Stabilization Strategies for Preventing Secondary Reactions During Lignin Depolymerization and Valorization

by

Vivek Patil

A dissertation submitted to the Graduate Faculty of
Auburn University
in partial fulfillment of the
requirements for the Degree of
Doctor of Philosophy

Auburn, Alabama

May 1, 2021

Keywords: Lignin, Hydrothermal Liquefaction, Phenolic Monomers, Pyrolysis

Approved by

Sushil Adhikari, Chair, Professor, Department of Biosystems Engineering

Oladiran Fasina, Professor, Department of Biosystems Engineering

Brian Via, Professor, School of Forestry and Wildlife Sciences

Zhihua Jiang, Assistant Professor, Department of Chemical Engineering

Abstract

Lignin-derived phenolic and aromatic monomers are rapidly being recognized as forerunners in the race to make sustainable biopolymers that can fulfill the world's demands for materials in the future. However, lignin being highly recalcitrant to the cleavage of its interunit linkages, requires harsh conditions for its depolymerization. These harsh conditions often make lignin react in an undesired way, leading to the formation of unwanted products, such as biochar through secondary reactions such as oligomerization, repolymerization and condensation. Specifically, certain reactive groups in the phenylpropanoid structure of lignin, such as Cα-OH and Cγ-OH, and open positions on the aromatic ring are majorly responsible for the recondensation of lignin during its valorization. To overcome these challenges, the structure of lignin can be modified in certain ways to make it more stable and less prone to the unwanted secondary reactions. Similar stabilization strategies can also be applied to lignin-derived fragments, which can be prevented from attacking each other after their formation in the depolymerization medium.

This dissertation is focused on investigating four strategies for stabilization of lignin and lignin-derived fragments during various stages of lignin valorization. In Chapter 2, fragments derived from fast pyrolysis of dealkaline lignin were stabilized with the help of vapors from low-density polyethylene (LDPE) and polystyrene (PS) through their co-pyrolysis at 500°C in a micro-pyrolyzer. The synergistic effect between these two feedstocks was quantified and this strategy was found to have about 1.4- 6.9 times increase in the yields of certain lignin and plastic-derived compounds on their depolymerization. The use of a locally sourced low-cost red clay catalyst and quantification of synergistic effect in co-pyrolysis were the highlights of this study.

The problems with dry-feed mechanism for lignin valorization can be overcome by using the feedstock in the form of a slurry. For this, solvent liquefaction at high pressures is a suitable process, as it is resilient to the higher moisture contents of feedstock and also achieves depolymerization at a lower temperature. However, the highly reactive environment provided by the liquefaction medium also leads to rapid re-condensation of lignin-derived fragments soon after they are formed. These fragments can be trapped by stabilizing them with hydrogen in radical form, which is a more effective way to avoid the handling issues related to gaseous hydrogen. In

Chapter 3, we provided hydrogen to these fragments using an *in-situ* hydrogen donor solvent 1,2,3,4-tetrahydronaphthalene (tetralin). It was revealed that the presence of *in-situ* hydrogen donor tetralin made the products from lignin depolymerization less dependent on composition of the solvent, ethanol-water. Also, it shifted the selectivity of monomeric products to be achieved at relatively lower concentration of ethanol in the solvent.

Modifying the lignin structure prior to its depolymerization can be achieved with the help of a chemical reagent such as phenol, which can be sourced from within a biorefinery itself. In Chapter 4, we explored a pretreatment to modify organosolv lignin at 80°C using phenol before depolymerizing it at 300°C with Ru/C as a catalyst and ethanol as a solvent. The presence of phenol led to biaryl formation with lignin, increasing its molecular weight, but also leading to a higher selectivity towards phenolic monomers compared with aliphatics. There was a 14% increase in the yield of phenolic monomers (excluding phenol) and a 27% decrease in the yield of biochar as a result of this pretreatment. Although, the consumption of phenol during this process renders it difficult to be economically feasible, this study contributes to the knowledge of lignin functional group protection through a pretreatment.

The most effective place within the lignin valorization pathway for stabilization of lignin is known to be during its isolation from biomass. In Chapter 5, we investigated the effect of adding boric acid to the biomass (poplar) fractionation medium while isolating lignin. We also used a biomass-derived solvent 2-methyl-tetrahydrofuran (2MeTHF) for lignin isolation. It was observed that there was an increase of ~20% in the relative abundance of Cγ-Hγ site in the β-O-4 linkage, whereas a decrease of ~3% in Cα-Hα site was seen. As a result of boric acid stabilization, the yield of monomers increased from 16% to 25%. Additionally, the nature of products was different with this stabilization strategy, yielding more of longer sidechains, lesser methoxy groups and slightly more saturation in the compounds.

In the end, the summary of all the chapters and overall learnings from the studies is presented in Chapter 6, where various strategies explored in this dissertation are tied together in a common theme. Additionally, future direction for this research area is discussed. Briefly, the use of a single solvent instead of a mixture, developing pretreatment strategies that can take a variable feed, removing the impurities from lignin and also performing depolymerization in a continuous reactor can be interesting areas to explore in the future.

Dedicated to my dear Mrunmayee (Wife), Pappa (Dad) and Mummy (Mom)

Acknowledgements

I want to express my heartfelt gratitude to all my colleagues, teachers and co-workers who made my Ph.D. journey at Auburn University memorable. I am highly grateful to have had an opportunity to work with my advisor and a great teacher, Dr. Sushil Adhikari, who has always inspired me to pursue my dreams. It was an incredible journey to spend nearly five years working with him at Auburn and learn many things from him not only about my research area, but also about life. The encouragement, wisdom and support I received from him was essential for me completing my doctoral research work.

My Ph.D. journey would not have been so enriching without the guidance and motivation provided by my committee members, Dr. Oladiran Fasina, Dr. Brian Via and Dr. Zhihua Jiang. I would also like to thank Dr. Maria Auad for serving as the Graduate School reader. I am greatly indebted to Walter and Virginia Woltosz, who supported my graduate studies through the 'Woltosz Fellowship' through their generous offer. I am also thankful to the Department of Biosystems Engineering, Samuel Ginn College of Engineering and Auburn University College of Agriculture for giving all the help and support throughout my graduate studies. I would also like to acknowledge here the research funding provided by 'United States Department of Agriculture-National Institute of Food and Agriculture' (Grant # USDA-NIFA-2015-67021-22842).

I am grateful to have met with very kind and supportive colleagues and friends at Biological Engineering Research Laboratory (BERL), who always taught me invaluable things- Dr. Hossein Jahromi, Dr. Pixiang Wang, Tawsif Rahman, and Poulami Roy. I am also thankful to people in the Department of Biosystems Engineering, working with whom was always a great experience- Kritika Malhotra, Hemendra Kumar and Dr. Haixin Peng.

Lastly, I owe it all to my family and my lovely wife, Mrunmayee, who always stood by my side throughout my pursuits. My wife, who always understood me, my father and mother, who always believed in me, and my brother Nikhil, who always cheered me up- I do not have words to express how much thankful I am to you!

Table of Contents

List of Figures

List of Tables

1. Introduction

Lignocellulosic biomass stands out among the various alternatives to crude oil, mainly due to its potential to be converted into liquid fuels and the economy of scale that it can afford (Lee et al., 2016; Vardon et al., 2016). It can be sourced from plants, forestry residues or agricultural wastes, and even municipal solid waste (Ramiah Shanmugam et al., 2019; Sequeiros et al., 2013). Roughly, the plant-derived biomass consists of about 40-45 wt.% cellulose, 25-35 wt.% hemicellulose and 15-30 wt.% lignin (Erdocia et al., 2016). Although, biomass alone cannot fulfill the existing requirement for liquid fuels and chemicals, it can contribute significantly to it (Patil et al., 2011). Removing the high amount of oxygen from lignocellulosic biomass through reactions such as hydrodeoxygenation is one of the purpose of conversion processes (Regmi et al., 2018). The use of a wide range of feedstock, including lignocellulosic biomass in the existing infrastructure for the biofuel and biodiesel-manufacturing plants is expected in the future (Aden and Foust, 2009). Because of its potential for creating chemical products, biomass is an important future resource for the process industries. A typical process for deriving value from biomass components involves their isolation and chemical transformation into the desired products (Rinaldi et al., 2016a).

Lignin (Figure 1.1) is one of the most abundant naturally found polymers in the world, second only to cellulose (Vardon et al., 2015). The main function of lignin in plants is to provide structural rigidity and help in water conduction (Regmi et al., 2018). The efforts for the utilization of biomass as a renewable source of fuels and chemicals often miss out on the opportunity to capture the potential of lignin (Laskar et al., 2014; Patil et al., 2020). The recent rise in interest in lignin utilization is due to the rapid increase in the production of second-generation biofuels. The idea of converting lignin into lower-molecular weight compounds originated around half-a-century ago, as a way of additional revenue-generation for the paper and pulp industry (Ma et al., 2018). The heterogeneous and irregular structure of lignin is said to be the main challenge in the production of widely useful acidic compounds such as vanillic, ferulic, and cinnamic acids (Agarwal et al., 2018). It is an amorphous polymer with a three-dimensional structure that mainly constitutes phenylpropane units connected to each other by a series of C-C and C-O-C linkages

(Deepa and Dhepe, 2015; Patil et al., 2018). The uniqueness of the structure of lignin comes from random crosslinking of C_9 units (Y. Wang et al., 2018). The other connections found in the structure of lignin are β-O-4, α-O-4, β-5, 4-O-5, 5-5, β-1, and β- β inter-unit linkages. A high carbon content, the aromaticity of its structure, and a universal abundance make lignin one of the most important renewable natural resources (Adhikari et al., 2020). Currently, the largest producer of lignin in the world is the paper and pulp industry accounting for about 50 million tons per year in the western hemisphere alone (Arturi et al., 2017). Yet, lignin has so far not found widespread industrial applications (Wen et al., 2013). Around 2% of industrially produced lignins find small applications such as chelating agents, binders, and surfactants (Y. Wang et al., 2018). As an energy source, lignin has about 60% energetic value as compared to that of crude oil (Beauchet et al., 2012). In a biomass-based economy, due to its highly aromatic structure, lignin can also be a valuable resource to produce aromatic chemicals (Jongerius et al., 2013). However, lignin is also the most recalcitrant among the three components of lignocellulosic biomass, posing serious difficulties in terms of selectivity and yield with its conversion (Kozliak et al., 2016). The stabilization of highly reactive groups in the lignin structure can be achieved in several ways and can lead to a more stable lignin structure that is suitable for depolymerization without condensation. We explore in the current research, the role of an *in-situ* hydrogen donor solvent tetralin (1,2,3,4-tetrahydronaphthalene), co-pyrolysis with plastics, and pretreatment with phenol and boric acid as stabilization strategies to aid lignin depolymerization (Chapter 2, Chapter 3, Chapter 4, Chapter 5).

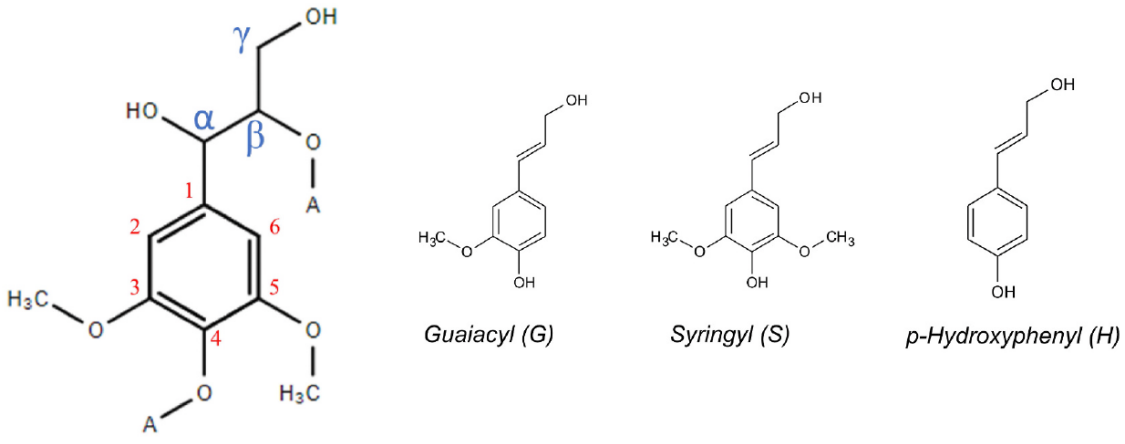

Figure 1.1 Structural units of lignin [adapted from (Patil et al., 2020); reproduced with permission from Elsevier]

Lignin is produced all over the world and has the potential to displace many products that are currently produced from petroleum-derived sources (Figure 1.2). The majority of those are pharmaceuticals, amines, and building blocks for synthetic polymers (Sun et al., 2018a). At the same time, the structure of lignin plays an important role in determining its reactivity. For example, G-type lignin, having only one methoxy substitution is more reactive than S-type lignin, which has two methoxy groups at C_3 and C_5 positions (Gordobil et al., 2016). Since lignin is likely to undergo structural changes during its extraction from biomass, it is advantageous to calculate the theoretical yield of monomers from lignin by subjecting the native lignin in biomass to the liquefaction conditions (Talebi Amiri et al., 2019). However, this is not possible with the commercially available lignins that have already undergone the modification during pulping. Hence, in the current study, a considerable focus is kept on technical lignins, such as commercially available alkaline lignin (TCI Chemicals, USA), dealkaline lignin (TCI Chemicals, USA), or organosolv lignin (prepared in the lab) while exploring the strategies for lignin depolymerization.

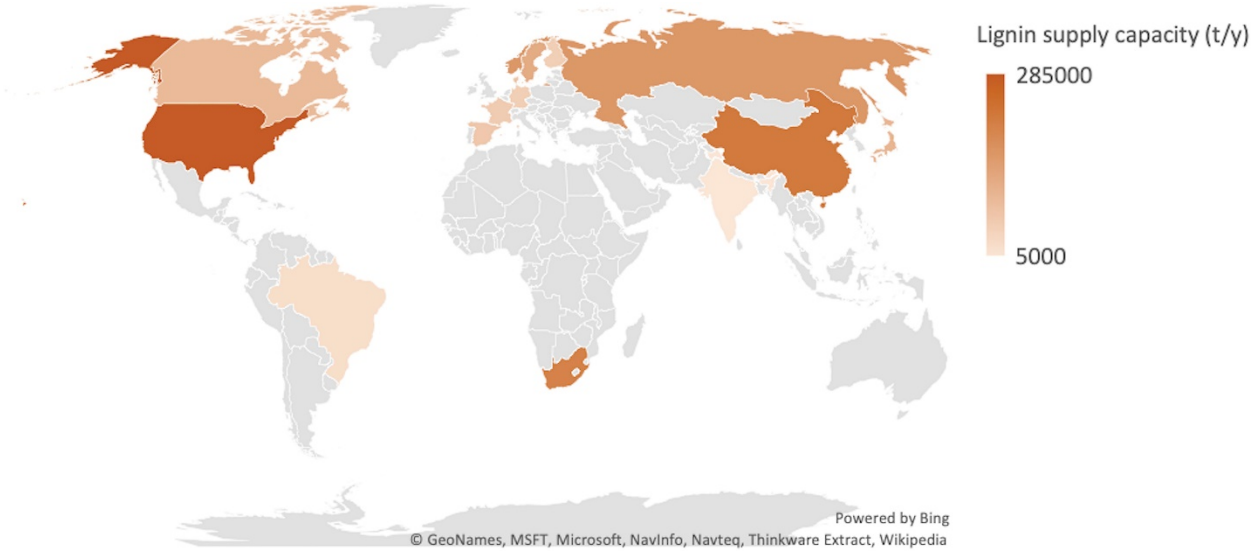

Figure 1.2 Global supply of lignin in 2017-18 [adapted from (Dessbesell et al., 2020); reproduced with permission from Elsevier]

The choice of catalyst for the depolymerization of lignin must be made wisely, as it changes the nature of lignin depolymerization products. For example, Raney Ni shows activity for hydrodeoxygenation of phenolics to produce ring saturation products, which would be more useful if the target products are renewable fuels rather than renewable chemicals (Regmi et al., 2018).

One strategy for the effective valorization of lignin for producing monomers is to combine lignin extraction with its depolymerization (Kumaniaev et al., 2017). In the same way, when lignin is obtained as a waste-stream from biomass fractionation processes, is likely to be in the form of a solution in lignocellulose-derived solvents, also known as "liquor". The presence of these solvents in the lignin stream can be made useful by effectively making use of their hydrodeoxygenation capabilities (Table 1.1). As novel techniques for the solvolysis of lignin, the current research explores biomass-derived reagents and solvents as sustainable alternatives to the existing industrial solvents for the isolation of lignin from biomass or for lignin pretreatment (Chapter 4 and Chapter 5).

The future direction of lignin depolymerization efforts should also include a focus on effective lignin extraction from the biomass so that the condensation of native lignin structure remains at the minimum possible level (Kim and Kim, 2018; Lan et al., 2019a; Shuai and Saha, 2017). There is enormous scope to find an economical way to cap the reactive groups in lignin, which can further assist in getting a high yield of phenolic monomers on depolymerization (Kim and Kim, 2018). The major reactive groups in lignin are formed because of the resonance structure of the benzene ring and include the benzylic cation and the electron-rich aromatic ring (Shuai and Saha, 2017). Oxidation, cyclization, and methoxylation are some of the common strategies followed for stabilization of the reactive groups in lignin (Kim and Kim, 2018). Oxidation of the benzylic alcohol present in the β-O-4 moiety of lignin makes the C_β-O ether bond weak, making its cleavage during depolymerization easier (W. Schutyser et al., 2018). The oxidation of lignin can either result in a high total bio-oil yield, or a high selectivity of certain products (Lancefield et al., 2016; Miles-Barrett et al., 2017; Rahimi et al., 2014; W. Schutyser et al., 2018). For example, syringyl-3-hydroxy-1-propanone is one such product that was obtained with high selectivity through lignin oxidation-depolymerization and can be used as a precursor to making an antimalarial agent, 4-(1-propenyl)-syringol) (Lancefield et al., 2016; Miles-Barrett et al., 2017; W. Schutyser et al., 2018; Sun et al., 2018b).

Table 1.1 Characteristics of various hydrogen donor solvents reported in the literature that were used for lignin depolymerization (from (Patil et al., 2020); reproduced with permission from Elsevier)

Solvent	Solvent characteristics	Mechanism of action	Yields (wt% of lignin)	Advantages	Drawbacks	Reference
Water	High dielectric constant	Hydrogen bonding with non-polar solute	39-79	Increasing the density with supercritical conditions can improve solvation	Dynamic equilibrium of solute can alter dissolution	(Holmelid et al., 2017; Wahyudiono et al., 2008)
Alcohols	Good solvent polarity index	Rapid dissolution of active species	54-85	Better molecular sources of active H_2	Do not act on all the lignin linkages	(Erdocia et al., 2016; Huang et al., 2015; Liu et al., 2019; Singh et al., 2014; Song et al., 2013)
Tetralin	Excellent hydrogen donor	Capping of reactive sites	11-40	Help avoid safety hazards of gaseous H_2	Solvent degradation at high temperatures	(Galkin and Samec, 2014; Haverly et al., 2018; K. H. Kim et al., 2014; Riaz et al., 2018; Rinaldi et al., 2016b)
Formic acid	Supplies H_2 during solvolysis	Provides H_2 through thermal decomposition	72-88	Active at relatively lower temperatures	Forms gaseous products at very high temperatures (~400°C)	(A. Das et al., 2018; Huang et al., 2014; Løhre et al., 2016; Rahimi et al., 2014)

Safe disposal of plastic waste has been a major environmental concern in the past few decades all over the world. The transformation of waste plastics to environmentally safe products is achievable through its thermochemical conversion. Out of the approximately 150 million tons of plastic waste generated annually, <10% is recycled (Rahimi and García, 2017; Zhang et al., 2016). With its high hydrogen content and lower oxygen content relative to lignin, plastics can be used together with lignin for an effective thermochemical conversion (Patil et al., 2018). In the context of the Circular Economy, recurring use of plastics for a higher-valued purpose will prevent it from

becoming a “waste” material after a short use (Ellen MacArthur Foundation, 2016). The co-pyrolysis of lignin and plastics offers a unique opportunity to take advantage of the complementary properties of the two waste sources, lignin, and plastics. There are many efforts to valorize biomass-derived lignin and plastics together (Dorado et al., 2014; Duan et al., 2017; Fan et al., 2017; Ojha and Vinu, 2015; Zhang et al., 2015; Zhou et al., 2015b). Micro-wave assisted co-pyrolysis of lignin and polypropylene at 200-350°C led to a synergistic effect between the two feedstocks, even though the bio-oil yield decreased (Duan et al., 2017). Whereas, the use of HZSM-5 catalyst for the co-pyrolysis of biomass and plastics had led to an increase in the bio-oil yield (Dorado et al., 2014). However, the use of expensive catalysts is not ideal because of the inherent low value for even a high volume of waste materials or products derived from them. Instead, the use of a locally-sourced catalyst, made with low-cost materials such as red clay can be an effective way to bring down the overall cost for the process and is explored in Chapter 2 (Anil et al., 2004; Lim et al., 2014).

1.1 Research problem

Effective conversion of lignin into useful phenolic monomers is difficult due to its tendency to undergo undesired secondary reactions leading to biochar. Solvent liquefaction was looked at as a technology to convert lignin into monomers at relatively lower temperatures compared to pyrolysis. However, a majority of the structural condensation of lignin occurs during its isolation from biomass. Additionally, the lignin fragments getting released after its depolymerization are highly reactive and often lead to self-condensation with one another. Therefore, strategies that can transform the structure of lignin or lignin-derived fragments so as to prevent their secondary reactions are valuable for ensuring that lignin reacts in the desired way. Preventing the self-condensation in this manner ensures that more bio-oil containing phenolic monomers is produced from lignin depolymerization. Some ways to achieve this can be forming a protective structure on the reactive sites of lignin, or capping the reactive radicals coming from lignin. The limitations of lignin utilization can be overcome to some extent by using several stabilization strategies that can be applied during various stages of lignin valorization. However, there is a research gap in the literature where these strategies have not been comprehensively looked at and have been applied only at one or two stages of lignin valorization. By using chemical reagents such as hydrogen from

plastics or donor solvent, and chemical stabilization agents such as phenol or boric acid, we can better understand how lignin reactivity changes for its depolymerization.

1.2 Research proposal and objectives

1.2.1 Objective 1- Co-Pyrolysis of Lignin and Plastics Using Red Clay as a Catalyst in a Micropyrolyzer

Goal: Investigate if the hydrogen provided by plastics during their fast pyrolysis can aid in the stabilization of reactive fragments from depolymerized lignin. Quantify the synergistic effect between the two feedstocks based on the changes in product yields.

Rationale: The disposal of waste plastics is a major issue all around the world. But this feedstock is oxygen-free and hence can be utilized to compensate for the highly oxygenated lignin during fast pyrolysis. Also, a low-cost catalyst such ad red clay can be useful in catalyzing this process, helping to bring down the overall cost of the thermochemical conversion. This type of catalyst had not been previously used for the co-pyrolysis of lignin and plastics and it can be useful knowledge for the development of this process.

1.2.2 Objective 2- The Role of an *in-situ* Hydrogen Donor Solvent in the Solvent Liquefaction of Lignin

Goal: Assess the effect of using a hydrogen donor solvent (tetralin) to the liquefaction medium during lignin depolymerization, on the resulting products.

Rationale: Hydrogen donor solvents can provide hydrogen in a radical form, which is more reactive. This hydrogen can effectively stabilize the reactive fragments from lignin in a liquefaction setting. Adding tetralin in addition to the ethanol-water solvent for lignin liquefaction had not been investigated before and hence this can be a valuable addition to the literature on this topic.

1.2.3 Objective 3- Lignin Depolymerization Aided with Biaryl Formation During a Pretreatment

Goal: Investigate the effect of a phenol-based pretreatment for lignin on its subsequent depolymerization by identification and quantification of resulting phenolic monomers.

Rationale: The reaction conditions used for lignin depolymerization are often quite harsh. Preventing the unwanted secondary reactions under such harsh conditions becomes difficult due to the limitations in controlling the process in this setting. Instead, modifying the structure of lignin in such as way that its reactivity is altered can be a better option to improve its depolymerization. Biaryl formation of lignin by using phenol in a pretreatment had not previously been studied and can help understand how lignin reacts to these conditions.

1.2.4 Objective 4- Effect of Boric Acid Capping During Biomass Fractionation on Subsequent Depolymerization of Lignin

Goal: To examine the effect of adding boric acid to the lignin isolation medium during biomass fractionation, on the subsequent depolymerization of lignin.

Rationale: Lignin structure is one of the most important factors that decide the yields of products on its depolymerization. However, once lignin is isolated from the biomass, it is difficult to change its structure. The most effective way to preserve the structure of lignin is to tune the conditions during its isolation from biomass. Although making these conditions milder help preserve the structure of lignin, it can negatively affect the yields of lignin isolation. Instead, forming a protective structure on lignin with the help of a chemical reagent such as boric acid is a better way to achieve this. Boric acid had not previously been used in an organosolv-type process for lignin stabilization during biomass fractionation, and this knowledge might open up a better way to preserve lignin structure.

These objectives are presented in Chapter 2, Chapter 3, Chapter 4, and Chapter 5, respectively. A summary of the research findings based on these studies, any limitations in those, and the future direction are presented in Chapter 6.

A literature review based on this chapter has been published and the citation is as follows:

Patil, V., Adhikari, S., Cross, P., Jahromi, H., 2020. Progress in the solvent depolymerization of lignin. Renew. Sustain. Energy Rev. 133, 110359. https://doi.org/https://doi.org/10.1016/j.rser.2020.110359

1.3 References

1. Aden, A., Foust, T., 2009. Technoeconomic analysis of the dilute sulfuric acid and enzymatic hydrolysis process for the conversion of corn stover to ethanol. Cellulose 16, 535–545. https://doi.org/10.1007/s10570-009-9327-8
2. Adhikari, S., Auad, M.L., Via, B., Shah, A., Patil, V., 2020. Production of Novolac Resin after Partial Substitution of Phenol from Bio-oil. Trans. ASABE 0. https://doi.org/10.13031/trans.13798
3. Agarwal, A., Rana, M., Park, J.H., 2018. Advancement in technologies for the depolymerization of lignin. Fuel Process. Technol. 181, 115–132. https://doi.org/10.1016/j.fuproc.2018.09.017
4. Anil, H., Cakici, A.I., Yanik, J., UCar, S., Karayildirim, T., 2004. Utilization of red mud as catalyst in conversion of waste oil and waste plastics to fuel. J. Mater. Cycles Waste Manag. 6, 20–26. https://doi.org/10.1007/s10163-003-0101-y
5. Arturi, K.R., Strandgaard, M., Nielsen, R.P., Sogaard, E.G., Maschietti, M., 2017. Hydrothermal liquefaction of lignin in near-critical water in a new batch reactor: Influence of phenol and temperature. J. Supercrit. Fluids 123, 28–39. https://doi.org/10.1016/j.supflu.2016.12.015
6. Beauchet, R., Monteil-Rivera, F., Lavoie, J.M., 2012. Conversion of lignin to aromatic-based chemicals (L-chems) and biofuels (L-fuels). Bioresour. Technol. 121, 328–334. https://doi.org/10.1016/j.biortech.2012.06.061
7. Deepa, A.K., Dhepe, P.L., 2015. Lignin Depolymerization into Aromatic Monomers over Solid Acid Catalysts. ACS Catal. 5, 365–379. https://doi.org/10.1021/cs501371q
8. Dessbesell, L., Paleologou, M., Leitch, M., Pulkki, R., Xu, C. (Charles), 2020. Global lignin supply overview and kraft lignin potential as an alternative for petroleum-based polymers. Renew. Sustain. Energy Rev. 123, 109768. https://doi.org/https://doi.org/10.1016/j.rser.2020.109768
9. Dorado, C., Mullen, C.A., Boateng, A.A., 2014. H-ZSM5 catalyzed co-pyrolysis of biomass and plastics. ACS Sustain. Chem. Eng. 2, 301–311. https://doi.org/10.1021/sc400354g
10. Duan, D., Wang, Y., Dai, L., Ruan, R., Zhao, Y., Fan, L., Tayier, M., Liu, Y., 2017. Ex-situ catalytic co-pyrolysis of lignin and polypropylene to upgrade bio-oil quality by microwave heating. Bioresour. Technol. 241, 207–213. https://doi.org/10.1016/j.biortech.2017.04.104
11. Ellen MacArthur Foundation, 2016. THE NEW PLASTICS ECONOMY: RETHINKING THE FUTURE OF PLASTICS & CATALYSING ACTION.
12. Erdocia, X., Prado, R., Fernández-Rodríguez, J., Labidi, J., 2016. Depolymerization of Different Organosolv Lignins in Supercritical Methanol, Ethanol, and Acetone to Produce Phenolic Monomers. ACS Sustain. Chem. Eng. 4, 1373–1380. https://doi.org/10.1021/acssuschemeng.5b01377
13. Fan, L., Chen, P., Zhang, Y., Liu, S., Liu, Y., Wang, Y., Dai, L., Ruan, R., 2017. Fast microwave-assisted catalytic co-pyrolysis of lignin and low-density polyethylene with HZSM-5

and MgO for improved bio-oil yield and quality. Bioresour. Technol. 225, 199–205. https://doi.org/10.1016/j.biortech.2016.11.072
14. Gordobil, O., Moriana, R., Zhang, L., Labidi, J., Sevastyanova, O., 2016. Assesment of technical lignins for uses in biofuels and biomaterials: Structure-related properties, proximate analysis and chemical modification. Ind. Crops Prod. 83. https://doi.org/10.1016/j.indcrop.2015.12.048
15. Jongerius, A.L., Bruijnincx, P.C.A., Weckhuysen, B.M., 2013. Liquid-phase reforming and hydrodeoxygenation as a two-step route to aromatics from lignin. Green Chem. 15, 3049–3056. https://doi.org/10.1039/c3gc41150h
16. Kim, K.H., Kim, C.S., 2018. Recent Efforts to Prevent Undesirable Reactions From Fractionation to Depolymerization of Lignin : Toward Maximizing the Value From Lignin 6, 1–7. https://doi.org/10.3389/fenrg.2018.00092
17. Kozliak, E.I., Kubátová, A., Artemyeva, A.A., Nagel, E., Zhang, C., Rajappagowda, R.B., Smirnova, A.L., 2016. Thermal Liquefaction of Lignin to Aromatics: Efficiency, Selectivity, and Product Analysis. ACS Sustain. Chem. Eng. 4, 5106–5122. https://doi.org/10.1021/acssuschemeng.6b01046
18. Kumaniaev, I., Subbotina, E., Sävmarker, J., Larhed, M., Galkin, M. V, Samec, J.S.M., 2017. Lignin depolymerization to monophenolic compounds in a flow-through system. Green Chem. 19, 5767–5771. https://doi.org/10.1039/C7GC02731A
19. Lan, W., de Bueren, J.B., Luterbacher, J.S., 2019. Highly Selective Oxidation and Depolymerization of α,γ-Diol-Protected Lignin. Angew. Chemie 131, 2675–2680. https://doi.org/10.1002/ange.201811630
20. Lancefield, C.S., Rashid, G.M.M., Bouxin, F., Wasak, A., Tu, W.C., Hallett, J., Zein, S., Rodríguez, J., Jackson, S.D., Westwood, N.J., Bugg, T.D.H., 2016. Investigation of the Chemocatalytic and Biocatalytic Valorization of a Range of Different Lignin Preparations: The Importance of β-O-4 Content. ACS Sustain. Chem. Eng. 4. https://doi.org/10.1021/acssuschemeng.6b01855
21. Laskar, D.D., Tucker, M.P., Chen, X., Helms, G.L., Yang, B., 2014. Noble-metal catalyzed hydrodeoxygenation of biomass-derived lignin to aromatic hydrocarbons. Green Chem. 16, 897. https://doi.org/10.1039/c3gc42041h
22. Lee, H., Jae, J., Ha, J.-M., Suh, D.J., 2016. Hydro- and solvothermolysis of kraft lignin for maximizing production of monomeric aromatic chemicals. Bioresour. Technol. 203, 142–149. https://doi.org/https://doi.org/10.1016/j.biortech.2015.12.022
23. Lim, X., Sanna, A., Andrésen, J.M., 2014. Influence of red mud impregnation on the pyrolysis of oil palm biomass-EFB. Fuel 119, 259–265. https://doi.org/10.1016/j.fuel.2013.11.057
24. Ma, R., Guo, M., Zhang, X., 2018. Recent advances in oxidative valorization of lignin. Catal. Today 302, 50–60. https://doi.org/10.1016/j.cattod.2017.05.101
25. Miles-Barrett, D.M., Montgomery, J.R.D., Lancefield, C.S., Cordes, D.B., Slawin, A.M.Z., Lebl, T., Carr, R., Westwood, N.J., 2017. Use of Bisulfite Processing To Generate High-β-O-4 Content Water-Soluble Lignosulfonates. ACS Sustain. Chem. Eng. 5, 1831–1839. https://doi.org/10.1021/acssuschemeng.6b02566
26. Ojha, D.K., Vinu, R., 2015. Fast co-pyrolysis of cellulose and polypropylene using Py-GC/MS and Py-FT-IR. RSC Adv. 5, 66861–66870. https://doi.org/10.1039/C5RA10820A
27. Patil, P.T., Armbruster, U., Richter, M., Martin, A., 2011. Heterogeneously catalyzed hydroprocessing of organosolv lignin in sub- and supercritical solvents. Energy and Fuels 25, 4713–4722. https://doi.org/10.1021/ef2009875

28. Patil, V., Adhikari, S., Cross, P., 2018. Co-pyrolysis of lignin and plastics using red clay as catalyst in a micro-pyrolyzer. Bioresour. Technol. 270, 311–319. https://doi.org/10.1016/j.biortech.2018.09.034
29. Patil, V., Adhikari, S., Cross, P., Jahromi, H., 2020. Progress in the solvent depolymerization of lignin. Renew. Sustain. Energy Rev. 133, 110359. https://doi.org/https://doi.org/10.1016/j.rser.2020.110359
30. Rahimi, A., García, J.M., 2017. Chemical recycling of waste plastics for new materials production. Nat. Rev. Chem. 1, 0046. https://doi.org/10.1038/s41570-017-0046
31. Rahimi, A., Ulbrich, A., Coon, J.J., Stahl, S.S., 2014. Formic-acid-induced depolymerization of oxidized lignin to aromatics. Nature 515, 249–252. https://doi.org/10.1038/nature13867
32. Ramiah Shanmugam, S., Adhikari, S., Nam, H., Patil, V., 2019. Adsorption and Desorption Behavior of Herbicide using Bio-Based Materials. Trans. ASABE 62, 1435–1445. https://doi.org/https://doi.org/10.13031/trans.13256
33. Regmi, Y.N., Mann, J.K., McBride, J.R., Tao, J., Barnes, C.E., Labbé, N., Chmely, S.C., 2018. Catalytic transfer hydrogenolysis of organosolv lignin using B-containing FeNi alloyed catalysts. Catal. Today 302, 190–195. https://doi.org/10.1016/j.cattod.2017.05.051
34. Rinaldi, R., Jastrzebski, R., Clough, M.T., Ralph, J., Kennema, M., Bruijnincx, P.C.A., Weckhuysen, B.M., 2016. Paving the Way for Lignin Valorisation: Recent Advances in Bioengineering, Biorefining and Catalysis. Angew. Chemie - Int. Ed. 55, 8164–8215. https://doi.org/10.1002/anie.201510351
35. Schutyser, W., Renders, T., Van Den Bosch, S., Koelewijn, S.F., Beckham, G.T., Sels, B.F., 2018. Chemicals from lignin: An interplay of lignocellulose fractionation, depolymerisation, and upgrading. Chem. Soc. Rev. https://doi.org/10.1039/c7cs00566k
36. Sequeiros, A., Serrano, L., Briones, R., Labidi, J., 2013. Lignin liquefaction under microwave heating. J. Appl. Polym. Sci. 130, 3292–3298. https://doi.org/10.1002/app.39577
37. Shuai, L., Saha, B., 2017. Towards high-yield lignin monomer production 19. https://doi.org/10.1039/c7gc01676j
38. Sun, Z., Bottari, G., Afanasenko, A., Stuart, M.C.A., Deuss, P.J., Fridrich, B., Barta, K., 2018a. Complete lignocellulose conversion with integrated catalyst recycling yielding valuable aromatics and fuels. Nat. Catal. 1, 82–92. https://doi.org/10.1038/s41929-017-0007-z
39. Sun, Z., Fridrich, B., De Santi, A., Elangovan, S., Barta, K., 2018b. Bright Side of Lignin Depolymerization: Toward New Platform Chemicals. Chem. Rev. 118, 614–678. https://doi.org/10.1021/acs.chemrev.7b00588
40. Talebi Amiri, M., Dick, G.R., Questell-Santiago, Y.M., Luterbacher, J.S., 2019. Fractionation of lignocellulosic biomass to produce uncondensed aldehyde-stabilized lignin. Nat. Protoc. 14, 921–954. https://doi.org/10.1038/s41596-018-0121-7
41. Vardon, D.R., Franden, M.A., Johnson, C.W., Karp, E.M., Guarnieri, M.T., Linger, J.G., Salm, M.J., Strathmann, T.J., Beckham, G.T., 2015. Adipic acid production from lignin. Energy Environ. Sci. 8, 617–628. https://doi.org/10.1039/C4EE03230F
42. Vardon, D.R., Rorrer, N.A., Salvachúa, D., Settle, A.E., Johnson, C.W., Menart, M.J., Cleveland, N.S., Ciesielski, P.N., Steirer, K.X., Dorgan, J.R., Beckham, G.T., 2016. cis,cis-Muconic acid: separation and catalysis to bio-adipic acid for nylon-6,6 polymerization. Green Chem. 18, 3397–3413. https://doi.org/10.1039/C5GC02844B

43. Wang, Y., Sun, S., Li, F., Cao, X., Sun, R., 2018. Production of vanillin from lignin: The relationship between β-O-4 linkages and vanillin yield. Ind. Crops Prod. 116, 116–121. https://doi.org/https://doi.org/10.1016/j.indcrop.2018.02.043
44. Wen, J.L., Xue, B.L., Xu, F., Sun, R.C., Pinkert, A., 2013. Unmasking the structural features and property of lignin from bamboo. Ind. Crops Prod. 42, 332–343. https://doi.org/10.1016/j.indcrop.2012.05.041
45. Zhang, H., Xiao, R., Nie, J., Jin, B., Shao, S., Xiao, G., 2015. Catalytic pyrolysis of black-liquor lignin by co-feeding with different plastics in a fluidized bed reactor. Bioresour. Technol. 192, 68–74. https://doi.org/10.1016/j.biortech.2015.05.040
46. Zhang, X., Lei, H., Chen, S., Wu, J., 2016. Catalytic co-pyrolysis of lignocellulosic biomass with polymers: a critical review. Green Chem. 18, 4145–4169. https://doi.org/10.1039/C6GC00911E
47. Zhou, H., Wu, C., Onwudili, J.A., Meng, A., Zhang, Y., Williams, P.T., 2015. Effect of interactions of PVC and biomass components on the formation of polycyclic aromatic hydrocarbons (PAH) during fast co-pyrolysis. RSC Adv. 5, 11371–11377. https://doi.org/10.1039/C4RA10639C

2. Co-Pyrolysis of Lignin and Plastics Using Red Clay as Catalyst in a Micropyrolyzer

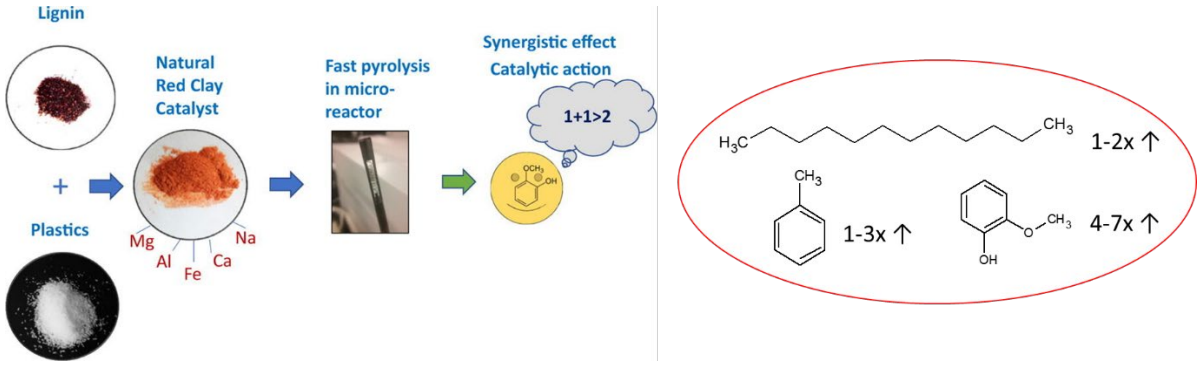

Abstract

In the current study, low-density polyethylene (LDPE) and polystyrene (PS) were co-pyrolyzed with dealkaline lignin in a micro-reactor. Lignin and plastics samples were co-pyrolyzed at 500°C with and without a low-cost red clay catalyst. The products were analyzed with GC-MS/FID to quantify phenolic compounds, alkanes and alkenes. The synergistic effect between lignin and plastics was studied by comparing the carbon yield of products from co-pyrolysis with that from individual pyrolysis. The co-pyrolysis of lignin and polystyrene was also performed at 600, 700 and 800°C. The study explores a novel approach to enhance lignin depolymerization with red clay catalyst while utilizing waste plastics.

Keywords: *lignin; co-pyrolysis; plastics; red clay.*

2.1 Introduction

Lignin, a major constituent of lignocellulosic biomass, can provide renewable fuels and chemicals when depolymerized via fast pyrolysis. However, high oxygen content of lignin leads to low quality of the inherently unstable bio-oil after fast pyrolysis (Karimi et al., 2014). Literature has reported high oxygen content and low hydrogen content of biomass components, including lignin as a problem in the large-scale commercialization of their pyrolysis (Zhang et al., 2016).

Co-feeding lignin with hydrogen-rich waste plastics can improve the quality of bio-oil (Zhang et al., 2016; Ojha and Vinu, 2015). Approximately 150 million tons of plastic waste is generated in the world annually (Rahimi and García, 2017), but only less than 10% of the waste plastic is recycled (Zhang et al., 2016). The plastic waste originates from a variety of sources, including household use, commercial applications, packaging and even agricultural activities (Dorado et al., 2014), and recycling could be very costly because of impurities that are present. Using plastics to provide *in-situ* hydrogen during the fast pyrolysis of lignin can also help mitigating plastic waste disposal problem (Dorado et al., 2014). The process of utilizing plastic via fast pyrolysis also eliminates the need to separate impurities from plastics, and has an edge over the conventional recycling (Scheirs and Kaminsky, 2006).

Alkaline lignin, from which dealkaline lignin is derived, resembles the waste stream from paper and pulp industry, also known as 'black liquor' (Rutten et al., 2017). Converting dealkaline lignin into liquid fuels and renewable chemicals represents an opportunity for its effective utilization (Duan et al., 2017). The quantity of lignin by-product generated in the paper and pulp industry is estimated to be 50 million tons annually (Sun et al., 2018b). About 97% of the lignin from paper and pulp processes is estimated to be burned directly as a low-grade heat source (Fan et al., 2017). The future biorefineries are likely to use soda process for separating the biomass components and will be producing thousands of tons of low-sulfur lignin as a by-product (Rutten et al., 2017). Effective utilization of this lignin will be a challenge for the biorefineries. The relatively lower hydrogen content of lignin molecules (H/C_{eff} molar ratio < 0.3) can be compensated by the higher hydrogen content of waste plastics, resulting in a higher quality of bio-oil (Duan et al., 2017). Low density polyethylene (LDPE) is a common plastic found in packaging and has an estimated recovery rate of about 5% for recycling (Rahimi and García, 2017); whereas, the recovery of polystyrene (PS), another common packaging plastic, is only 1% (Rahimi and García, 2017). Both of these plastics have a high hydrogen content (H/C_{eff} molar ratio= 1-2) (Zhang et al., 2014).

Several studies (Dorado et al., 2014; Duan et al., 2017; Fan et al., 2017; Mullen et al., 2016; Ojha and Vinu, 2015; Yao et al., 2015; Zhang et al., 2015, 2016; Zhou et al., 2015b) have reported co-pyrolysis of lignin and waste plastics as a means to improve the bio-oil properties. Co-pyrolysis of agricultural biomass and waste plastics with HZSM-5 at 600°C led to an improvement in the

yield of bio oil and the amount of aromatics as compared to the pyrolysis of individual feedstock (Dorado et al., 2014). On the other hand, the use of HZSM-5 catalyst in a microwave-assisted co-pyrolysis of alkali lignin and polypropylene at 200-350°C led to a decrease in bio-oil (Duan et al., 2017). Nonetheless, the synergistic effect between the two feedstock and subsequent improvement in the bio-oil yield as compared to pyrolysis of lignin was still present (Duan et al., 2017). In the current study, the goal is to investigate if a low-cost catalyst such as red clay can be effectively utilized for the co-pyrolysis of dealkaline lignin and LDPE or PS. The red clay catalyst is chosen based on the catalytic properties of "red mud", a bauxite industry by-product reported in the literature. The total amount of red mud produced in the world as a bauxite mining waste is estimated to be nearly 120 million tons per year (Karimi et al., 2014). The need for catalyst during fast pyrolysis of lignin is both to selectively produce the deoxygenated products and to upgrade the pyrolysis products (Rahimi and García, 2017). Lim et al. found that impregnation of red mud on oil palm biomass decreases the char formation during its pyrolysis (Lim et al., 2014). Red mud has been known to contain the oxides of Fe, Al, Si and Ti and has previously been utilized as a catalyst for polymer degradation (Anil et al., 2004). It was also reported that red mud as a catalyst plays a role in hydrogenation reaction (Kim et al., 2015); (Sushil and Batra, 2008). In this study, plastics supposedly donate hydrogen during co-pyrolysis that helps in depolymerization of lignin. Hence, studying a catalyst that can assist this process is important. However, red clay sourced locally is used in this study instead of the red mud from alumina industry. Biomass feedstock is often contaminated with red clay during its harvesting. The usefulness of plastics having a high hydrogen content in mitigating the adverse effect of contaminations such as clay in the lignin is also explored.

In this study, the catalyst is placed external to the feedstock so that pyrolysis vapors from both the feedstocks can interact with each other at the catalyst site. Duan et al. mentioned problems with *in-situ* arrangement of catalyst, such as difficulties in the recovery of catalyst after the reaction due to char formation (Duan et al., 2017). Separating the pyrolysis stage and the catalytic upgrading of pyrolysis vapors is also helpful in recovery of the catalyst after the reaction (Duan et al., 2017). HZSM-5, a widely used catalyst for the catalytic fast pyrolysis of biomass, suffers from a smaller catalyst lifetime, as well as low carbon efficiency (Dorado et al., 2014). The use of red clay for the co-pyrolysis of lignin and plastics, as explored in this study, has not been reported

previously. A mild catalyst such as red clay can assist the initial stages of lignin depolymerization, which could bring down the overall cost of the process. The further conversion of primary products from depolymerization of lignin, such as guaiacol to catechol and methanol can then be proceeded even without a catalyst (Wahyudiono et al., 2008). Also, the ash that comes during the harvesting of biomass, from which lignin is isolated, reflects into a high inorganic content of the bio-oil and hence affects its stability by catalyzing polymerization and condensation reactions (Nguyen Lyckeskog et al., 2016). The inorganic elements from the clay that comes with harvested biomass, including lignin, can instead catalyze the depolymerization of the plastics in co-pyrolysis and create *in-situ* availability of hydrogen in the process. The current study explores the co-pyrolysis of lignin and plastics with these things in mind.

2.2 Experimental

2.2.1 Materials and Catalyst Characterization

Dealkaline lignin was purchased from TCI America (Oregon, USA) and is hereafter referred to as just 'lignin'. This particular product was reported to have a molecular weight of 60,000 Da (Deepa and Dhepe, 2014). It was sieved to get the size of particles between 105 and 595 microns and used without further processing. Polyethylene powder, low density (500 micron, M.W. 3-6 million Da.) and polystyrene standard (M.W. 3,350 Da.) was purchased from Alfa Aesar (Massachusetts, USA). Mettler Toledo XS205 Dual Range weighing balance (resolution: 0.01 mg) was used to measure the weights of raw materials. Ultimate analysis of the raw materials was performed using 'Vario MICRO cube' elemental analysis system (Elementar Americas Inc., NY, USA). Fourier Transform Infrared (FTIR) analysis of lignin was performed using Thermo-Nicolet iS10 (Thermo Scientific, Massachusetts, USA).

The red clay used in this study was collected from local construction site (Auburn, Alabama, USA). It was dried at 105°C for 24 hours, sieved to particle size <105 μm and calcined at 500°C for 4 hours before use. The fresh red clay sample lost its mass by about 9 wt.% during the calcination. The weight reduction is likely to be due to the intrinsic moisture and organic impurities in the red clay. Autosorb IQ (Quantachrome instruments, FL, USA) was used to measure the Brunauer-Emmett-Teller (BET) surface area of the catalysts, based on the theory of physical adsorption of gas molecules on a solid surface. Degassing of about 1 g of sample was carried out

at 300°C for 24 hours under vacuum. The surface area measurement was carried out at -196°C using liquid nitrogen as the adsorbate. X-ray diffraction (XRD) analysis of catalyst was performed on Bruker D2 Phaser X-Ray Diffractometer, while the X-ray fluorescence (XRF) analysis was performed on a portable Bruker Elemental Tracer IV-ED XRF system. The catalyst was calcined at 500°C for 4 hours before using it for the fast pyrolysis experiments. The amount of various metals in the red clay was determined using ICP-AES analysis with SPECTRO-CIROS ICP-AES instrument (SPECTRO Analytical Instruments Inc., Germany). Prior to that, the samples were digested in nitric acid using CEM Mars X microwave digestion system (CEM Corporation, North Carolina, USA) according to EPA method 3051.

2.2.2 Thermogravimetric analysis (TGA)

Thermogravimetric analysis of raw materials was carried out in TGA-50 (Shimadzu Scientific Instruments, Inc., Maryland, USA). The thermal degradation of raw materials was studied in a thermo-gravimetric analyzer under nitrogen atmosphere. For PS and LDPE, a known amount (about 5-10 mg) of sample was placed in an aluminum crucible and was heated to 600°C and 700°C, respectively at a rate of 15°C/min. For lignin, with the same sample size, alumina crucible was used and the samples were heated up to 900°C 15°C/min. The samples were held at that temperature for 5 minutes and then cooled down to room temperature. For the mixture of lignin and plastics, they were mixed in a 1:1 weight ratio and alumina pans were used. Also, lignin, plastics and red clay were mixed in equal amount (lignin: LDPE: RC = 1:1:1 or lignin: PS: RC = 1:1:1 ratio of weights) and used. The amount of sample for the mixture of feedstock was about 6 – 15 mg. In the current study, the combined char and coke yield was determined from the TGA curves for the feedstocks.

2.2.3 Fast pyrolysis experiments

The fast pyrolysis of either lignin or plastics alone is termed as ‘individual pyrolysis’, while that of their mixtures is termed as ‘co-pyrolysis.’ The fast pyrolysis without red clay is termed as ‘thermal pyrolysis’, while that using red clay is termed as ‘catalytic pyrolysis.’ Thermal and catalytic fast co-pyrolysis was performed in a micro reactor (CDS Pyroprobe® 5200, CDS Analytical LLC, Pennsylvania, USA) connected to a gas chromatography unit by Agilent 7890A

GC/ 5975C MS using a DB-1701 column (30 m; 0.25 mm i.d.; 0.25mm film thickness). The initial temperature of the Pyroprobe® was kept at 40°C and then it was increased at the rate of 2°C/mS to 500°C and kept steady for 90s. Helium (He) gas (ultra-high purity, 99.999%) supplied by Airgas Inc. (Charlotte, NC) was used to purge the non-condensed gases. Inside the Pyroprobe®, the pressure was equal to that of the Helium (He) cylinder. He-gas swept the pyrolysis vapors from Pyroprobe® to the adsorbent trap, which was kept at 40°C. Adsorption of condensed pyrolysis vapors occurred on the trap. This study does not include the analysis of non-condensable gases. The desorption of condensed pyrolysis vapors was carried out by heating the trap to 300°C and sweeping the vapors with He gas to be analyzed by GC. The samples were placed between about 1 mm packing of quartz wool in an open-ended quartz tube (25 mm long with 1.9 mm i.d.). For co-pyrolysis, lignin and plastics were added and then mixed with a needle. In the case of catalytic pyrolysis, red clay was placed external to the feed, in the mass ratio of 1:1 with the lignin and plastics mixture. About 1 mm length of quartz wool packing was used between the lignin-plastics mixture and red clay. All of the pyrolysis experiments were carried out twice.

The GC system was connected to Polyarc® (Activated Research Company, Minnesota, USA), and the samples were passed through Poyarc® prior to flame ionization detector (FID). The transfer line temperature was kept at 300°C between Pyroprobe® and GC to avoid the condensation of gases. The GC oven used for product analysis was set at 40°C for 4 minutes initially, then heated to 100°C at 10°C min^{-1}, to 235°C at 5°C min^{-1} and then to 280°C at 20°C min^{-1} and maintained steady for 10 minutes. A split-ratio of 10:1 was used. The flow of helium gas that was used for sweeping the products was 3 mL/min. Ionization of compounds was carried out at 70eV electron impact conditions and a mass per charge (m/z) range of 30-550 was used for analysis. The sample stream was divided into two parts and then sent to MS and FID simultaneously. The compounds that appeared in all of the runs and had the highest likelihood measured using with NIST (National Institute of Standards and Technology) MS library and from literature were confirmed and then quantified.

The amount of lignin, LDPE or PS used for each run varied for each trial. However, this amount was noted and incorporated in the subsequent calculations. About 1 mg of sample was used for individual pyrolysis, whereas about 2 mg mixtures of lignin and plastics (1:1 wt/wt) were used for the co-pyrolysis experiments. The variation in the amount of lignin or plastics in each

sample affected the FID area. Hence, the FID area of each compound was normalized for the weight of the sample. The assumption here is that the FID areas linearly change as per the sample weight. This linearity was checked for various compounds. For example, five standards with different concentrations of guaiacol in dichloromethane (DCM) were prepared and a calibration curve was plotted for FID area against the amount of guaiacol injected in GC for each sample. There was a good correlation coefficient (R^2) of 0.998 between FID area and the amount of guaiacol injected in GC when a linear equation (y=mx; y: FID area; x: guaiacol amount; m= 3.55E+10) was used to fit the data. This confirmed that the FID area changes linearly with the amount of guaiacol injected in GC. In the same way, correlation coefficients (R^2) for ethylbenzene (0.963), indane (0.975), creosol (0.973), 1-methylnaphthalene (0.984), indene (0.968), n-dodecane (0.960) was determined. Whenever one of these compounds was present in the fast pyrolysis products, its concentration (g sample^{-1}) was determined using this calibration and it was termed as 'internal standard'. This compound was then used as a reference for calculating amount of other compounds. The concentration (g sample^{-1}) of other compounds was calculated using the 'relative mass response factor' for that compound, as described later in this section, using the concentration of this particular compound (Hoang and Ana, n.d.). The Polyarc® system used in the present study converts all of the compounds into methane before passing it through FID. Hence, the differences arising from different responses of compounds in FID are taken care of. It is also important to note that the FID calibrations were carried out by using a solution of standard compounds in DCM. Whereas, in the fast pyrolysis experiments, GC detects the compounds coming out of Pyroprobe® directly in the vapor form. Hence, the subsequent quantification of compounds based on the former calibration has certain limitations. The equations used for arriving at concentration (g GC-eluted vapors^{-1}) of a compound are given below ("Quantification with the Polyarc ®," n.d.).

Note that the amount of each detected compound (g GC-eluted vapors^{-1}) is directly correlated with the amount of that compound injected in GC from Pyroprobe®. Hence, the unit of concentration g GC-eluted vapors^{-1} can also be taken as g sample^{-1}.

$$Normalized\ FID\ area = \frac{FID\ area * (total\ mass\ of\ initial\ sample)}{(mass\ of\ lignin\ or\ plastic\ in\ the\ initial\ sample)} \qquad \textit{(Equation 2.1)}$$

$$RMRF_A = \frac{MW_A}{MW_S} . \frac{\#C_S}{\#C_A} \quad \textit{(Equation 2.2)}$$

$$C_A = C_S(\frac{Area_A}{Area_S})RMRF_A \qquad \textit{(Equation 2.3)}$$

Where,

C_A: concentration of analyte (g g^{-1} GC-eluted vapors)

C_S: concentration of internal standard (g g^{-1} GC-eluted vapors)

$Area_A$: Integrated FID peak area of analyte

$Area_S$: Integrated FID peak area of internal standard

MW_A: Molecular weight of the analyte

MW_S: Molecular weight of the standard

$\#C_A$: Number of carbon atoms in a molecule of analyte

$\#C_S$: Number of carbon atoms in a molecule of standard

RMRF: Relative mass response factor

MW: Molecular Weight (g mol^{-1})

#C: Number of C-atoms in the molecule

A: Analyte, S: Standard

The carbon content of a detected compound was determined using its molecular formula, as per Equation 2.4. The weight percentage of a compound (g g^{-1} GC-eluted vapors) was determined using Equation 2.3. The carbon yield was calculated by comparing the weight of carbon in each compound by that in the initial feed sample, as per Equation 2.5.

$$C - content\ of\ a\ compound\ detected\ in\ GC = [Carbon\ fraction\ in\ the\ compound] * [weight\ percentage\ of\ compound] \qquad \textit{(Equation 2.4)}$$

$$C - yield\ (wt.\%) = \frac{C-content\ of\ compound\ detected\ in\ GC\ (mg)}{C-content\ of\ feed\ material\ (mg)}\ \textit{(Equation 2.5)}$$

It is important to note that in the case of thermal and catalytic co-pyrolysis, the carbon yields of GC-detected compounds are based on the amount of feedstock, either lignin or plastic,

from which a compound is formed. Also, the total C-yield of GC-detected compounds is the sum of C-yields of only those compound that can be detected using the NIST spectra and literature. Hence, some compounds that showed small FID-peaks, but could not be identified with MS are not listed in the table.

2.3 Results and discussion

2.3.1 Thermogravimetric analysis

From the TGA analysis of samples shown in Figure 2.1(a), it was found that dealkaline lignin has two regions of thermal degradation, at around 80-200°C and 400-600°C; whereas, LDPE and PS both had a common thermal degradation region at around 400-550°C. The temperature range for the thermal degradation of lignin that is mentioned in the literature is 180-670°C (Jin et al., 2016). This is slightly different from what was observed in the current study. Variations in the thermogravimetric data are likely to be due to the specific source of lignin. Similarly, the pyrolysis temperature range reported in the literature for LDPE is 447-493°C and that for PS is 393-441°C (Jin et al., 2016). The difference in the sources of these plastics is likely to be the reason for the slightly different temperature ranges observed in the current study. It can be seen from the DTG curve in Figure 2.1(c) that dealkaline lignin degrades slowly, although its degradation starts earlier as compared to the plastics. Whereas, the two plastics LDPE and PS, degrade quickly at a higher temperature.

The TG and DTG curves for the mixture of lignin and plastics is represented in Figure 2.1(b) and Figure 2.1(d) respectively. It was observed that the mixtures of lignin and both the plastics degrade in roughly the same temperature range, that of 500-600°C and again between 600-900°C. The mixture of lignin with LDPE leaves more residue as compared to that of lignin with PS. The LDPE sample used in this study has a much higher molecular weight (3-6 million Da.) as compared to the PS sample (3,500 Da.). This might be resulting in a higher rate of degradation exhibited by PS as compared to LDPE. From the DTG curve in Figure 2.1(d), the rates of degradation for these mixtures show a peak at a slightly higher temperature as compared to the individual components from Figure 2.1(c). However, all of the mixtures, including the ones with red clay achieved maximum mass loss rates in 400-600°C region. As expected, the mixtures with red clay ended up with a high residue at the end. The presence of red clay slightly decreased the maximum rates at which the mixture of feedstock degraded.

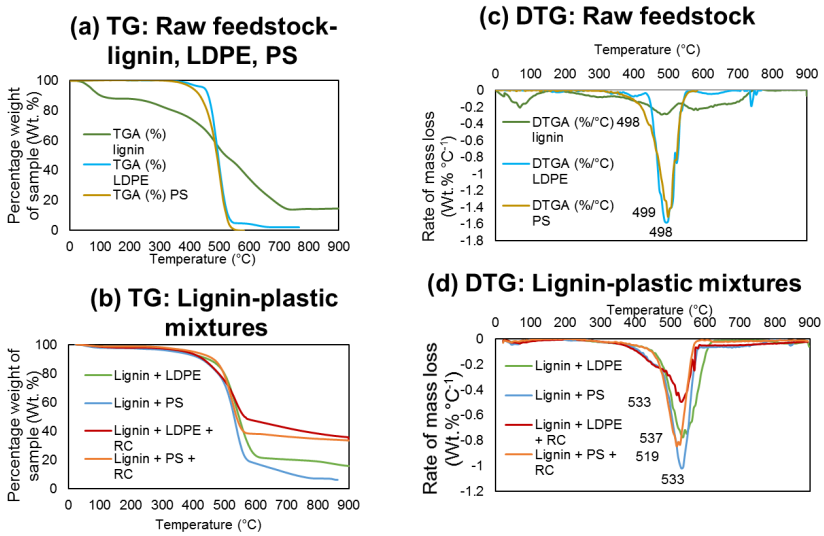

	T_i (°C)	T_{end} (°C)	T_{max} (°C)	DTG_{max} (wt% °C^{-1})
Lignin	283	733	498	-0.27
LDPE	378	558	498	-1.6
PS	343	563	498	-1.5
Lignin + LDPE	278	623	537	-0.8
Lignin + PS	293	778	533	-1.0
Lignin + LDPE + RC	314	883	533	-0.5
Lignin + PS + RC	304	579	519	-0.8

Figure 6. Thermo-gravimetric analysis (TGA) of feedstock in nitrogen atmosphere

Lignin: Plastic = 1 : 1 (weight ratio)
Lignin: Plastic: Catalyst = 1 : 1 : 1 (weight ratio)

Figure 2.1 Thermo-gravimetric analysis (TGA) of feedstock in nitrogen atmosphere

Here, the estimated quantity of residue from TGA results is considered as the amount of char and coke. Zhang et al. determined coke yield during the catalytic conversion of certain biomass-derived organic chemicals using TGA analysis (Zhang et al., 2011). The authors observed that a lower H/C_{eff} of feedstock results in a lower coke yield (Zhang et al., 2011). In a similar fashion, the combined char and coke yield was determined to be around 14.9 wt.% for lignin, 1.96 wt.% for LDPE and around 0.02 wt.% for PS. The mixture of lignin and LDPE left about 15.78 wt.% residue, while that of lignin and PS left about 6.04 wt.% residue. Similarly, lignin and LDPE with red clay left 34.09 wt.% residue, whereas lignin and PS with red clay left 33.54 wt.% residue. Note that these values cannot not be considered exactly equal to the char and coke values for pyrolysis, as the heating rates in the case of TGA studies were much lower.

2.3.2 Elemental composition of raw materials

The proximate and ultimate analyses of the raw materials are given in Table 2.1. No information is available about the isolation method that was used to separate lignin from its source.

However, it can be inferred that high sulfur content seen from the ultimate analysis of lignin is the result of Kraft process used for lignin isolation, which involves the use of Na_2S (Deepa and Dhepe, 2014). The high sulfur in the dealkaline lignin is expected to be converting into non-condensable H_2S gas during the fast-pyrolysis. The ultimate analyses of the commercial samples of LDPE and PS samples show high hydrogen contents and almost no oxygen or moisture.

Table 2.1 Proximate and ultimate analysis of raw materials (values after ± sign indicate the standard deviation)

		Lignin (dealkaline)	Polystyrene (PS)	Low density Polyethylene (LDPE)
Elemental composition on dry ash-free basis (average wt.%)	C	45.7 ± 2.0	91.6 ± 0.0	85.0 ± 0.0
	H	3.4 ± 0.3	8.0 ± 0.0	15.0 ± 0.0
	N	0.2 ± 0.1	0.0 ± 0.0	0.0 ± 0.0
	S	5.3 ± 0.3	0.0 ± 0.0	0.0 ± 0.0
	O (by difference)	45.3 ± 1.8	0.4 ± 0.0	0.0 ± 0.0
(Proximate analysis on as-received basis)	Moisture content (wt.%)	10.9 ± 0.4	0.0 ± 0.0	0.0± 0.0
	Volatile matter (wt.%)	60.5 ± 1.2	100 ± 0.0	100 ± 0.0
	Ash content (wt.%)	13.9 ± 0.2	0.0 ± 0.0	0.0 ± 0.0
	Fixed C (wt.%), by difference	14.7 ± 0.6	0.0 ± 0.0	0.0 ± 0.0

2.3.3 FTIR analysis of lignin

The functional groups present in the dealkaline lignin sample used for this work were studied using FTIR analysis. The aromatic skeletal vibrations, typical of lignin molecules, were observed between 1400-1600 cm^{-1} wavenumber region. Also, a peak was observed at 1700cm^{-1} that represented the stretching of unconjugated ketones, carbonyls and esters. However, this peak was relatively weak as compared to that seen in organosolv lignin. The 'dealkaline' lignin used in this study is likely to be derived from 'alkaline' lignin. The process of alkaline lignin extraction may

be resulting in a smaller extent to which the β-O-4 bonds are cleaved, which could be the reason for the smaller extent of compounds containing carbonyl groups in the lignin structure.

2.3.4 Catalyst characterization

2.3.4.1 XRF/XRD analysis

The XRF spectra for the calcined (500°C, 4 h) red clay samples revealed the presence of elements such as of Mg, Al, Si, Ca, Ti and Fe. The amount of these elements in the calcined red clay catalyst, as determined using ICP-AES analysis was found to be 7.2±0.2 wt.% Al, 3.7±0.1 wt.% Fe, 1.1±0.0 wt.% Ca, 0.3±0.0 wt.% Mg and the majority of the rest being silica, measurement of which was not possible due to certain limitations in the ICP-AES setup. The composition of red clay seen in this study is different from most of the red mud compositions reported in the literature. The reason being that typically 'red mud' is sourced from alumina industry, whereas the natural 'red clay' explored in this study is sourced from a local construction site. Iron and aluminum in red mud have been known for their catalytic properties, whereas calcium and sodium are known to cause sintering of catalysts (Kim et al., 2015). In the present study, all of these four elements are present in the catalyst used and hence are likely to alter the reaction paths during lignin depolymerization.

From the XRD plots of fresh and calcined red clay catalyst, it was seen that some of the mineral groups disappear from catalyst during the heating process. The $Na_5Al_3CSi_3O_{15}$ (2θ=10-15° and 23-25°) and Fe_2O_3 (2θ= ~25°) peaks present in fresh red clay were not seen in the calcined samples. It is likely that these minerals goes to an amorphous or more oxidized state at a high temperature and hence are not detected in the XRD spectrum. Additionally, the catalyst was also calcined at a higher temperature (575°C) for 6 hours and subjected to the XRD analysis to detect any changes in it as an effect of providing additional heat.

2.3.4.2 BET surface area and pore size

The BET surface area of red clay was found to be 28.6 ±0.6 m^2/g. This area is smaller than that reported by Karimi et al. for red mud, which was about 104 m^2/g (Karimi et al., 2014). The average pore size of the red clay was found to be 963.7±43.3 nm and is subsequently categorized as a macroporous catalyst.

2.3.5 Thermal and catalytic co-pyrolysis of lignin with and LDPE and PS

2.3.5.1 Lignin and LDPE

The mass percentages in condensable pyrolysis vapors and carbon yields for the major GC-detected compounds from the fast pyrolysis are reported in Table 2.2. The thermal fast pyrolysis of lignin produced majority of 2-methoxyphenol (0.49±0.09 wt.%C), which comes from the guaiacyl (G) unit in a lignin molecule. The other products derived from the G-unit were creosol (0.10±0.01 wt.%C), 2-methoxy-4-vinylphenol (0.07±0.01 wt.%C) and vanillin (0.11±0.01 wt.%C). Also, phenol, 2,6-dimethoxy, which is derived from the syringyl (S) unit in lignin, was seen in a small amount (0.04±0.00 wt.%C). The total C-yield for G-type condensable pyrolysis products was 0.78 wt.%C. These C-yield values for dealkaline lignin are very small as compared to what was seen in an earlier study on organosolv lignin derived from switchgrass at 500°C, where the total C-yield for G-type and S-type products was 17.9 wt.% and 3.1 wt.% respectively (Mahadevan et al., 2016). The proportion of p-hydroxyphenyl (H), guaiacyl (G) and syringyl (S) groups in the lignin structure can be determined from the pyrolysis products (Lopes et al., 2011). Based on the compound mass yields calculated using standard calibration, a ratio of (H:G:S = 0 : 20.2 : 1) was seen for the dealkaline lignin sample used in this study.

The high amount of error observed in guaiacol amount in fast co-pyrolysis products indicates that the interaction between lignin and LDPE is sensitive to variations in the relative amount of these two feedstocks, resulting in higher standard deviation in the results. Although the calculations took into consideration the exact amount of each of these feedstocks used for the co-pyrolysis experiments, their interaction is complex in nature and results in variable amounts of certain compounds in the products vapors. The sample size used in these experiments was very small and hence using a consistent amount was challenging.

Guaiacol is the only lignin-derived compound seen in the thermal or catalytic co-pyrolysis products. Also, compounds from individual pyrolysis of LDPE, such as cyclopropane, 1-methyl-2-pentyl- (C_9), 1-Decene (C_{10}), 1-Undecene (C_{11}), 1-Tridecene (C_{13}), 1-Tetradecene (C_{14}), 3-Eicosene, (E)- (C_{20}) do not appear in the co-pyrolysis products. It is noted here that the results can also be seen from the perspective of studying the role of waste plastics in mitigating the adverse effect of clay contamination that is found on the biomass samples, including lignin, especially

during its harvesting and transport. Lignin, as such will produce different fast-pyrolysis products when contaminated with clay, as can be seen from the section-c in Table 2.2. However, adding hydrogen-rich plastics to this system will change the reaction path towards selectively producing guaiacol from lignin, rest being products derived from LDPE, as can be seen from section (e) in Table 2. Comparing the C-yields from section (c) with section (e), it can also be observed that the addition of LDPE to lignin contaminated with red clay improves the C-yield of guaiacol.

The co-pyrolysis of biomass components and plastics has been known to differ from that of individual feedstocks (S. Wang et al., 2018). Vasile et al. studied the co-pyrolysis of various plastics with lignin and cellulose and found that the lignin had a smaller tendency to produce saturated compounds at the expense of unsaturated and aromatic compounds, as compared to cellulose (Vasile et al., 2010). This observation for cellulose differs from what was seen during the current study with lignin, where the oxygenated product guaiacol, was formed from lignin at the expense of other aromatic compounds, as seen from Table 2.2(d). The aromatic compounds will require additional energy in the system to carry out demethoxylation of the lignin-derived compound guaiacol. A general observation is that LDPE takes up more of the heat energy very quickly and that results in very less amount of energy available for the further demethoxylation reaction. A similar observation was noted for the catalytic fast pyrolysis of lignin, when red clay was placed *in-line* to the feed. Comparing the results in section (c) with section (a) of Table 2.2, it is seen that C-yield of guaiacol decreased upon using red clay in the system, even though it remained the major product. The amount of guaiacol, either the weight percentage in condensable pyrolysis vapors or the C-yield, changes with the addition of LDPE. This clearly indicates that there is a role of LDPE in influencing the products formation during fast pyrolysis of lignin.

Overall, the fast thermal co-pyrolysis of dealkaline lignin and LDPE led to an increase in the amount of certain lignin- derived compounds, such as guaiacol, as compared to the individual pyrolysis of lignin, from 0.49 wt.%C to 2.57 wt.%C due to an improved heat transfer observed to lignin molecules. Due to the complex interaction of lignin and LDPE, the amount of each compound detected in GC is highly sensitive to the proportion of both the feedstocks in a particular sample. During the co-pyrolysis of lignin and LDPE, the compounds derived from LDPE occupy a larger proportion of C-yield as compared to the ones derived from LDPE. This can be due to the high molecular weight of the LDPE samples used for this study (3-6 milllion Da.). This might have

led to a lower extent to which LDPE is depolymerized to smaller molecules that can be detected by GC.

Table 2.2 Mass percentage and carbon yield of major compounds detected from individual and co-pyrolysis of (a) lignin (b) low density polyethylene, LDPE (c) lignin with red clay (d)lignin and LDPE together (e) lignin and LDPE with red clay (f) polystyrene (PS) (g) Lignin and PS (h) Lignin and PS with red clay

Compound	Wt.% of condensable pyrolysis vapors	S.D.	C yield (wt%)	S.D.
(a) Lignin				
Phenol, 2-methoxy- {Guaiacol} (C7)	60.41	3.64	0.49	0.09
Phenol, 2-methoxy-4-methyl- {Creosol} (C8)	11.17	0.02	0.10	0.01
2-Methoxy-4-vinylphenol (C9)	7.84	0.18	0.07	0.01
Vanillin (C8)	15.49	2.72	0.11	0.01
Phenol, 2,6-dimethoxy (C8)	5.09	1.09	0.04	0.00
		Total	**0.81**	
(b) Low density polyethylene (LDPE)				
1-Octene (C8)	12.63	1.16	0.23	0.11
Cyclopropane, 1-methyl-2-pentyl- (C9)	9.25	0.24	0.17	0.09
1-Decene (C10)	10.63	0.05	0.20	0.11
1-Undecene (C11)	9.84	0.09	0.19	0.11
1-Dodecene (C12)	8.96	0.18	0.17	0.10
1-Tridecene (C13)	8.62	0.56	0.17	0.10
1-Tetradecene	10.94	0.65	0.20	0.11
1-Pentadecene (C15)	9.86	0.39	0.19	0.11

3-Eicosene, (E)- (C20)	9.80	0.70	0.19	0.12
1-Heptadecene (C17)	9.46	0.18	0.18	0.11
		Total	**1.91**	

(c) Lignin with red clay

Phenol, 2-methoxy- {Guaiacol} (C7)	67.37	1.56	0.80	0.08
2-Methoxy-4-vinylphenol (C9)	8.79	0.28	0.11	0.01
Vanillin (C8)	21.23	0.77	0.10	0.10
Benzaldehyde, 3-hydroxy-4-methoxy- (C8)	2.62	2.62	0.03	0.03
		Total	**1.04**	

(d) Lignin and LDPE

Phenol, 2-methoxy- {Guaiacol} (C7)	28.12	19.05	2.57	1.74
1-Heptene (C7)	12.42	0.79	0.18	0.01
1-Dodecene (C12)	10.61	1.59	0.31	0.05
1-Dodecene (C12)	9.65	2.03	0.41	0.09
1-Pentadecene (C15)	11.94	3.79	0.79	0.25
		Total	**4.25**	

(e) Lignin and LDPE with red clay

Phenol, 2-methoxy- {Guaiacol} (C7)	47.31	1.05	3.41	0.60
1-Octene (C8)	11.03	1.03	0.34	0.00
Cyclopropane, 1-methyl-2-pentyl- (C9)	7.63	0.13	0.30	0.03
1-Decene (C10)	6.05	0.19	0.12	0.02
1-Undecene (C11)	13.10	3.22	0.34	0.11
1-Dodecene (C12)	9.31	0.24	0.24	0.02
1-Tridecene (C13)	5.57	0.58	0.14	0.00
		Total	**4.89**	

(f) Polystyrene

Styrene (C8)	94.06	0.41	5.82	0.89

Toluene (C7)	3.46	0.10	0.21	0.03
Benzene, hexyl- (C12)	0.92	0.09	0.00	0.00
Benzene, (1-methylenepentyl)- (C12)	1.56	0.21	0.00	0.00
		Total	**6.03**	

(g) Lignin and PS

Phenol, 2-methoxy- {Guaiacol} (C7)	3.12	0.30	0.19	0.00
Styrene (C8)	70.22	16.91	4.22	0.58
Toluene (C7)	3.54	0.79	0.21	0.03
Benzene, (1-methylenepentyl)- (C12)	1.23	0.24	0.07	0.01
Benzene, hexyl- (C12)	1.26	0.23	0.07	0.01
Ethylbenzene (C8)	1.62	0.54	0.09	0.02
		Total	**4.67**	

(h) Lignin and PS with red clay

Phenol, 2-methoxy- {Guaiacol} (C7)	4.53	2.66	2.16	0.55
Styrene (C8)	86.86	4.03	10.62	1.61
Toluene (C7)	4.27	0.10	0.56	0.08
Ethylbenzene (C8)	2.46	0.31	0.36	0.05
Benzene, hexyl- (C12)	0.80	0.80	0.20	0.03
Benzene, (1-methylenepentyl)- (C12)	1.08	0.18	0.16	0.02
		Total	**14.06**	

2.3.5.2 Lignin and PS

From the co-pyrolysis of lignin and PS, the trend seen for the C-yield of guaiacol was different from that seen for the co-pyrolysis of lignin and LDPE. The C-yield of guaiacol decreased from 0.49±0.09 wt.%C during individual lignin fast pyrolysis to 0.19±0.00 wt.%C during its thermal co-pyrolysis with PS. However, during the catalytic co-pyrolysis of lignin with PS, the C-yield of guaiacol was again increased to 2.16±0.55 wt.%C. Also, the total C-yield of GC-detected compounds increased from 4.67 wt.%C during thermal co-pyrolysis to 14.06 wt.%C upon addition of red clay to the system. This can be a result of a lower amount of compounds converting into the

non-condensable gases or solid residue, when red clay is present in the system. It can be seen from Table 2.2 that either the thermal or catalytic co-pyrolysis of lignin and PS, styrene molecules make up the majority of the C-yield. Based on the TGA results, it was also seen that PS results in very small amount of residue. This can be a result of the ready availability of styrene polymer for pyrolysis reaction and hence a reduced amount of heat energy available for the depolymerization of lignin. This result indicates that co-pyrolysis of PS with lignin during fast pyrolysis at 500°C has considerable limitations due to unequal heat transfer to the two feedstocks.

2.3.5.3 Role of red clay catalyst

The use of red clay catalyst for the co-pyrolysis of lignin with LDPE and lignin with PS was observed to increase the C-yield of lignin-derived guaiacol. To understand the role of red clay in this process, it is also important to take into consideration the reaction set-up and the role played by the particular placement of catalyst in the reactor tube. Karimi et al. found that the oxygen content of bio-oil obtained from pyrolysis of lignocellulosic biomass was reduced from 43.1 wt% to 3.5 wt% after upgrading with the use of red mud catalyst (Karimi et al., 2014). Based on their observations, the *in-line* placement of catalyst in the current study is expected to serve a purpose of upgrading the co-pyrolysis vapors. Red clay has been reported to act through Fe_2O_3 as the major iron species in its role as a catalyst (Djeffal et al., 2014). Yathvan et al. found that red mud could catalyze the fractional catalytic pyrolysis of biomass (Yathavan and Agblevor, 2013). It was reported that the activity of the low-cost catalysts such as red clay is lower compared to the metal-based commercial catalysts (Karimi et al., 2014). However, another considerable role played by the red clay catalyst in this study was apparently in altering the heat absorbed by different feedstock. The dealkaline lignin used in this study may not be undergoing pyrolysis to full extent at 500°C. This can be the reason for a lower C-yield of these compounds. At the same time, the C-yield of guaiacol increases to 2.57±1.74 wt.%C during the thermal co-pyrolysis with LDPE and to 3.41±0.60 wt.%C when red clay is used as a catalyst. The reason for this observation can be that the presence of LDPE or red clay leads to an increased activity of lignin depolymerization in the system. The lignin molecules are likely to have failed to absorb enough heat energy to depolymerize into guaiacol during individual pyrolysis. However, in the presence of red clay, they are likely to spend more time in the quartz tube used for reaction, leading to a slightly higher energy absorption and depolymerization. This can be seen from the slightly higher C-yield of

guaiacol (0.80±0.08 wt.%C) and overall C-yield of GC-detected compounds (1.04 wt.%C) during the fast pyrolysis of lignin with red clay (Table 2-c). The presence of LDPE is likely to have helped in making more hydrogen available to enable the depolymerization of lignin. Additionally, the presence of red clay in the system slows down the rate of heat energy taken up by the LDPE molecules and hence allows the lignin molecules to absorb a slightly higher amount of heat energy. As a result, in the presence of red clay, guaiacol formation increases again to 0.94±0.00 wt.%C. The macroporous structure of red clay probably acts as heat-sink and allows a greater residence time for the lignin and LDPE molecules to absorb the heat and have interactions that result in hydrogen transfer.

The current study used very high heating rates during the reaction (2000ºC s^{-1}). According to literature, it is likely that the feedstocks are not uniformly heated in this type of set-up and the extent of reaction is high only at the interface (Sophonrat et al., 2017). Even though the feed was introduced in the reaction in the form of powder, there might be certain limitations regarding the heat transfer inside bulk of the materials. Since the breaking of lignin to form guaiacol has been known to occur via the Bronsted acid action, this reaction indeed seems to have occurred in thermal and catalytic co-pyrolysis of lignin and LDPE. It is likely that red clay is slightly catalyzing some hydrogen donor activity that is responsible for the Bronsted acid catalyzed reaction of guaiacol formation. Although the source of hydrogen in the catalytic co-pyrolysis reaction is most probably LDPE, it has a considerable amount of hydrogen (~15 wt.%).

The Fe_2O_3 (hematite) phase detected from the XRD spectra of red clay is known to consume a molecule of hydrogen and be converted into Fe_2O_3 (magnetite), released a molecule of water in the process (Yathavan and Agblevor, 2013). From this reaction, it can be inferred that the hydrogen made available in the system by the LDPE molecules was likely consumed by the red clay. Hence, the role of red clay in hydrogenation of lignin to form guaiacol via Bronsted acid catalyzed mechanism is probably very limited. Instead, the changes that occur in heat transfer to the molecules of lignin and plastic, when red clay is introduced in the system, play the major role in determining the primary products of fast pyrolysis. By comparing the results for the co-pyrolysis of lignin with LDPE and PS, we could deduce that polystyrene molecules, owing to the low molecular weight of the samples (~3,350 Da.), depolymerize into styrene molecules very

quickly. However, the same was not observed for LDPE, which has a much higher molecular weight (~3-6 million Da.) and does not readily depolymerize into smaller compounds.

2.3.6 Temperature effect in the thermal co-pyrolysis of lignin and PS

Co-pyrolysis of dealkaline lignin and polystyrene (PS) was carried out at higher temperatures. Temperature has been reported to control the cracking reactions and pyrolysis products yields (Fan et al., 2017). The areas under total ion chromatogram (TIC) obtained using GC-FID can be useful for comparing the amount of the same product under different conditions (Sophonrat et al., 2017). Here, the C-yields are calculated based on FID areas with prior calibration of standard, and are presented in Table 2.3. Statistical analysis of the C-yield values was performed.

Table 2.3 Carbon yields of compounds from the co-pyrolysis of polystyrene and lignin

	C-yield (wt.%)							
	PS+DL_500		**PS+DL_600**		**PS+DL_700**		**PS+DL_800**	
Compound	**Avg**	**S.D.**	**Avg**	**S.D.**	**Avg**	**S.D.**	**Avg**	**S.D.**
Styrene	4.22^{A}	0.58	2.75^{AB}	0.37	2.45^{AB}	0.06	1.57^{B}	0.32
Toluene	0.21^{A}	0.03	0.14^{AB}	0.02	0.13^{AB}	0.01	0.09^{B}	0.02
Ethylbenzene	0.09^{A}	0.02	0.04^{A}	0.01	0.04^{A}	0.00	0.03^{A}	0.01
Phenol, 2-methoxy- {Guaiacol}	0.19^{A}	0.00	0.15^{A}	0.01	0.16^{A}	0.04	0.14^{A}	0.02
Benzene, hexyl-	0.07^{A}	0.01	0.05^{AB}	0.00	0.05^{AB}	0.00	0.03^{B}	0.01
	0.07^{A}	0.01	0.05^{AB}	0.01	0.04^{B}	0.00	0.03^{B}	0.01

Benzene, (1-methylenepentyl)-				
Total	**4.87**	**3.17**	**2.86**	**1.89**

[PS: polystyrene, DL: dealkaline lignin, RC: red clay; Numbers indicated by the same letter in superscript are not significantly different from each other (Tukey's HSD test, α=0.05)]

It can be seen from Table 2.3 that the C-yield of guaiacol statistically does not change when the pyrolysis temperature is increased from 500°C to 800°C. However, the C-yield of styrene, the major product from depolymerization of PS, decreased significantly with the increased temperature. The same trend can be seen for all the other PS-derived compounds, which are toluene, hexyl benzene, and 1-methylpentyl benzene, the C-yield of all of which significantly decreased at higher temperatures. The decrease in C-yield of ethylbenzene, however, was not significant.

The trends observed for increased pyrolysis temperatures for the thermal co-pyrolysis of lignin and PS were different from that observed for the other biomass components. Sophonrat et al. studied the co-pyrolysis of polystyrene and cellulose in a microreactor and found that the yield of light products from both the feedstock increased with higher pyrolysis temperatures (Sophonrat et al., 2017). Previous studies exploring the interaction between biomass components and PS found that the co-pyrolysis was not beneficial due to the high water formation (Kositkanawuth et al., 2017). Lignin has a distinct set of reactions that are more common at higher temperatures. For example, lignin is reported to undergo primary and secondary cracking reactions during its pyrolysis at higher temperatures (Jin et al., 2016). This combined with the early depolymerization of polystyrene in the mixture results in a poor interaction between both the feedstock. The total C-yield of major products decreased from 4.87 wt.% at 500°C to 1.89 wt.% at 800°C. Overall, higher pyrolysis temperatures played a role in altering the interaction of polystyrene with lignin. However, the result was a lower C-yield of compounds detected in the condensable pyrolysis vapors detected by GC. Since there was not a significant change in the guaiacol yield at higher temperatures, we can say that temperature has a limited role in the co-pyrolysis of lignin and PS.

2.3.7 Determination of synergistic effects

Synergistic effects in the co-pyrolysis of biomass components and plastics have previously been reported in the literature (Dorado et al., 2014; Mullen et al., 2016; Ojha and Vinu, 2015; Zhang et al., 2016). To quantify the extent of synergistic effects observed in the formation of certain pyrolysis products, an arbitrary parameter 'S-ratio' is defined here:

$$S - ratio\ for\ a\ compound = \frac{C\text{-}yield\ (wt.\%C)\ in\ co\text{-}pyrolysis}{C\text{-}yield\ (wt.\%C)\ in\ individual\ pyrolysis}$$ *(Equation 2.6)*

S-ratio greater than 1 is attributed to the presence of synergistic effect. The values of this parameter for the thermal and catalytic co-pyrolysis of lignin and LDPE are shown in Table 2.4. Note that S-ratio is calculated for only those compounds that were seen in both individual as well as co-pyrolysis. Looking at the S-ratio based on the C-yields of compounds, a positive synergistic effect can be observed in the formation of 1-dodecene and 1-pentadecene for the thermal co-pyrolysis of lignin and LDPE and for guaiacol, 1-dodecene, 1-dodecene, 1-octene, 1-methyl-2-pentyl cyclopropane, and 1-undecene during the catalytic co-pyrolysis of lignin and LDPE. For the lignin-derived compound guaiacol, S-ratio is much larger than 1 for thermal and catalytic co-pyrolysis, indicating a presence of positive synergistic effect and an increase in the C-yield of the lignin-derived products in thermal co-pyrolysis. Also, using red clay in the system improves the heat transfer to both the feedstock and results in a higher amount of C-yield for guaiacol during the co-pyrolysis, which is seen from the higher S-ratio. In the case of thermal co-pyrolysis of lignin and PS, the lignin-derived compound guaiacol, as well as the PS-derived compounds styrene and toluene do not show positive synergistic effect. However, all of them show positive synergistic effect, indicated by an S-ratio greater than 1, when red clay is used as a catalyst. These observations can be attributed to the complex interactions between lignin and LDPE or lignin and PS, together with the unequal heat transfer to the two feedstock, as discussed in the previous section. Overall, the co-pyrolysis of dealkaline lignin with LDPE or PS resulted in a positive synergistic effect only after the addition of red clay catalyst for most of the major products. Whereas, the lignin-derived compounds were detected to be in a small quantity using GC-MS/FID during thermal co-pyrolysis, owing to the less amount of heat absorption by lignin molecules in the presence of plastics.

Table 2.4 S-ratios for compounds in the thermal and catalytic co-pyrolysis of lignin and LDPE (500°C)

S-ratio (based on C-yields)	Thermal co-pyrolysis	Catalytic co-pyrolysis
Lignin and low density polyethylene (LDPE)		
Phenol, 2-methoxy- {Guaiacol} (C7)	5.20	6.91
1-Decene (C8)	0.00	0.57
1-Dodecene (C12)	1.80	1.37
1-Pentadecene (C15)	4.09	-
1-Octene (C8)	-	1.49
Cyclopropane, 1-methyl-2-pentyl- (C9)	-	1.73
1-Undecene (C11)	-	1.82
1-Tridecene (C13)	-	0.83
Lignin and polystyrene (PS)		
Styrene	0.73	1.83
Toluene	1.00	2.66
Guaiacol (C7)	0.39	4.38

2.4 Conclusion

The carbon yield of lignin-derived compound guaiacol increased during co-pyrolysis of lignin with LDPE and PS when red clay was used as a catalyst. However, the co-pyrolysis with PS did not improve the carbon yield of guaiacol from lignin without red clay. Temperature had a limited role in the thermal co-pyrolysis of lignin with PS. Lignin and plastics were seen to take up an unequal amount of heat energy during co-pyrolysis. This problem was resolved to some extent by using red clay as a catalyst. The waste plastics can be a resource when combined with lignin utilization efforts.

2.5 Acknowledgements

The author would like to express sincere gratitude towards Dr. Jianping Wang for help and guidance during the ICP-AES analysis.

An article based on this chapter has been published and the citation is as follows:

Patil, V., Adhikari, S., Cross, P., 2018. Co-pyrolysis of lignin and plastics using red clay as catalyst in a micro-pyrolyzer. Bioresour. Technol. 270, 311–319.
https://doi.org/10.1016/j.biortech.2018.09.034

2.6 References

1. Anil, H., Cakici, A.I., Yanik, J., UCar, S., Karayildirim, T., 2004. Utilization of red mud as catalyst in conversion of waste oil and waste plastics to fuel. J. Mater. Cycles Waste Manag. 6, 20–26. https://doi.org/10.1007/s10163-003-0101-y
2. Djeffal, L., Abderrahmane, S., Benzina, M., Fourmentin, M., al, et, 2014. Efficient degradation of phenol using natural clay as heterogeneous Fenton-like catalyst. Environ. Sci. Pollut. Res. Int. 21, 3331–3338. https://doi.org/http://dx.doi.org/10.1007/s11356-013-2278-5
3. Dorado, C., Mullen, C.A., Boateng, A.A., 2014. H-ZSM5 catalyzed co-pyrolysis of biomass and plastics. ACS Sustain. Chem. Eng. 2, 301–311. https://doi.org/10.1021/sc400354g
4. Duan, D., Wang, Y., Dai, L., Ruan, R., Zhao, Y., Fan, L., Tayier, M., Liu, Y., 2017. Ex-situ catalytic co-pyrolysis of lignin and polypropylene to upgrade bio-oil quality by microwave heating. Bioresour. Technol. 241, 207–213. https://doi.org/10.1016/j.biortech.2017.04.104
5. Fan, L., Chen, P., Zhang, Y., Liu, S., Liu, Y., Wang, Y., Dai, L., Ruan, R., 2017. Fast microwave-assisted catalytic co-pyrolysis of lignin and low-density polyethylene with HZSM-5 and MgO for improved bio-oil yield and quality. Bioresour. Technol. 225, 199–205. https://doi.org/10.1016/j.biortech.2016.11.072
6. Hoang, C., Ana, S., n.d. Quantification of Monomer Concentration without Calibration and Internal Standard using GC / Pyrolysis and the Polyarc ® Reactor Application Note Pyrolyzer 1–4.
7. Http://www.activatedresearch.com/Public_Documents/Quantification%20with%20the%20Polyarc.pdf, n.d. Quantification with the Polyarc ®.
8. Jin, W., Shen, D., Liu, Q., Xiao, R., 2016. Evaluation of the co-pyrolysis of lignin with plastic polymers by TG-FTIR and Py-GC/MS. Polym. Degrad. Stab. 133, 65–74. https://doi.org/10.1016/j.polymdegradstab.2016.08.001
9. Karimi, E., Teixeira, I.F., Gomez, A., de Resende, E., Gissane, C., Leitch, J., Jollet, V., Aigner, I., Berruti, F., Briens, C., Fransham, P., Hoff, B., Schrier, N., Lago, R.M., Kycia, S.W., Heck, R., Schlaf, M., 2014a. Synergistic co-processing of an acidic hardwood derived pyrolysis bio-oil with alkaline Red Mud bauxite mining waste as a sacrificial upgrading catalyst. Appl. Catal. B Environ. 145, 187–196. https://doi.org/https://doi.org/10.1016/j.apcatb.2013.02.007

10. Karimi, E., Teixeira, I.F., Gomez, A., de Resende, E., Gissane, C., Leitch, J., Jollet, V., Aigner, I., Berruti, F., Briens, C., Fransham, P., Hoff, B., Schrier, N., Lago, R.M., Kycia, S.W., Heck, R., Schlaf, M., 2014b. Synergistic co-processing of an acidic hardwood derived pyrolysis bio-oil with alkaline Red Mud bauxite mining waste as a sacrificial upgrading catalyst. Appl. Catal. B Environ. 145, 187–196. https://doi.org/https://doi.org/10.1016/j.apcatb.2013.02.007
11. Kim, S.C., Nahm, S.W., Park, Y.K., 2015. Property and performance of red mud-based catalysts for the complete oxidation of volatile organic compounds. J. Hazard. Mater. 300, 104–113. https://doi.org/10.1016/j.jhazmat.2015.06.059
12. Kositkanawuth, K., Bhatt, A., Sattler, M., Dennis, B., 2017. Renewable Energy from Waste: Investigation of Co-pyrolysis between Sargassum Macroalgae and Polystyrene. Energy and Fuels 31, 5088–5096. https://doi.org/10.1021/acs.energyfuels.6b03397
13. Lim, X., Sanna, A., Andrésen, J.M., 2014. Influence of red mud impregnation on the pyrolysis of oil palm biomass-EFB. Fuel 119, 259–265. https://doi.org/10.1016/j.fuel.2013.11.057
14. Mullen, C.A., Dorado, C., Boateng, A.A., 2016. Co-pyrolysis of biomass and polyethylene over HZSM-5 : effects of plastic addition on coke formation and catalyst deactivation Biomass Fast Pyrolysis-oil.
15. Nguyen Lyckeskog, H., Mattsson, C., Åmand, L.E., Olausson, L., Andersson, S.I., Vamling, L., Theliander, H., 2016. Storage Stability of Bio-oils Derived from the Catalytic Conversion of Softwood Kraft Lignin in Subcritical Water. Energy and Fuels 30, 3097–3106. https://doi.org/10.1021/acs.energyfuels.6b00087
16. Ojha, D.K., Vinu, R., 2015. Fast co-pyrolysis of cellulose and polypropylene using Py-GC/MS and Py-FT-IR. RSC Adv. 5, 66861–66870. https://doi.org/10.1039/C5RA10820A
17. Rahimi, A., García, J.M., 2017. Chemical recycling of waste plastics for new materials production. Nat. Rev. Chem. 1, 0046. https://doi.org/10.1038/s41570-017-0046
18. Rutten, C., Ramírez, A., Posada Duque, J., 2017. Hydrotreating and hydrothermal treatment of alkaline lignin as technological valorization options for future biorefinery concepts: a review. J. Chem. Technol. Biotechnol. 92, 257–270. https://doi.org/10.1002/jctb.5103
19. Scheirs, J., Kaminsky, W., 2006. Feedstock Recycling and Pyrolysis of Waste Plastics: Converting Waste Plastics into Diesel and Other Fuels, Feedstock Recycling and Pyrolysis of Waste Plastics: Converting Waste Plastics into Diesel and Other Fuels. https://doi.org/10.1002/0470021543
20. Sophonrat, N., Sandström, L., Johansson, A.C., Yang, W., 2017. Co-pyrolysis of Mixed Plastics and Cellulose: An Interaction Study by Py-GC×GC/MS. Energy and Fuels 31, 11078–11090. https://doi.org/10.1021/acs.energyfuels.7b01887
21. Sun, Z., Fridrich, B., De Santi, A., Elangovan, S., Barta, K., 2018. Bright Side of Lignin Depolymerization: Toward New Platform Chemicals. Chem. Rev. 118, 614–678. https://doi.org/10.1021/acs.chemrev.7b00588
22. Sushil, S., Batra, V.S., 2008. Catalytic applications of red mud, an aluminium industry waste: A review. Appl. Catal. B Environ. 81, 64–77. https://doi.org/10.1016/j.apcatb.2007.12.002
23. Vasile, C., Brebu, M., Darie, H., Cazacu, G., 2010. Effect of some environmentally degradable materials on the pyrolysis of plastics II: Influence of cellulose and lignin on the pyrolysis of complex mixtures. J. Mater. Cycles Waste Manag. 12, 147–153. https://doi.org/10.1007/s10163-009-0282-0

24. Wahyudiono, Sasaki, M., Goto, M., 2008. Recovery of phenolic compounds through the decomposition of lignin in near and supercritical water. Chem. Eng. Process. Process Intensif. 47, 1609–1619. https://doi.org/10.1016/j.cep.2007.09.001
25. Wang, S., Lin, X., Li, Z., Yi, W., Bai, X., 2018. Thermal and Kinetic Behaviors of Corn Stover and Polyethylene in Catalytic Co-pyrolysis 13, 4102–4117.
26. Yao, W., Li, J., Feng, Y., Wang, W., Zhang, X., Chen, Q., Komarneni, S., Wang, Y., 2015. Thermally stable phosphorus and nickel modified ZSM-5 zeolites for catalytic co-pyrolysis of biomass and plastics. RSC Adv. 5, 30485–30494. https://doi.org/10.1039/C5RA02947C
27. Yathavan, B.K., Agblevor, F.A., 2013. Catalytic pyrolysis of pinyon-juniper using red mud and HZSM-5. Energy and Fuels 27, 6858–6865. https://doi.org/10.1021/ef401853a
28. Zhang, H., Cheng, Y.-T., Vispute, T.P., Xiao, R., Huber, G.W., 2011a. Catalytic conversion of biomass-derived feedstocks into olefins and aromatics with ZSM-5: the hydrogen to carbon effective ratio. Energy Environ. Sci. 4, 2297. https://doi.org/10.1039/c1ee01230d
29. Zhang, H., Cheng, Y.-T., Vispute, T.P., Xiao, R., Huber, G.W., 2011b. Catalytic conversion of biomass-derived feedstocks into olefins and aromatics with ZSM-5: the hydrogen to carbon effective ratio. Energy Environ. Sci. 4, 2297. https://doi.org/10.1039/c1ee01230d
30. Zhang, H., Nie, J., Xiao, R., Jin, B., Dong, C., Xiao, G., 2014. Catalytic co-pyrolysis of biomass and different plastics (polyethylene, polypropylene, and polystyrene) to improve hydrocarbon yield in a fluidized-bed reactor. Energy and Fuels 28, 1940–1947. https://doi.org/10.1021/ef4019299
31. Zhang, H., Xiao, R., Nie, J., Jin, B., Shao, S., Xiao, G., 2015. Catalytic pyrolysis of black-liquor lignin by co-feeding with different plastics in a fluidized bed reactor. Bioresour. Technol. 192, 68–74. https://doi.org/10.1016/j.biortech.2015.05.040
32. Zhang, X., Lei, H., Chen, S., Wu, J., 2016. Catalytic co-pyrolysis of lignocellulosic biomass with polymers: a critical review. Green Chem. 18, 4145–4169. https://doi.org/10.1039/C6GC00911E
33. Zhou, H., Wu, C., Onwudili, J.A., Meng, A., Zhang, Y., Williams, P.T., 2015. Effect of interactions of PVC and biomass components on the formation of polycyclic aromatic hydrocarbons (PAH) during fast co-pyrolysis. RSC Adv. 5, 11371–11377. https://doi.org/10.1039/C4RA10639C

3. The Role of an *in-situ* Hydrogen Donor Solvent in the Solvent Liquefaction of Lignin

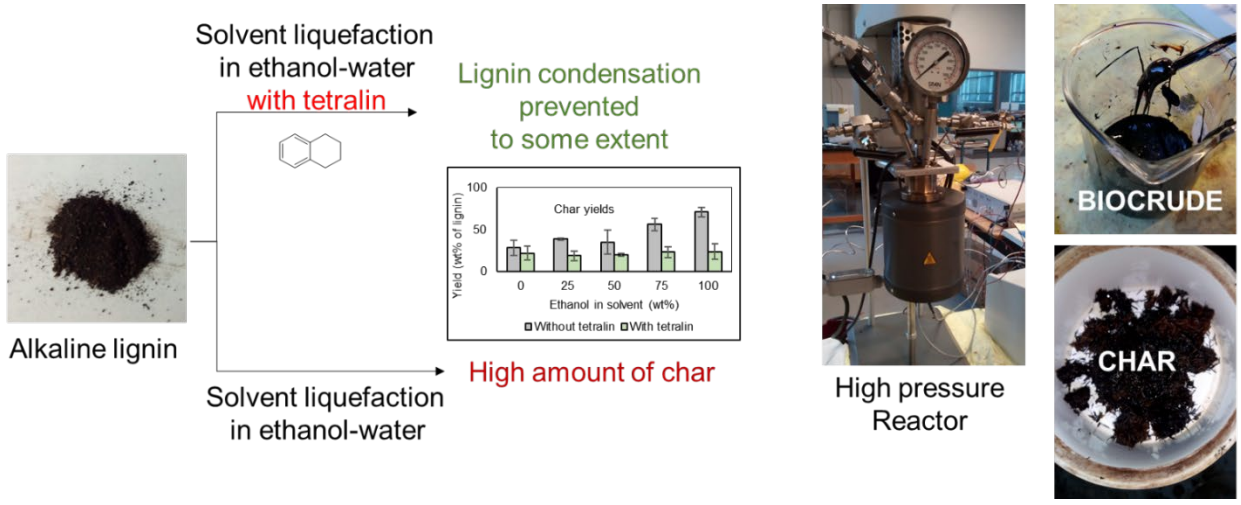

Abstract

The second-generation bioethanol industry produces lignin as a waste stream. Lignin, which constitutes 25-35% of lignocellulosic biomass is the most abundant aromatic biopolymer on earth and an untapped resource. Bio-oil produced from the solvent liquefaction of lignin cannot be used as a fuel directly because of its high viscosity. In addition, hydrothermal liquefaction of lignin results in a high amount of solid bio-char. The objective of the current research is to study the hydrothermal liquefaction of alkaline lignin using organic solvents. Alkaline lignin was chosen for the experiment for its resemblance with the black liquor lignin. The hypothesis is that the use of *in-situ* hydrogen donor decreases solid residue formation and improves the bio-oil yield. Liquefaction experiments for alkaline lignin were performed in a batch reactor at 310 (±10) °C with ethanol-water mixture as solvent. In addition, in another set of experiments, tetralin (1,2,3,4-tetrahydronaphthalene) was added to the reaction mixture as an *in-situ* hydrogen donor. The products were characterized with FTIR, GC-MS, total acid number (TAN), elemental analysis, and water content. The results exhibited that the solvent liquefaction of alkaline lignin in the presence of *in-situ* hydrogen donor made the conditions for maximum yield of phenolic monomers to shift towards a lower ethanol concentration in the solvent. Additionally, char yields were reduced with the use of tetralin for lignin liquefaction.

Keywords: *Alkaline Lignin, Hydrothermal Liquefaction, Hydrogen Donor, Tetralin*

3.1 Introduction

Rapid urbanization and population rise all over the world is putting enormous stress on the availability of raw materials required for industries. The traditional crude-oil based sources of these raw materials can be substituted by lignocellulosic biomass, a renewable resource, which is also a source of 'second-generation' biofuels. Biomass has a higher rate of regeneration than its fossil-based counterparts. Combined with the various strategies for utilization of solid waste streams, one can create a circular economy model of energy and material use with the help of biomass (Patil et al., 2020). With the second-generation bioethanol production industry rising all over the world, the need to diversify the products from this process becomes important for making it economically attractive (Agarwal et al., 2017). These industries use woody crops or agricultural residue as their feed source. The process involves separation of sugars, which mainly comes from cellulose and hemicellulose present in the biomass, which then undergoes fermentation to product ethanol. The leftover biomass has lignin as the major component. Traditionally, it finds application in direct heat and power generation (Xu et al., 2014), owing to its substantial energy content. However, considering the aromatic nature of its building blocks, as well as the potential to produce variety of chemicals, this path leads to under-utilization of lignin. Another major source of lignin is the 'black liquor', which is produced as a waste stream in paper and pulp industry

Due to the unique chemical structure of lignin, it can be best utilized by depolymerizing it to get lower-molecular weight compounds. According to an estimate, out of the 50 million tons of alkaline lignin produced annually by the pulp and paper industry, only 2% is utilized for commercial applications (Laurichesse and Avérous, 2013; Patil et al., 2018). The 'billion-ton initiative' by the United States for lignocellulosic biofuels also indicates generation of around 150-300 million tons of waste containing lignin as major compound, which needs to be diverted into different product streams (Langholtz et al., 2016). Utilizing this waste for manufacturing of materials, instead of only energy is required for financial viability. Lignin contains three structural units, connected to each other by any of the seven typical linkages (Kang et al., 2013; Xu et al., 2014). The three aromatic units are para-coumaryl alcohol, coniferyl alcohol and sinapyl alcohol. The latter two are methoxylated and di-methoxylated derivatives of the former one. The five

bonding patterns are β-O-4 (β-aryl ether), α-O-4 (α-aryl ether), 5-5 (dibenzodioxicine/ biphenyl), β-5 (phenylcoumaran), β- β' (pinoresinol) , 4-O-5 (diphenyl ether) and β-1' (diphenyl methane) (Xu et al., 2014). Researchers have investigated various thermochemical processes such as pyrolysis, gasification, wet oxidation, hydrothermal liquefaction etc. for depolymerization of the complex structure of lignin. Among these, hydrothermal liquefaction (HTL) can take wet feed and can give selective compounds with appropriate reaction conditions. The HTL process used in our study is conventional isothermal HTL process in which a constant temperature is applied to the feedstock for a moderate time (20-60 minutes). As mentioned by Qian et al., fast HTL is when a set-point temperature is reached and maintained for a very small amount of time such as 1 minute (Qian et al., 2017). An organic solvent, ethanol was used in addition to water in our study for dissolution and proper mixing of alkaline lignin in the reaction media. Additionally, tetralin (1,2,3,4-tetrahydronaphthalene) was used as an *in-situ* hydrogen donor to the mixture of solvents.

Fang et al. found that organic solvents dissolve lignin and make a homogeneous phase (Fang et al., 2008). The additional advantages of organic solvents are lower temperature and lower pressure required for subcritical conditions as compared to that of water (Barta et al., 2010). Combined with hydrogen donor, availability of *in-situ* hydrogen decreases oxygen content of bio-oil products (Alemán-Vázquez et al., 2012). Tetralin, the hydrogen donor solvent used in this study has hydrogen in its structure that can be transferred to other molecules during the reaction (Alemán-Vázquez et al., 2012). It is expected that the use of *in-situ* hydrogen donor will prevent the re-polymerization of smaller lignin fragments and reduce the solid residue formation. The broader objective of the current study is to explore novel methods to improve the bio-oil yield from the solvent liquefaction of lignin. The specific objective of this study is to examine the role of hydrogen donor solvent in altering the product yields. It is expected that the use of hydrogen donor solvents will result in prevention of re-polymerization of lignin during its liquefaction. Also, the effect of different compositions of the solvent will also be explored on the product yield and quality.

3.2 Experimental

3.2.1 Materials

Alkaline lignin used in this study (20-29% ignition sulfate residue, calcd. on anh. substance) was purchased from TCI America (Oregon, USA). The molecular weight of this lignin was not provided by the manufacturers. The hydrogen donor solvent 1,2,3,4-tetrahydronaphthalene, also known as 'tetralin', was purchased from Alfa Aesar (Massachusetts, USA). N-hydroxy-5-norbornene-2,3- dicarboximide (NHND), chloroform-D, and 2-chloro-4,4,5,5-tetramethyl-1,3,2-dioxaphospholane (TMDP) were purchased from Millipore-Sigma (Burlington, Massachusetts, USA). Ethanol used was 190 proof, ACS/USP grade, purchased from Pharmaco-Aaper (Belmont, North Carolina, USA). All chemicals were reagent grade. Water used in the experiments was of Ultrapure (Type 1) quality (Synergy Ultrapure Water Systems, EMD Millipore, Burlington, Massachusetts, USA). All the chemicals were used in solvent liquefaction experiments without modification.

The alkaline lignin for this study was used without further purification. The values for other characterization results from the batch of alkaline lignin used, such as the methoxyl group content, pH, ignition residue and water content, were taken from the supplier (TCI Chemicals) website.

3.2.2 Methodology

3.2.2.1 Experimental Setup and Instruments

Hydrothermal liquefaction of alkaline lignin was performed in a Parr ® Reactor having 1 L volume (Model 4567, Parr Instrument, Moline, Illinois, USA). IKA RV-10 rotary evaporator with RV10 and HB10 control was used to separate solvent from product mixture (IKA Works, Inc., Wilmington, North Carolina, USA). A temperature of 40°C and 175 mbar vacuum was used for the separation of ethanol. The weighing balances used for measurement of raw material and products were Mettler Toledo XS205 Dual Range weighing balance (Resolution: 0.01 mg), Adventurer AR 3130 by OHAUS corporation USA (Resolution: 1 mg) and Mettler Toledo AB 204-S / FACT (Resolution: 0.1 mg).

3.2.2.2 Solvent liquefaction

Alkaline lignin was mixed with ethanol-water mixture in the ratio 1:10 (w/w) in a glass beaker. Tetralin was added to this mixture in the equal quantity of alkaline lignin (1:1 wt/wt ratio). The mixture was poured slowly into the reactor and it was tightened with bolts. Pressure test was performed with 3 MPa nitrogen. The reactor with its mixture was pressurized and depressurized with 2 MPa nitrogen with continuously stirring at 300 rpm, to purge the air from the system. The stirring at the purging stage ensured that the gas is penetrating inside the liquid and hence removing all the gases that might be present in mixture. It was pressurized again at 2 MPa nitrogen before starting the reaction. The reaction was performed at 310 (±10) °C in the inert atmosphere of nitrogen with stirring at 300 rpm. The reaction time was kept short at 20 minutes, considering most of the alkaline lignin depolymerization occurred in this time span (Kozliak et al., 2016). Shorter reaction time is also supposed to avoid any further re-condensation of products. After 20 minutes, the heating was stopped, and water was circulated through pipes inside the reaction mixture for indirect removal of heat. The reaction products are known to undergo re-condensation reaction very quickly. Hence, to avoid further reactions of the mixture, the reactor was immersed in an ice bath for increasing the rate of heat removal.

In another set of experiments, tetralin was eliminated from the ingredients and reaction was performed with 1:8 ratio of alkaline lignin: ethanol/water mixture, at 310 (±10) °C for 20 minutes. In addition to both experiments, liquefaction of alkaline lignin a 50-50 wt.% ethanol-water mixture was performed six times to observe the variation in elemental composition of bio-oil and biochar with the same reaction conditions. The values of bio-oil are reported after adjusting the amount of water present in it.

3.2.2.3 Separation of products

The product of the solvent liquefaction of alkaline lignin is a viscous mixture of bio-oil, biochar, aqueous phase, and gases. Dichloromethane was used as a solvent to clean the reactor and take out the product from reactor. This product mixture was filtered using Whatman filter paper number 4 (pore size 20-25 μm). The solid residue was dried at 80°C in a 'Single Wall Transite Oven' purchased from Blue M Electric Company (White Deer, Pennsylvania, USA).

The solvent DCM was separated in a rotary evaporator at 40°C and atmospheric pressure. The unreacted solvent ethanol in the product mixture was also separated in rotary evaporator at 40°C and 175-mbar vacuum. The temperature of rotary evaporator was increased from 40°C to 65°C to improve the heat transfer and subsequent solvent removal. In that process, some water also evaporated with ethanol. This phenomenon is difficult to avoid and affects the mass balance. Aqueous phase in the bio-oil product was separated by decantation. Due to the presence of impurities in the initial alkaline lignin, some of which act as surfactants, the water was not completely separated from the bio-oil.

In the experiments where tetralin was used as an additional hydrogen donor, it was difficult to separate tetralin from the product mixture with distillation because of its high boiling point (207°C), which exceeded that of many of the compounds in bio-oil. Hence, the unreacted tetralin was still present in the product mixture. In another set of experiments, tetralin alone (without alkaline lignin) was mixed with the five compositions of ethanol-water and subjected to the solvent liquefaction conditions. Compounds formed from this reaction were considered as the base case for the mixture of three solvents for the given reaction conditions. Accordingly, the mass balance was adjusted by considering the formation of various compounds from the solvent degradation.

3.2.3 Characterization of reactants and products

3.2.3.1 Proximate analysis

The volatile matter and ash content of lignin was measured using ASTM E 872 and ASTM E 1755 standards, respectively. The ash content of alkaline lignin was measured using Thermolyne muffle furnace (Thermo Fisher Scientific, Massachusetts, USA) with the procedure given by NREL (Sluiter et al., 2008). Briefly, the samples were subjected to a temperature of 105ºC for 24 hours for moisture content measurement. Thereafter, the dried samples were heated at 950ºC for 7 minutes for volatile combustible matter (VCM) measurement. The ash content was measured by subjecting the residual solids from the VCM measurement to 575ºC for 4 h. The amount fixed carbon was estimated by subtracting the above contents from total dry weight of initial lignin.

3.2.3.2 ^{31}P NMR spectroscopy

The ^{31}P NMR characterization of lignin and a few bio-oil samples was performed using the method described in the literature (Meng et al., 2019). Briefly, a stock solution was prepared by

mixing deuterated chloroform ($CDCl_3$) and pyridine in a 1: 1.6 (v/v) ratio. About 40 mg of N-hydroxy-5-norbornene-2,3- dicarboximide (NHND) and about 40 mg of Cr(III) acetylacetonate were added to this mixture as internal standard and relaxation agent, respectively. About 20-25 mg of lignin was added to ~1 mL of this mixture and vortexed for 2 minutes. Thereafter, ~100 mg of a phosphitylating agent (2-chloro-4,4,5,5-tetramethyl-1,3,2-dioxaphospholane, or TMDP) was added to the solution and again vortexed for 2 minutes. The solution was filtered using a 0.45 µm nylon syringe filter and was added to an NMR tube up to the 5.5 cm height. The spectra was recorded using Bruker Avance 500MHz spectrometer (Bruker BioSpin Corporation, Billerica, Massachusetts, USA) with 64 scans, 350 ppm spectral width and 0.40 s acquisition time. The analysis was performed using Bruker TopSpin 4.0.6 software.

3.2.3.3 ^{1}H-^{13}C 2D-HSQC NMR spectroscopy

Lignin was characterized using ^{1}H-^{13}C 2D Heteronuclear Single Quantum Coherence-Nuclear Magnetic Resonance (HSQC-NMR) spectroscopy to understand its chemical structure as per the literature protocol (Talebi Amiri et al., 2019). About 20-25 mg of lignin was dissolved in ~1 mL of deuterated dimethyl sulfoxide (DMSO-d_6). The mixture was vortexed for 2 minutes and filtered using 0.45 µm nylon syringe filter before adding to the NMR tube. The spectrum was recorded using a Bruker Avance 500 MHz spectrometer having a z-gradient triple resonance 'Cryo-probe' (Bruker BioSpin Corporation, Billerica, Massachusetts, USA). Also, Bruker standard pulse sequence 'hsqcetgp' was used during the experiment. The acquisition was performed at 298.1 K for 10.49 minutes using 16 scans for ^{1}H, 32 scans for ^{13}C, additional 2 scans for HSQC, and 16 dummy scans ensuring steady state of the equipment. The analysis was performed using Bruker TopSpin 4.0.6 software.

To increase the solubility of samples in deuterated solvents, acetylation of lignin was performed (Gan and Pan, 2019; Sameni et al., 2017). Briefly, lignin (~100 mg) was dissolved in an equal-volume mixture (~4 mL) of pyridine and acetic anhydride and vortexed for 2 minutes. The mixture was then kept under dark at room temperature with mixing for 24 h. After the reaction, lignin was precipitated by adding this solution dropwise to ~120 mL of ice-cold water containing ~1 mL of concentrated hydrochloric acid. The precipitated lignin was washed with deionized water and dried at 50°C for 48 hours before the NMR characterization.

3.2.3.4 GC-MS

Bio-oil was characterized using GC-MS to know its chemical composition. The GCMS characterization of samples was performed using Agilent 7890A GC/5975C MS equipped with a DB-1701 column having dimensions of 30 m x 0.25 mm i.d. x 0.25 mm film thickness (Agilent Technologies, Santa Clara, California, USA). The oven was heated at 50°C for 2 minutes. Then the temperature was increased to 250°C at a rate of 5°C/minute. It was held there for 10 minutes. The helium flow was kept at 1.76 mL/minute. A 1 µL injection with the splitless mode was used. The compounds were analyzed with comparison of their mass spectra with those of pure compounds using NIST 05 library database, and also by their retention times and literature. Naphthalene, 1-methyl present in the product was used as an internal standard, and its yield was calculated using a standard calibration curve. The yield of other phenolic monomers was estimated using the effective carbon number method as follows (Shuai et al., 2016; Szulejko et al., 2013):

$$C_{monomer} = \frac{A_{monomer}}{A_{std}} x \frac{C_{std}}{MW_{std}} x \frac{ECN_{std}}{ECN_{monomer}} x\, MW_{monomer} \quad \textit{(Equation 3.1)}$$

Where,

$C_{monomer}$: Monomer concentration

$A_{monomer}$: Area under the curve for a monomer in a GC-MS spectrum

A_{std}: Area under the curve for a standard compound in a GC-MS spectrum

C_{std}: Concentration of standard, estimated using a calibration curve

MW_{std}: Molecular weight of the standard

ECN_{std}: The effective carbon number of the standard

$ECN_{monomer}$: The effective carbon number of a monomer

$MW_{monomer}$: Molecular weight of the monomer

The yield of a compound was calculated in the following way:

$$Y_{monomer} = \frac{C_{monomer}\, x\, W_{product\ mixture}}{W_{lignin}} \quad \textit{(Equation 3.2)}$$

$\Sigma Y_{monomer}$: Sum of mass yields of all monomers, based on dry lignin

$S_{monomer} = \frac{Y_{monomer}}{\Sigma Y_{monomer}} x100$ *(Equation 3.3)*

Where,

$S_{monomer}$: Selectivity of a monomer

$\Sigma Y_{monomer}$: Sum of mass yields of all monomers, based on the weight of bio oil

3.2.3.5 FTIR spectroscopy

Lignin and biochar were characterized using FTIR spectroscopy to know the major functional groups in them. Thermo Nicolet iS10 was used for FTIR analysis of alkaline lignin and products (Thermo Scientific, Waltham, MA). The analysis used 34 scans of the samples over a range of 400-4000 cm^{-1}.

3.2.3.6 Elemental Analysis

Elemental analysis of lignin, bio-oil and biochar was performed with 'Vario MICRO cube' elemental analysis system (Elementar Americas Inc., New York, USA). Sulfanilamide was used as a standard to calculate daily factor values and 2 mg of samples were used for the characterization.

3.2.3.7 Total organic carbon (TOC) measurement

Total organic carbon (TOC) measurement of the aqueous phase was performed to know the carbon lost to this phase. The TOC of aqueous phase was measured by diluting the samples 1000-times with DIW using a TOC-L analyzer (Shimadzu Corp., Japan).

3.2.3.8 Titration

Total Acid Number (TAN) measurement of bio-oil was performed using titration to know the acidity of bio-oil. The TAN of bio-oil was measured with 'Mettler Toledo T50 Titrator' (Mettler Toledo, Columbus, Ohio, USA). ASTM D664 method was followed for this purpose. The calibration was done initially with a solution of potassium hydrogen phthalate (KHP) (80 mg of KHP in 60 mL de-ionized water (DIW)) (Crystal baker analyzed ACS reagent, purchased from Avantor Performance Materials Inc.). The mixture was titrated with a blank solvent (ASTM D664)

as well as buffer solutions of pH 4 and 11. About 0.1 g bio-oil sample was mixed with 50 mL of blank solution for TAN measurement.

Bio-oil was characterized for its water content using Karl-Fischer titration using 'V20 Volumetric KF Titrator' (Mettler Toledo, Columbus, Ohio, USA). Any organic phase that might be present in aqueous phase samples was removed prior to this using centrifugation.

3.3 Results and discussion

3.3.1 Proximate analysis

The ash content of lignin, as provided by the supplier was 2%, which was found to be 19.5 wt% when measured in the lab. The moisture content of the lignin was 5.5%, as provided by the supplier, which was measured to be 8.4 wt% in the lab. Additionally, other properties of lignin, as provided by the supplier were 11.9% methoxyl group, pH of 9.0, and ignition residue (sulfate) of 23.6%. Also, the fixed carbon in the lignin was determined to be 31.3 wt% on dry, ash-free basis and the volatile matter was determined to be 49.2 wt% on dry basis using proximate analysis. The fixed carbon content of alkaline lignin used here was higher than what is generally seen for other types of lignins, such as organosolv lignin. This lignin also had a relatively higher amount of ash, which can be a result of the specific pretreatment used to isolate lignin from biomass.

3.3.2 NMR

3.3.2.1 ^{31}P NMR spectroscopy

The ^{31}P NMR spectrum of lignin is shown in Figure 3.1. The alkaline lignin used in this study had majority of phenolic hydroxyl groups (2.2 mmol g^{-1}) in its total hydroxyl concentration (4.0 mmol g^{-1}). The hydroxyl content of alkaline lignin was lower than that for organosolv lignin, but comparable to the biorefinery lignin (Yang et al., 2014).

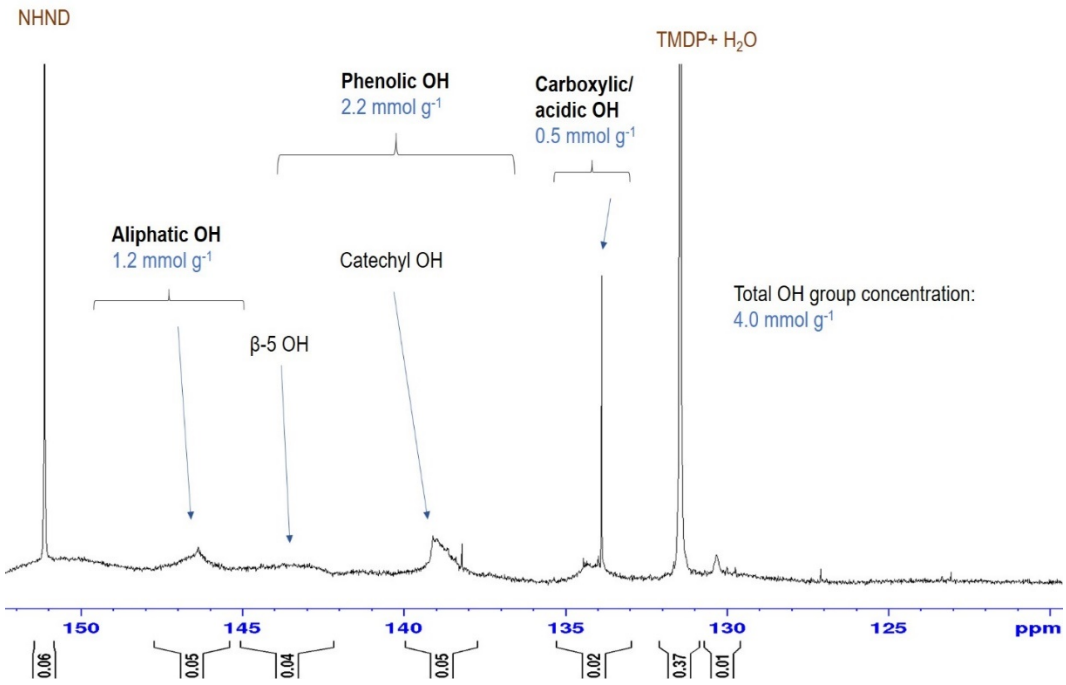

Figure 3.1 ^{31}P NMR spectrum of alkaline lignin

Additionally, the ^{31}P NMR characterization of bio-oil (not shown in the figure) made with only water as a solvent revealed that the addition of tetralin to the solvent medium caused an increase in hydroxyl concentration from 3.5 mmol g^{-1} to 4.5 mmol g^{-1}. This can be a result of the hydrogen provided by tetralin temporarily capping the reactive fragments from lignin and preventing them from recondensation. Subsequently, these fragments might have retained the hydroxyl groups present in them, which could have led to an increased hydroxyl group concentration. Also, with water as a solvent, and without adding tetralin to the liquefaction medium, the hydroxyl group concentration of the bio-oil decreased a bit compared to that in lignin. This can be a result of self-condensation of lignin during bio-oil formation, which was higher without the presence of a hydrogen donor solvent. Overall, the cleavage of ether linkages in lignin causes $C_{aromatic}$-O-R groups to be converted into $C_{aromatic}$-O-H groups (Pu et al., 2019). Therefore, the decrease in hydroxyl groups in absence of tetralin suggests higher condensation of lignin.

3.3.2.2 ^{1}H-^{13}C 2D-HSQC NMR spectroscopy

The ^{1}H-^{13}C 2D-HSQC NMR spectrum of alkaline lignin (Figure 3.2) revealed the structural features, including its constituent units and the linkages. The lignin used in this study had majority of guaiacyl (G)-type units, connected to each other mainly with β-O-4 and β-β linkages. From the volume integration of regions in the spectrum, it could be estimated that the relative abundance of β-O-4 and β-β linkages in the lignin was 95% and 5% respectively. Overall, it can be inferred from the weak spectral regions that the alkaline conditions used to isolate lignin were harsh and hence the lignin structure being relatively condensed.

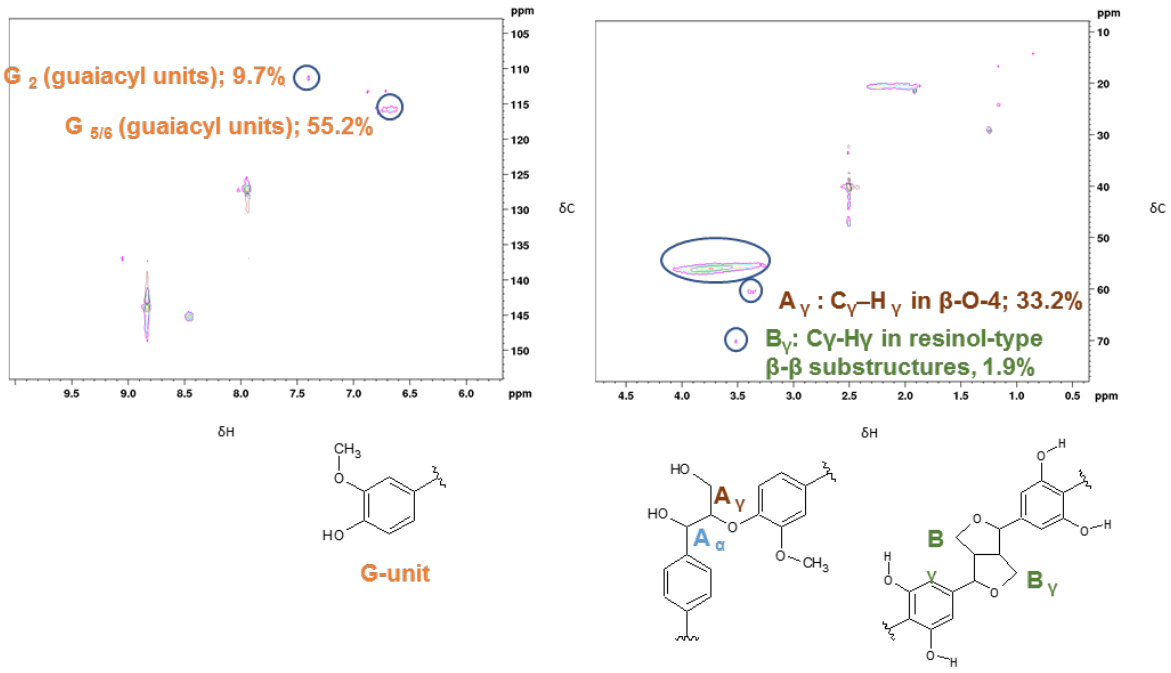

Figure 3.2 ^{1}H-^{13}C 2D HSQC NMR spectrum of alkaline lignin

3.3.3 GC-MS

The compounds seen from the gas chromatography-mass spectrometry (GC-MS) of bio-oil made with solvent liquefaction of lignin of are shown in Figure 3.3. For the analysis of bio-oil, its qualitative assessment is primarily considered in this article, as it gives a better idea of the formation of desired products, rather than its quantitative assessment. In the case of liquefaction with the use of tetralin, with a higher ethanol to water ratio, higher chromatogram area of total aromatic compounds was seen, which is shown as the last bar in black color in each case. However,

when the hydrogen donor solvent tetralin was used, the higher ethanol to water ratio did not result in the highest fraction of total aromatics. At the same time, the GC-MS area itself had increased in this case (not shown in the figure), which indicated an increase in the amount of the aromatic compounds, as the parameters for gas chromatography analysis remained the same. It also suggested that tetralin enhanced the depolymerization leading to aromatics formation already initiated by the ethanol-water solvent mixture.

The observations suggested that when tetralin was used, the ethanol-water ratio no longer remained the determining factor for the fraction of total aromatics in bio-oil. Since the aromatics represent monomeric compounds, most of which were deoxygenated, their proportion and selectivity compared to other type of compounds in bio-oil was also indicative of the depolymerization and deoxygenation reaction. Note that analysis based on each compound was not possible, as the number of compounds detected in GCMS was in several hundreds, and in some cases more than 500. Based on the observation from product characterizations, it can be proposed that tetralin provided its hydrogen to the depolymerized lignin fragments, stabilizing them, and making them available for further deoxygenation. Hence, the condensation of these compounds into solid biochar was slowed down. At the same time, tetralin was also seen to get other substitutions in its structure.

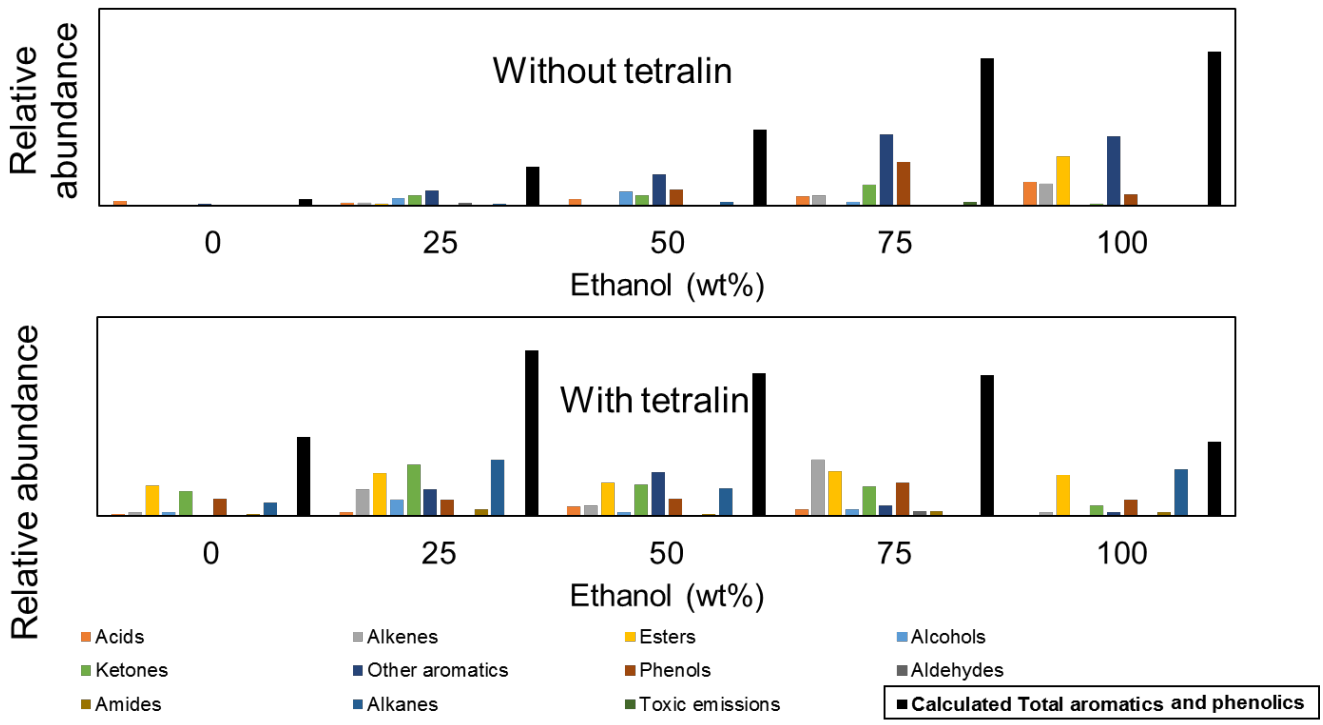

Figure 3.3 Compounds in bio-oil made with the solvent liquefaction of alkaline lignin with and without using tetralin as *in-situ* hydrogen donor, detected using GCMS [note that both plots differ in their scale and only the comparative data is presented]

Overall, the major compounds in the bio-oil recovered were mostly phenolics, aromatics and substituted benzene-compounds (Figure 3.4). Alkoxy phenols were the major compounds in the category of phenolics. Total 56.7 wt% of bio-oil made from lignin with ethanol as a solvent in the presence of tetralin was identified to be comprised of various phenolic monomers. The tetralin-derived products were also present in the product in residual amounts, but their yields were subtracted while calculating the selectivity of desired phenolic monomers. The major compounds seen in bio-oil and their selectivity based on their mass percentage in bio-oil were methanone, (5-hydroxy-3-benzofuryl)(2,5-dimethoxyphenyl)- (11.1 wt%), propenoic acid, 3-[4-methoxy-3-(4-methylphenoxy)phenyl]-, ethyl ester (5.1 wt%), phenol, 2,2'-methylenebis[6-(1,1-dimethylethyl)-4-ethyl- (4.8 wt%) and phenol (4.0 wt%). The presence of many oligomeric products could be a results of their saturation due to the presence of hydrogen radicals, which hinders their further cleavage (Schuler et al., 2019). The dimeric phenolic compounds are considered to have better

antioxidant properties compared to monomeric phenolic compounds, and hence are valuable for lignin valorization (Kang et al., 2013). There were many more compounds in the bio-oil other than those mentioned here. Previously, homovanillic acid was reported to be the major compound from lignin in presence of hydrogen donor solvent (Lee et al., 2016). As a common observation from all the experiments performed with solvent liquefaction of alkaline lignin, the number of compounds and their distribution varied slightly from trial to trial. Yet, there are few compounds that were present in bio-oil from all the trials. However, there are limitations in the detection of compounds using GCMS, as not all the compounds in bio-oil are eluted in the GC. Hence, there is a well-acknowledged possibility that the compounds with higher molecular weight are also generated in the reaction, which need other methods for their detection. This is mentioned later in the future work section of this article.

Ouyang et al. performed ethanol enhanced liquefaction of alkaline lignin using formic acid instead of tetralin, as *in-situ* hydrogen donor (Ouyang et al., 2015). The major compounds mentioned by them, as components of 'bio-oil' were different from the one observed in this study. Ouyang et al. reported vanillin, 4-((1E)-3-hydroxy-1-propenyl)-2-methoxyphenol, phenol, 2,6-dimethoxy, syringaldehyde, acetylsyringone, syringic acid, benzoic acid, 4- hydroxyl-, 3-hydroxy-4-methoxycinnamic acid as the major compounds (Ouyang et al., 2015). Unlike the distribution mentioned by Ouyang et al., where only a few compounds were in majority, no single major compound was observed in the present study. The maximum peak area for a compound was not found to be more than 6-7% of total chromatogram area. The residence time of majority of GC-eluted compounds in this study was ranging from 14 to 24 minutes, whereas in the case of Ouyang et al., majority of compounds eluted from 8 to 19 minutes (Ouyang et al., 2015). The average molecular weight of GC-eluted compounds detected in this study was 189 g mol^{-1}. This was comparable to the compounds detected by Ouyang et al., whose molecular weight ranges from 94 to 210 (Ouyang et al., 2015). As per the analysis by Ouyang et al., ethanol plays a greater role in avoiding repolymerization of bio-oil (Ouyang et al., 2015). However, the current study presents a more complex role of ethanol on the chemical composition of bio-oil.

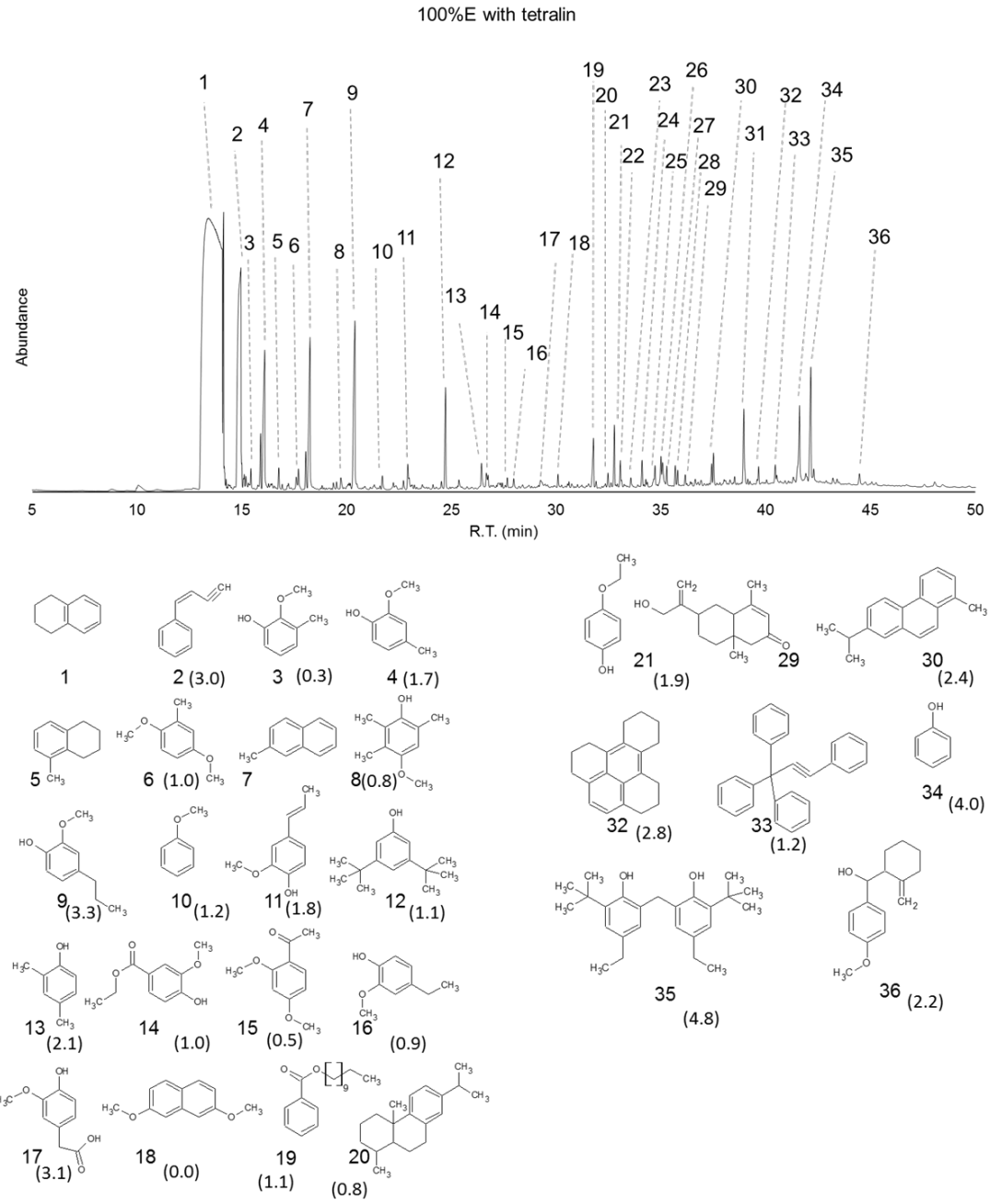

Figure 3.4 Compounds seen in the bio-oil made from liquefaction of alkaline lignin in ethanol as a solvent in presence of tetralin (300°C, 20 min, 100 psi N_2) [compounds where selectivity is not given in parentheses are the tetralin-derived residual compounds in bio-oil, which have been excluded from total yield calculation]

3.3.4 FTIR

Lignin isolation from biomass is known to result is alteration in the structure of lignin to varying degrees. This happens mostly during pulping of wood, and the result is often a condensed structure of lignin. Hence, it was necessary to study the functional groups present in alkaline lignin. From the FTIR spectrum of alkaline lignin shown in Figure 3.5, it can be seen that there are distinct peaks around the region of wavenumber 1400 to 1600 cm^{-1}. This represents aromatic skeletal vibrations, a common characteristic seen in the FTIR spectra of lignin. However, for this sample of alkaline lignin, a peculiarity was observed in the smaller size of the peak around wavenumber of 1700 cm^{-1}. This peak represents a C=O bond, which be carbonyl, aldehyde or ester groups. This peak was relatively smaller compared to the spectra for lignin reported elsewhere. This was maybe because, during the alkaline process used by the supplier, β-O-4 bond cleavage in lignin might have also occurred to some extent.

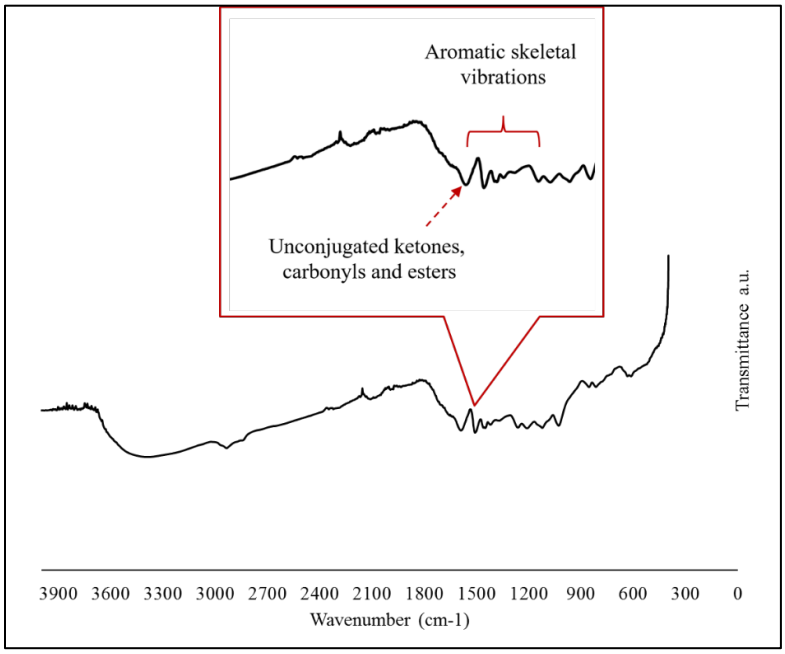

Figure 3.5 FTIR analysis of alkaline lignin

Figure 3.6 shows the FTIR spectra of bio-oil made with the solvent liquefaction of lignin without using tetralin in the system. As the ethanol in the solvent increased, the Sp^3 C-H spectra became stronger. Additionally, the spectrum for O-H group of alcohols went from very weak to

moderate. With a higher ethanol in the solvent, O-H for acids became weak and C-O bond spectrum went from very weak to moderate. This suggests that the total amount of acidic compounds formed went down with a higher ethanol content in the solvent. This is in conformity with the results from Total Acid Number (TAN) and pH measurement for bio-oil, as discussed in previous sections. Increased amounts of esters in the bio-oil was also observed with a higher ethanol content in the solvent.

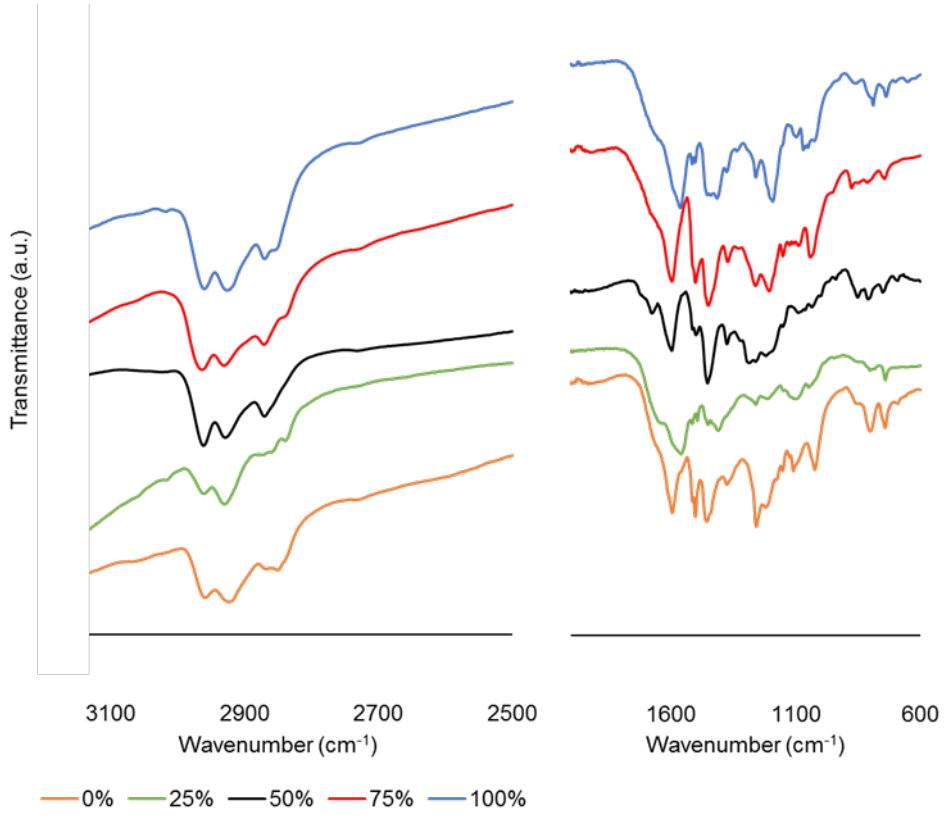

Figure 3.6 FTIR spectra of bio-oil made using solvent liquefaction of lignin in ethanol-water without tetralin

3.3.5 Elemental analysis

The alkaline lignin used in this study was found to contain 55.6 wt% C, 5.4 wt% H, 0.1 wt% N, 3.9 wt% S, and 35.0 wt% O on dry basis. Comparison of the elemental composition with that reported by other researchers shows that there was certain variation in the amounts of individual elements. For example, wheat straw alkali lignin was reported to have a comparable

amount of carbon on dry basis (56.5%), but a much smaller amount of sulfur (0.4%) (Ouyang et al., 2015). Most of the sulfur from alkaline lignin in this study is likely to have ended up in the biochar or would have been lost in the gaseous products. The lignin obtained from alkaline liquor and precipitated with sulfuric acid had 31.5 wt% C, 4.4 wt% H, 0.1 wt% N, and 3.7 wt% S on dry basis (Ház et al., 2019). Since the biomass sources of lignin are not mentioned by the suppliers, it was not possible to assess what could have led to the relatively higher carbon or sulfur content of the lignin used in the present study.

Elemental analysis of bio-oil obtained with the solvent liquefaction of alkaline lignin in ethanol- water mixture when tetralin was added to the system, is presented in Figure 3.7. The cases with 100% ethanol or 100% water have previously been reported to lead to an entirely different type of reaction leading to bio-oil, and hence are not compared in this table (Lee et al., 2016). Here, the purpose of elemental analysis is to see the trend of carbon content of bio-oil samples and predict the extent to which repolymerization of fragmented lignin molecules must be taking place during the reaction. It can be seen that except for the amount of carbon, the mass fraction of other elements is not changing as distinctly with the change in the solvent composition. From the figure, it is seen that overall, the carbon and hydrogen content of bio-oil is highest with 50% ethanol in the solvent without tetralin. Also, the elemental O/C of bio-oil was about 0.26 with 50% ethanol in solvent, which was lower than that reported previously with the use of hydrogen donor solvent for lignin liquefaction (Pu et al., 2019). This indicates that in the present study, the condensation of phenolic moieties was prevented to a great extent. The variation in elemental composition has also been higher from previous results in the literature (Pu et al., 2019). It was still higher for 25%E and 75%E in the present study, around 0.50-0.57, suggesting higher condensation under these conditions. There is considerable amount of sulfur detected in bio-oil if tetralin is not used in the system, as seen in Figure 3.7. Hence, there must be a substantial sulfur removal strategy if this bio-oil must be upgraded to be used as a fuel, in contrast to what was observed when tetralin was present in the system. In the present study, sulfur is also likely getting released in the form of gas (H_2S).

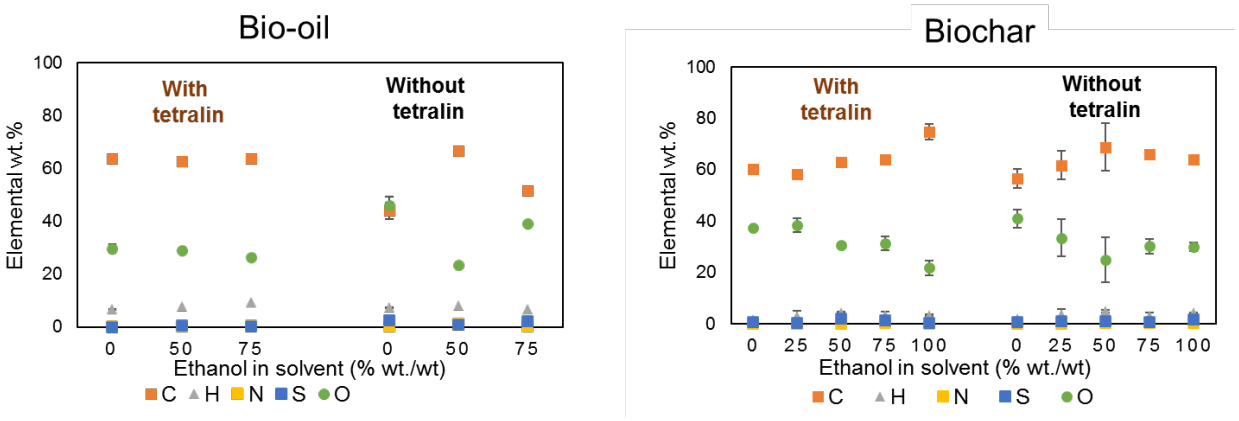

Figure 3.7 Elemental composition of bio-oil and biochar made from lignin liquefaction in ethanol-water

Also, the values of calorific values for a set of six biochar samples and six bio-oil samples, made with the same solvent composition (50%E, without tetralin) and with the same reaction conditions is shown in Table 3.1 to emphasize the challenges with reproducibility of the experiments in the present study. Note that these trials are not considered for the results elsewhere in this study.

Table 3.1 Elemental composition of biochar and bio-oil produced from solvent liquefaction of alkaline lignin in ethanol-water mixture (50-50 wt%) without tetralin

	Average wt. %*					**C.V. (MJ/kg, predicted using Dulong's formula)**
	N	**C**	**H**	**S**	**O**	
Biochar	0.4	75.2	5.4	1.2	17.8	30.7
	0.3	82.7	5.7	0.7	10.6	34.7
	1.4	66.6	5.1	1.6	25.4	25.5
	0.3	72.9	5.0	<0.1	21.8	27.9
	0.2	79.2	5.1	<0.1	15.5	31.4
	1.3	65.2	4.5	0.7	28.3	23.6
Average	0.6 ± 0.5	73.6 ± 6.3	5.2 ± 0.4	0.7 ± 0.6	19.9 ± 6.0	**29.9** ± 3.0

Bio-oil	1.6	72.2	9.2	1.7	15.3	35.0
	1.1	63.1	7.3	1.0	27.6	26.9
	2.5	76.3	8.5	1.3	11.4	36.2
	1.5	76.8	8.5	0.2	13.0	35.9
	1.5	73.3	9.2	0.6	15.3	35.4
	1.2	63.8	7.4	0.3	27.3	27.4
Average	1.6 ± 0.4	70.9 ± 5.5	8.4 ± 0.8	0.8 ± 0.5	18.3 ± 6.6	**32.8** ± 4.0

[*Values from all experimental trials are presented]

3.3.6 Yields

The products of hydrothermal liquefaction of alkaline lignin, with ethanol-water mixture as solvent and tetralin as *in-situ* hydrogen donor were categorized into organic phase (bio-oil), aqueous phase and solid residue. The residual solvents were separated using rotary evaporation at reduced pressures. The gaseous products from the reaction were not analyzed in this study. The variation in proportion of solid and liquid products with different amounts of ethanol in the solvent was studied. Previously, continuous feeding of gaseous H_2 to a lignin-tetralin system was reported to have resulted in a higher mass transfer of H_2 to the liquid phase (Pu et al., 2019). However, the present study shows that the effect of H_2 made available in-situ from tetralin can affect the products as well.

The weight of bio-oil produced increased as the proportion of ethanol went up from 0% to 25% (Figure 3.8). It started decreasing as the ethanol in solvent was further increased from 25% to 75%. It increased again when 100% ethanol was used as the solvent. It can be inferred that with 50% to 75% ethanol in water, the combined effect of both the solvents at subcritical temperature hindered the bio-oil formation. An effort was made to quantify the residual tetralin in the product mixture by observing tetralin in bio-oil using GC-MS and the bio-oil yield was adjusted according to this value. An excessive variation in the bio-oil yield and difficulty in separation of tetralin and other solvent after liquefaction of lignin was previously reported (Haverly et al., 2018; Lee et al., 2016; Pu et al., 2019). This suggests that the use of solvents having higher boiling points can cause challenges in separation of products downstream in the process. Additionally, the presence of three

different solvents might be leading to azeotropic mixtures and even occasional evaporation of bio-oil components. This uncertainty in solvent removal can be a reason for the variation in bio-oil yields.

The total of bio-oil and biochar yields are lower for the trials with 50% and 75% ethanol in the solvent. Here, a higher proportion of compounds in the product might have ended up in the aqueous phase. Later, the measurement of total organic carbon (TOC) of aqueous phase confirmed this hypothesis, which is described later in the article. As the amount of ethanol in the solvent increased from 25% to 50%, the amount of biochar in product increased significantly and then remained almost steady until ethanol in the solvent was 100%. This indicates that higher proportions of ethanol in the solvent favors the formation of biochar. Previously, the ethanol-water composition of 50-50 wt.% and a temperature of 300°C was reported to give the highest yield of bio-oil in the hydrothermal liquefaction of loblolly pine on similar reactor set-up (Celikbag et al., 2016; Lee et al., 2016). From this study, the presence or absence of tetralin was observed to affect bio-oil yields more than the ethanol-water concentration, which in turn plays a larger role in absence of hydrogen donor solvents (Lee et al., 2016). Tetralin used as a hydrogen donor also decomposes to produce several organic products, which may appear in the bio-oil phase. Also, the residual water as well as solvent ethanol (after the decantation and rotary evaporation) in the bio-oil mixture is responsible for skewed mass balance of these products.

Also, some more trends can be observed from the yields of bio-oil and biochar as the ethanol concentration in the solvent is changed. The yields are calculated based on the initial weight of lignin. From Figure 3.8, we can see that the bio-oil yields when tetralin is present in the system are somewhat higher than the case when tetralin is absent. From the biochar yield data shown in Figure 3.9, we can see that the biochar yields are almost always lower when tetralin is used. Since biochar is formed due to repolymerization of fragmented lignin, the lower biochar yields mean that the repolymerization has occurred to a smaller extent when tetralin is used. This explains the higher bio-oil yields with the use of tetralin in addition to the solvent system of ethanol-water. Note that due to the difficulties in separation of solvents due to the viscous and hydrophilic nature of bio-oil, the yields are not very consistent.

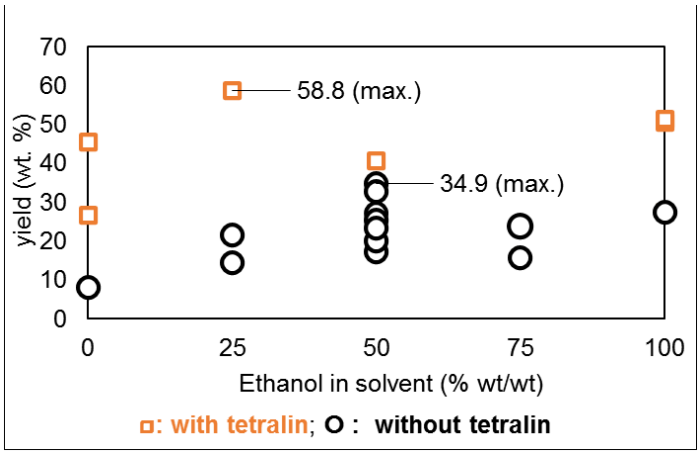

Figure 3.8 Bio oil yields from the solvent liquefaction of lignin without tetralin

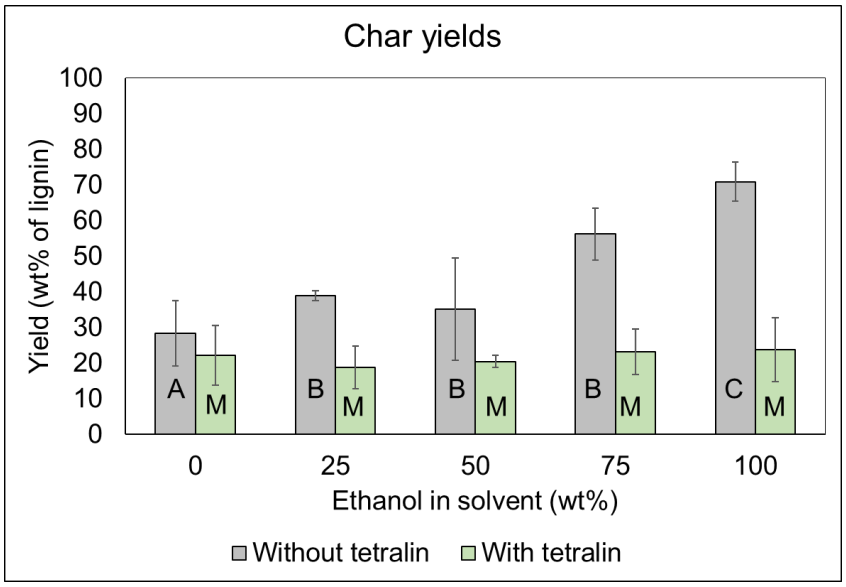

Figure 3.9 Biochar yield from the solvent liquefaction of lignin [Numbers indicated by the same letter are not significantly different from each other (Tukey's HSD test at α=0.1)]

The liquefaction of alkaline lignin in ethanol-water mixture was also repeated without the use of tetralin as hydrogen donor in two more sets of experiments. In one set, the solvent used for extraction of liquid bio-oil product was DCM and in other case, it was ethanol. It can be seen from Figure 3.10 that using ethanol to extract the products of solvent liquefaction of alkaline lignin gives better average yields of bio-oil as well as biochar. Whereas, in the case of using DCM as the

extraction solvent, the aqueous phase recovery is better. The reason for this can be that DCM and water are immiscible and hence can be easily separated into phases. This yield of bio-oil is comparable to the one mentioned by Kang et al., which was around 25-28% (Kang et al., 2011). The temperature range for the experiments by Kang et al. was 270-330°C and the liquefaction was performed for 30 minutes (Kang et al., 2011). It is clearly seen that the bio-oil yield values obtained without the use of tetralin are lower, yet well within a reasonable range. When tetralin was used as an *in-situ* hydrogen donor, it was difficult to separate it after the reaction during solvent removal due to its degradation into other products. Hence, any attempts to consider the tetralin degradation products while measuring the bio-oil yield had limitations. Here, for the sake of simplicity, we assume that some of the tetralin degradation products distribute themselves in the bio-oil, and some are evaporated with the solvent during rotary evaporation at reduced pressure.

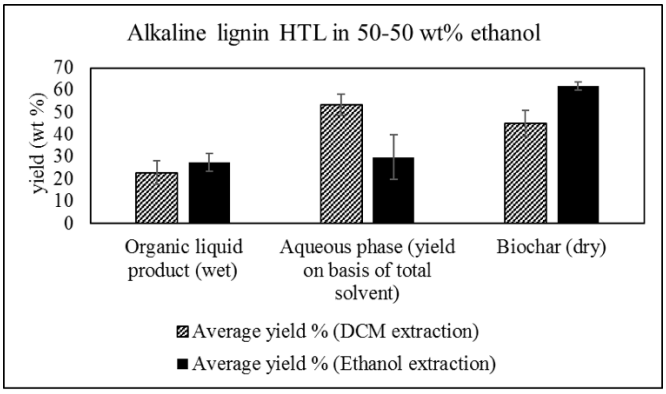

(a)

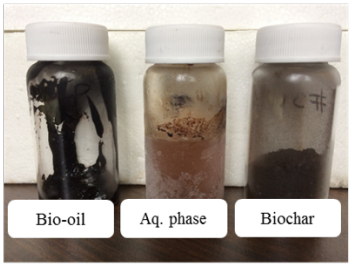

(b)

Figure 3.10 Products from the solvent liquefaction of alkaline lignin in 50-50 wt.% ethanol-water mixture without using tetralin (a) yields (b) pictures of products

3.3.7 TOC

As seen in Figure 3.11, as the amount of ethanol in solvent mixture went up from 0% to 75%, the organic carbon present in aqueous phase increased from 25 mg/L to 232 mg/L. With 50% to 75% ethanol in solvent, total amount of bio-oil and biochar decreased. The TOC measurement confirmed this observation, suggesting formation of higher amounts of water-soluble organics in the liquefaction product for this range of solvent composition. However, the higher concentration of organic carbon could also be due to the lesser amount of water present in those cases. As the amount of ethanol in solvent approached to 100%, all the organic compounds formed were seen only in biochar and bio-oil, in absence of any aqueous phase to dissolve the water-soluble compounds.

The total organic carbon in aqueous phase of product mixture from the solvent liquefaction of alkaline lignin without using tetralin was found to be 24.9-28.9 mg/L (not shown in the figure). As a general observation, comparing the values of TOC of aqueous phase with and without the use of tetralin indicated that the presence of tetralin increased the amount of total organic carbon present in the aqueous phase. This extra amount of organic carbon in aqueous phase could have come either at the expense of lesser quantity of bio-oil or at the expense of that of biochar. However, the yield of biochar was higher when tetralin was not used. Hence organic carbon in aqueous phase could have come at the expense of lower bio-oil yield when tetralin was used.

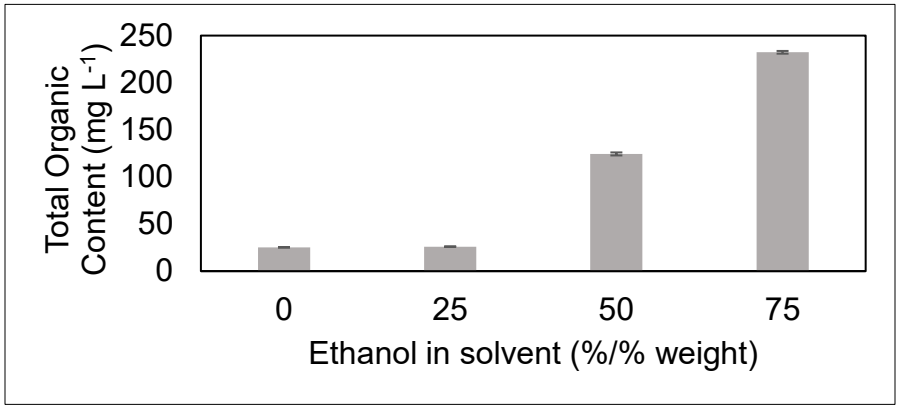

Figure 3.11 Total Organic Carbon (TOC) of aqueous phase in product of solvent liquefaction of alkaline lignin in the presence of tetralin

3.3.8 TAN

It can be seen from Figure 3.12 that the total acid number (TAN) for the bio-oil dropped from 2.47 to 0.05 when ethanol in solvent was increased from 0 to 50%. Note that, typical TAN for (petroleum) acid crude is >0.5 mg KOH/ g and for high TAN crude is >1.0 mg KOH/ g. The higher TAN seen in the bio-oil from the current study during lower concentration of ethanol in solvent can be because of the higher amount of organic acids formed during the liquefaction reactions. The reactions leading to the formation of organic acids could have been catalyzed by presence of water being in a higher quantity in the solvent for those particular conditions. It can be inferred that, in the presence of higher amounts of water in the solvent (>50%), the building blocks of alkaline lignin undergo reactions to form various acidic compounds.

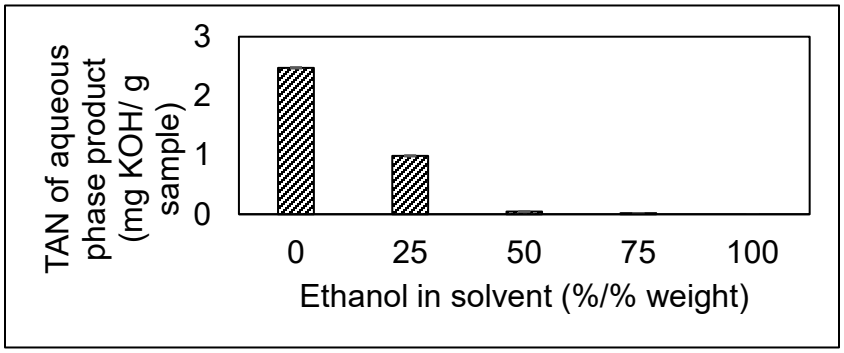

Figure 3.12 Total Acid Number (TAN) of bio-oil made with lignin in ethanol-water in presence of tetralin

3.3.9 Limitations due to lignin source variability

There were certain limitations to this study. First, the surfactant impurities present in alkaline lignin made it difficult to separate water from the bio-oil phase during downstream steps. This affected the mass balance and other product properties. Second, the solvents formed an azeotropic mixture and hence caused an uneven evaporation even after using vacuum and harsh conditions, which affected product composition. The biomass used to extract alkaline lignin can affect various chemical properties of lignin, such as the ratio of S/G/H-type units, methoxy and aliphatic hydroxyl group contents, fraction of aryl-ether bonds among all the interunit linkages, molecular weight etc. For example, a lignin with lower molecular weight and methoxy content, and higher

aliphatic hydroxyl and aryl-ether content will result in a higher bio-oil yield on liquefaction (Muraleedharan et al., 2018). The S/G ratio of lignin may also influence the formation of catechol-type compounds, as the rates of guaiacyl and syringyl decomposition are different (Schuler et al., 2019). The physical properties of biomass also affect lignin extraction and depolymerization processes. For example, a higher initial moisture content can reduce the hydration time in the beginning of HTL and hence speed up the depolymerization process (Williams et al., 2016). Reducing the particle size of lignin may not affect heat transfer when there is a solvent mixture as a reaction medium, but may affect the pumpability of lignin slurry during continuous operations (Elliott et al., 2015; Zhang et al., 2009). Additionally, lignin with a higher ash content will lead to an increased char formation on HTL (Toor et al., 2011). The best ways to address the challenges with lignin variability are selecting the right conversion process, considering a pretreatment process, and blending another feedstock with lignin to achieve the desired feed properties (Williams et al., 2016). For example, the higher ash content of wheat-straw derived alkaline lignin used in this study could have been mitigated by blending it with a woody biomass-derived lignin.

3.3.10 Potential of lignin to make sustainable alternatives to crude-oil derived products

Demonstrating the depolymerization of alkaline lignin at pilot scale is necessary before it can make its way up into the industry. For enabling pilot scale demonstration of bio-oil production, one needs to have established continuous liquefaction of alkaline lignin, as it is the requirement for industry. The desired properties of bio-oil from any lignin is low moisture and oxygen content, thermal stability, miscibility with hydrocarbon streams etc. However, the use of HTL is advantageous, as this process has a little effect due to variability in the moisture content of feed lignin (Williams et al., 2016). Also, the problems faced in thermochemical conversion through HTL due to biomass source variability can be mitigated by using extracted lignin as the feed to get targeted products. Whereas, densification strategies such as pelleting or briquetting can help overcome the variability in physical characteristics of feed lignin (Ray et al., 2013). According to Upton et. al., alkaline lignin has previously been used for the synthesis of polyurethanes, polysters, epoxide resins and phenolic resins (Upton and Kasko, 2016). It was also mentioned in the same article that alkaline lignin, without any valorization, can replace the macropolyol component of

polyurethanes easily (Upton and Kasko, 2016). Also, such lignin-derived bio-based polyols are supposed to have better biodegradability as compared to petroleum-based polyols (Cateto et al., 2013; Hu et al., 2013).

Haverly et al., distilled the bio-oil made from continuous liquefaction of southern yellow pine lignin (Haverly et al., 2018). The distillate was called "medium oil" and it was found to have potential to be used as a fuel. They mentioned the average mass fraction of water in their bio-oil to be 13.4 wt.%. Also, the average oxygen content of bio-oil was reported to be 55.6%. However, the initial oxygen content of biomass in that case was 41.7% and hence there was net increase in the oxygen content after the conversion to bio-oil. Whereas the oxygen content of bio-oil in the present study was reduced to 23-46% from around 40% in the alkaline lignin. The oxygen content of biochar was 19-27 wt%. The oxygen content of bio-oil in the case where tetralin was used additionally was higher. this indicates that the process of solvent liquefaction is seen to produce bio-oil with higher oxygen content than the feed in case of southern yellow pine lignin, but lower oxygen content in case of alkaline lignin.

The laboratory scale experiments performed for solvent liquefaction of alkaline lignin in this study suggested that, a mixture of water and ethanol was itself an effective solvent for this process. Shorter reaction time and relatively lower acidic content in products were some of the advantages achieved by the reaction setup. However, there were no substantial differences visible in functional groups present in the organic liquid or biochar products when different amount of ethanol was used in the solvent along with water. As seen from total organic content measurement, more amount of ethanol in solvent led to higher total organic carbon in the aqueous phase of product. It can be concluded that using the solvents like water, ethanol or tetralin one at a time, is better than using their mixture. The alkaline lignin used dispersed easily in deionized water after stirring for several minutes. Hence, there will not be any problem for using this slurry even in a continuous reactor.

3.4 Conclusion

In conclusion, the results of this study suggest that the extent of repolymerization of bio-oil compounds into condensed structures was reduced with the use of hydrogen donor solvent tetralin.

Also, this reduction in product condensation resulted in higher selectivity towards monomeric compounds, which was confirmed from the number of total aromatics in bio-oil. The alkaline lignin structure was relatively condensed, which was verified using NMR characterization. The structures of phenolic monomers produced and the yields of major compounds in bio-oil were elucidated using GC-MS. Most importantly, when a strong hydrogen donor solvent such as tetralin was used in the system, the amount of ethanol became less important as a factor in deciding the extent of depolymerization and deoxygenation reactions. Instead, tetralin took the control of the extent of these reactions. The location of maximum phenolic monomer yield shifts towards lower concentrations of ethanol in the solvent. The absence of a specific trend in product yields with respect to lignin properties such as S/G ratio during the depolymerization of lignin was recently highlighted by Anderson et al (Anderson et al., 2019). The current study adds a similar observation for the depolymerization of lignin, but in the case of solvent composition when *in-situ* hydrogen donor is used. Overall, the solvent liquefaction of alkaline lignin resulted in deoxygenated products, which had a substantial number of phenolic compounds. Hence, the bio-oil from this process could be used as fuel directly or can be polymerized to make phenolic resins. Further research can explore the potential to make biodegradable plastics from this bio-oil.

3.5 Acknowledgements

The authors would like to acknowledge the United States Department of Agriculture and the National Institute of Food and Agriculture for funding this research project (Grant # USDA-NIFA-2015-67021-22842).

3.6 References

1. Agarwal, S., Chowdari, R.K., Hita, I., Heeres, H.J., 2017. Experimental Studies on the Hydrotreatment of Kraft Lignin to Aromatics and Alkylphenolics Using Economically Viable Fe-Based Catalysts. ACS Sustain. Chem. Eng. 5, 2668–2678. https://doi.org/10.1021/acssuschemeng.6b03012
2. Alemán-Vázquez, L.O., J.L.Cano-Domínguez, García-Gutiérrez, J.L., 2012. Effect of Tetralin, Decalin and Naphthalene as Hydrogen Donors in the Upgrading of Heavy Oils. Procedia Eng. 42, 532–539. https://doi.org/https://doi.org/10.1016/j.proeng.2012.07.445
3. Anderson, E.M., Stone, M.L., Katahira, R., Reed, M., Muchero, W., Ramirez, K.J., Beckham, G.T., Román-Leshkov, Y., 2019. Differences in S/G ratio in natural poplar variants do not predict catalytic depolymerization monomer yields. Nat. Commun. 10, 2033. https://doi.org/10.1038/s41467-019-09986-1

4. Barta, K., Matson, T.D., Fettig, M.L., Scott, S.L., Iretskii, A. V., Ford, P.C., 2010. Catalytic disassembly of an organosolv lignin via hydrogen transfer from supercritical methanol. Green Chem. 12, 1640–1647. https://doi.org/10.1039/c0gc00181c
5. Cateto, C.A., Barreiro, M.F., Ottati, C., Lopretti, M., Rodrigues, A.E., Belgacem, M.N., 2013. Lignin-based rigid polyurethane foams with improved biodegradation. J. Cell. Plast. 50, 81–95. https://doi.org/10.1177/0021955X13504774
6. Celikbag, Y., Via, B.K., Adhikari, S., Buschle-Diller, G., Auad, M.L., 2016. The effect of ethanol on hydroxyl and carbonyl groups in biopolyol produced by hydrothermal liquefaction of loblolly pine:31P-NMR and19F-NMR analysis. Bioresour. Technol. 214, 37–44. https://doi.org/10.1016/j.biortech.2016.04.066
7. Elliott, D.C., Biller, P., Ross, A.B., Schmidt, A.J., Jones, S.B., 2015. Hydrothermal liquefaction of biomass: Developments from batch to continuous process. Bioresour. Technol. 178, 147–156. https://doi.org/https://doi.org/10.1016/j.biortech.2014.09.132
8. Fang, Z., Sato, T., Smith, R.L., Inomata, H., Arai, K., Kozinski, J.A., 2008. Reaction chemistry and phase behavior of lignin in high-temperature and supercritical water. Bioresour. Technol. 99, 3424–3430. https://doi.org/10.1016/J.BIORTECH.2007.08.008
9. Gan, L., Pan, X., 2019. Phenol-Enhanced Depolymerization and Activation of Kraft Lignin in Alkaline Medium. Ind. Eng. Chem. Res. 58, 7794–7800. https://doi.org/10.1021/acs.iecr.9b01147
10. Haverly, M.R., Okoren, K. V, Brown, R.C., 2018. Optimization of Phenolic Monomer Production from Solvent Liquefaction of Lignin. ACS Sustain. Chem. Eng. 6, 12675–12683.
11. Ház, A., Jablonský, M., Šurina, I., Kačík, F., Bubeníková, T., Ďurkovič, J., 2019. Chemical Composition and Thermal Behavior of Kraft Lignins. Forests 10, 483.
12. Hu, S., Luo, X., Li, Y., 2013. Polyols and Polyurethanes from the Liquefaction of Lignocellulosic Biomass. ChemSusChem 7, 66–72. https://doi.org/10.1002/cssc.201300760
13. Kang, S., Li, X., Fan, J., Chang, J., 2013. Hydrothermal conversion of lignin: A review. Renew. Sustain. Energy Rev. 27, 546–558. https://doi.org/10.1016/j.rser.2013.07.013
14. Kang, S., Li, X., Fan, J., Chang, J., 2011. Classified separation of lignin hydrothermal liquefied products. Ind. Eng. Chem. Res. 50, 11288–11296. https://doi.org/10.1021/ie2011356
15. Kozliak, E.I., Kubátová, A., Artemyeva, A.A., Nagel, E., Zhang, C., Rajappagowda, R.B., Smirnova, A.L., 2016. Thermal Liquefaction of Lignin to Aromatics: Efficiency, Selectivity, and Product Analysis. ACS Sustain. Chem. Eng. 4, 5106–5122. https://doi.org/10.1021/acssuschemeng.6b01046
16. Langholtz, M.H., Stokes, B.J., Eaton, L.M., Brandt, C.C., Davis, M.R., Theiss, T.J., Turhollow Jr, A.F., Webb, E., Coleman, A., Wigmosta, M., 2016. 2016 Billion-ton report: advancing domestic resources for a thriving bioeconomy, volume 1: economic availability of feedstocks. Oak Ridge National Lab.(ORNL), Oak Ridge, TN (United States).
17. Laurichesse, S., Avérous, L., 2013. Chemical modification of lignins: Towards biobased polymers, Progress in Polymer Science. https://doi.org/10.1016/j.progpolymsci.2013.11.004

18. Lee, H. shik, Jae, J., Ha, J.M., Suh, D.J., 2016. Hydro- and solvothermolysis of kraft lignin for maximizing production of monomeric aromatic chemicals. Bioresour. Technol. 203, 142–149. https://doi.org/10.1016/j.biortech.2015.12.022
19. Meng, X., Crestini, C., Ben, H., Hao, N., Pu, Y., Ragauskas, A.J., Argyropoulos, D.S., 2019. Determination of hydroxyl groups in biorefinery resources via quantitative 31P NMR spectroscopy. Nat. Protoc. https://doi.org/10.1038/s41596-019-0191-1
20. Muraleedharan, M.N., Zouraris, D., Karantonis, A., Topakas, E., Sandgren, M., Rova, U., Christakopoulos, P., Karnaouri, A., 2018. Effect of lignin fractions isolated from different biomass sources on cellulose oxidation by fungal lytic polysaccharide monooxygenases. Biotechnol. Biofuels 11, 296. https://doi.org/10.1186/s13068-018-1294-6
21. Ouyang, X., Huang, X., Zhu, Y., Qiu, X., 2015. Ethanol-Enhanced Liquefaction of Lignin with Formic Acid as an in Situ Hydrogen Donor. Energy & Fuels 29, 5835–5840. https://doi.org/10.1021/acs.energyfuels.5b01127
22. Patil, V., Adhikari, S., Cross, P., 2018. Co-pyrolysis of lignin and plastics using red clay as catalyst in a micro-pyrolyzer. Bioresour. Technol. 270, 311–319. https://doi.org/10.1016/j.biortech.2018.09.034
23. Patil, V., Adhikari, S., Cross, P., Jahromi, H., 2020. Progress in the solvent depolymerization of lignin. Renew. Sustain. Energy Rev. 133, 110359. https://doi.org/https://doi.org/10.1016/j.rser.2020.110359
24. Pu, J., Nguyen, T.-S., Leclerc, E., Lorentz, C., Laurenti, D., Pitault, I., Tayakout-Fayolle, M., Geantet, C., 2019. Lignin catalytic hydroconversion in a semi-continuous reactor: An experimental study. Appl. Catal. B Environ. 256.
25. Qian, L., Wang, S., Savage, P.E., 2017. Hydrothermal liquefaction of sewage sludge under isothermal and fast conditions. Bioresour. Technol. 232, 27–34. https://doi.org/https://doi.org/10.1016/j.biortech.2017.02.017
26. Ray, A.E., Hoover, A.N., Nagle, N., Chen, X., Gresham, G.L., 2013. Effect of pelleting on the recalcitrance and bioconversion of dilute-acid pretreated corn stover under low- and high-solids conditions. Biofuels 4, 271–284. https://doi.org/10.4155/bfs.13.14
27. Sameni, J., Krigstin, S., Sain, M., 2017. Solubility of Lignin and Acetylated Lignin in Organic Solvents. Bioresour. Vol 12, No 1.
28. Schuler, J., Hornung, U., Dahmen, N., Sauer, J., 2019. Lignin from bark as a resource for aromatics production by hydrothermal liquefaction. GCB Bioenergy 11, 218–229. https://doi.org/10.1111/gcbb.12562
29. Shuai, L., Amiri, M.T., Questell-Santiago, Y.M., Héroguel, F., Li, Y., Kim, H., Meilan, R., Chapple, C., Ralph, J., Luterbacher, J.S., 2016. Formaldehyde stabilization facilitates lignin monomer production during biomass depolymerization. Science (80-.). 354, 329–333. https://doi.org/10.1126/science.aaf7810
30. Sluiter, A., Hames, B., Ruiz, R., Scarlata, C., Sluiter, J., Templeton, D., 2008. Determination of ash in biomass.
31. Szulejko, J.E., Kim, Y., Kim, K., 2013. Method to predict gas chromatographic response factors for the trace-level analysis of volatile organic compounds based on the effective carbon number concept. J. Sep. Sci. 36, 3356–3365.

32. Talebi Amiri, M., Dick, G.R., Questell-Santiago, Y.M., Luterbacher, J.S., 2019. Fractionation of lignocellulosic biomass to produce uncondensed aldehyde-stabilized lignin. Nat. Protoc. 14, 921–954. https://doi.org/10.1038/s41596-018-0121-7
33. Toor, S.S., Rosendahl, L., Rudolf, A., 2011. Hydrothermal liquefaction of biomass: A review of subcritical water technologies. Energy 36, 2328–2342. https://doi.org/10.1016/j.energy.2011.03.013
34. Upton, B.M., Kasko, A.M., 2016. Strategies for the Conversion of Lignin to High-Value Polymeric Materials: Review and Perspective. Chem. Rev. 116, 2275–2306. https://doi.org/10.1021/acs.chemrev.5b00345
35. Williams, C.L., Westover, T.L., Emerson, R.M., Tumuluru, J.S., Li, C., 2016. Sources of Biomass Feedstock Variability and the Potential Impact on Biofuels Production. BioEnergy Res. 9, 1–14. https://doi.org/10.1007/s12155-015-9694-y
36. Xu, C., Arancon, R.A.D., Labidi, J., Luque, R., 2014. Lignin depolymerisation strategies: towards valuable chemicals and fuels. Chem. Soc. Rev. 43, 7485–7500. https://doi.org/10.1039/C4CS00235K
37. Yang, S., Wen, J.-L., Yuan, T.-Q., Sun, R.-C., 2014. Characterization and phenolation of biorefinery technical lignins for lignin–phenol–formaldehyde resin adhesive synthesis. RSC Adv. 4, 57996–58004. https://doi.org/10.1039/C4RA09595B
38. Zhang, B., von Keitz, M., Valentas, K., 2009. Thermochemical liquefaction of high-diversity grassland perennials. J. Anal. Appl. Pyrolysis 84, 18–24. https://doi.org/https://doi.org/10.1016/j.jaap.2008.09.005

4. Lignin Depolymerization Aided with Biaryl Formation During a Pretreatment

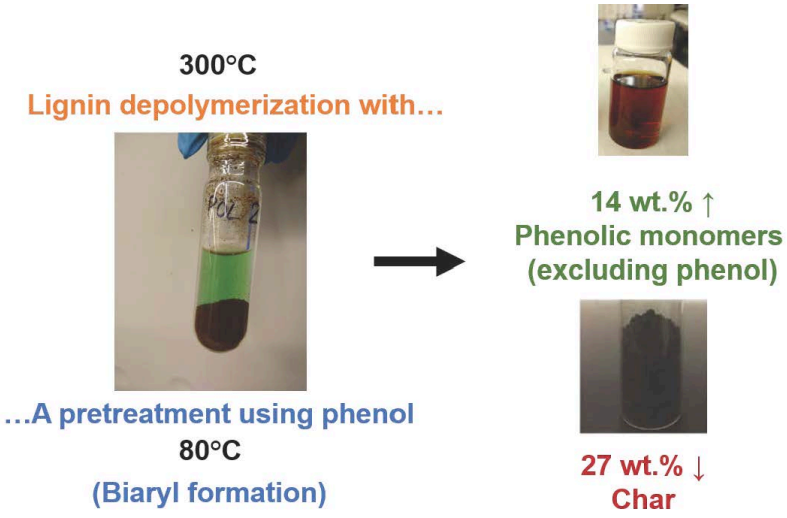

Abstract

Plant-based lignin is a renewable resource that can help attain sustainable development goals of clean and affordable energy. Herein, we explored a pretreatment at 80°C to modify lignin using phenol, which also happens to be one of the major products from the thermolysis of lignin. Catalytic Transfer Hydrogenolysis using Ru/C as a catalyst in ethanol at 300°C was used to break down lignin. Through biaryl formation, additional compounds can be formed from lignin, leading to an increase in the yield of desired products. The relation between modified lignin structure and its effect on the depolymerization process was investigated with ^{1}H-^{13}C-2D-HSQC, ^{31}P NMR and FTIR spectroscopy, GC-MS/FID, TGA, and elemental analysis. Biaryl formation during the pretreatment enabled different product formation routes compared with simply adding phenol to the lignin depolymerization medium. There was a 14% increase in phenolic monomers yield (excluding phenol) and a 27% decrease in biochar yield with the pretreatment. This study contributes to the prior knowledge of lignin functional group protection by exploring the use of phenol in a pretreatment.

Keywords: *Lignin, Depolymerization, Stabilization, Biaryl formation*

4.1 Introduction

Achieving sustainable development goals of 'Affordable and Clean Energy,' 'Responsible Consumption and Production,' and 'Climate Action' requires the use of renewable sources of chemicals and fuels (Issa et al., 2019; Ragauskas et al., 2006). Biomass-derived lignin is a promising resource that can fulfill the demands of commodity and specialty chemicals needed as plastics, pharmaceuticals, and flavoring agents (Jahromi et al., 2020; Patil et al., 2020). One-third (on a mass basis) of the lignocellulosic biomass is lignin. The lignin waste is expected to reach 225 million tons annually by 2030 from the second-generation bioethanol industry (Cotana et al., 2014).

Lignin is derived from up to three phenylpropanoid units, namely syringyl, guaiacyl and p-hydroxyphenyl, linked with several inter-unit linkages. These linkages are C-O bonds, such as β-O-4, α-O-4, and 4-O-5, or they are C-C bonds, such as 5-5, β-1, β-5, and β-β, as shown in Figure 4.1. During the extraction of lignin from source biomass, native lignin structure is altered, forming recalcitrant C-C bonds (Guadix-Montero and Sankar, 2018). Many strategies have previously been proposed to make the lignin structure more resilient to recondensation. The use of phenolic reagents as stabilizing agents is one such strategy, in which phenolic groups are attached to highly reactive lignin sites, altering the course of reaction during subsequent depolymerization (Shuai and Saha, 2017). Phenol can attach itself to lignin with its para- or ortho-position, hence stabilizing the sites from recondensation (Podschun et al., 2015).

The presence of phenol in the reaction medium during lignin depolymerization is shown to have an effect on suppressing unwanted cross-linking reactions, otherwise known as 'oligomerization' or 'char formation' (Patil et al., 2018; Roberts et al., 2011; Saisu et al., 2003). While the maximum yield of phenolic monomers obtained was about 19 wt% with this strategy, the presence of extra phenol could have led to this apparent increase (Saisu et al., 2003). On the other hand, just adding phenol to the reaction mixture during lignin liquefaction in near-critical water led to about 1.8 - 14.7 wt% of phenol-free monomer yield based on initial lignin (Arturi et al., 2017). The use of phenol in the lignin depolymerization medium also opens the possibility of

a 'redistribution mechanism' (Gan and Pan, 2019; Saito et al., 2003). Briefly, a monomeric 'phenoxyl' radical can attack a long chain made of phenoxyl radicals, leading to intermediate and subsequent cleavage of polymer chains (Saito et al., 2003). This radical-based reaction is also shown in Figure 4.1.

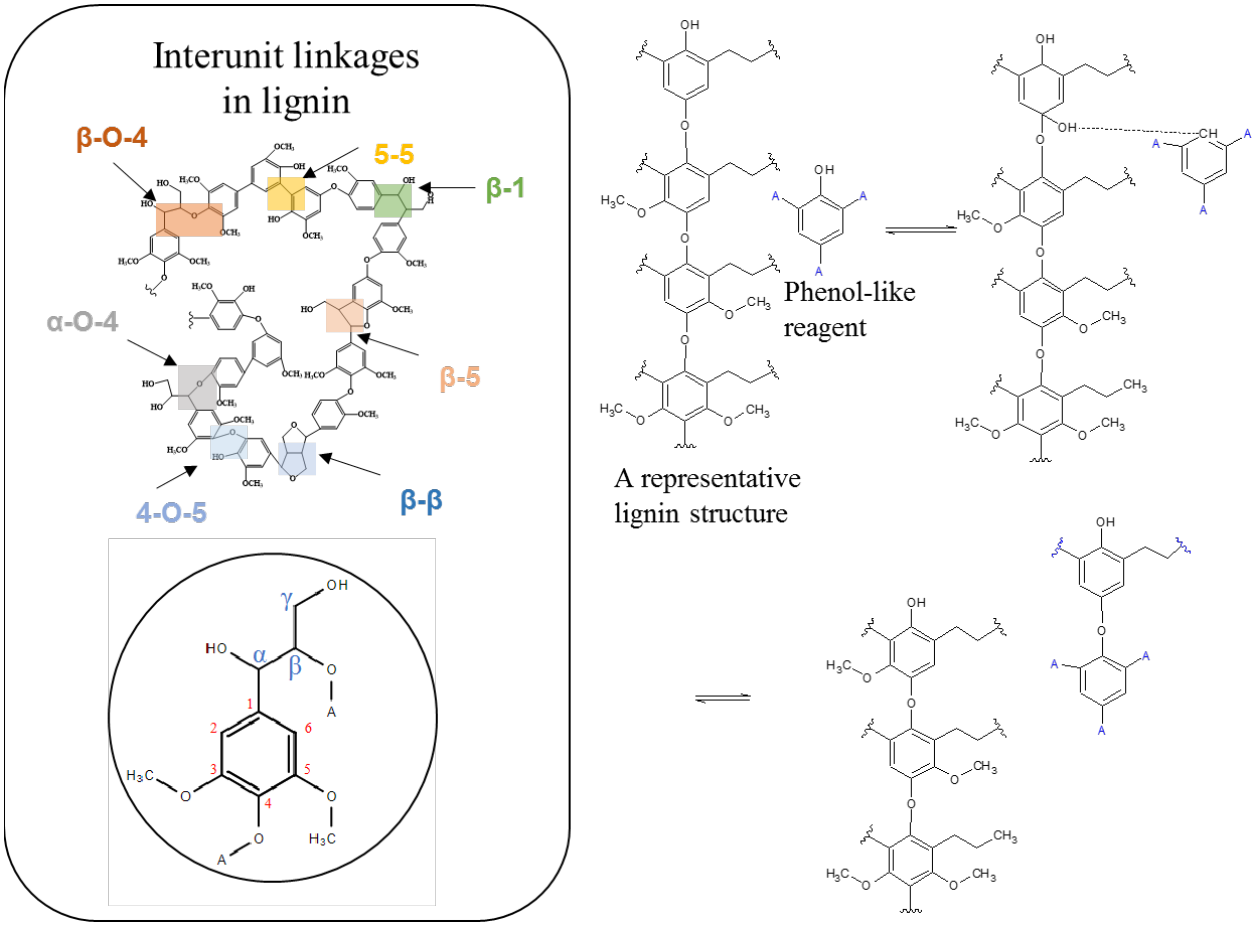

Figure 4.1 Phenol redistribution mechanism based on (Saito et al., 2003) Note: 'A' indicates alkyl substitutions or hydrogen.

Decoupling of biaryl formation during pretreatment and depolymerization was investigated in this study while using a known lignin cleavage method called Catalytic Transfer Hydrogenolysis (CTH) (L. Das et al., 2018). Previously, total lignin monomer yields were reported only as high as 6 % with CTH of lignin, although bio-oil yield could be higher due to the presence of oligomers (Limarta et al., 2018). Phenolic yield for wheat straw protobind (soda) lignin at 400°C in ethanol without a catalyst was only 0.7 wt% (Güvenatam et al., 2016). Selective bond-cleavage by prior

modification of lignin structure is a valuable strategy for lignin depolymerization. The effect of adding phenol directly to the liquefaction medium on lignin depolymerization has been explored in the literature (Arturi et al., 2017; Toledano et al., 2014). However, investigation of biaryl formation as a pretreatment strategy to modify lignin before depolymerization has not been previously examined. Additionally, there has not been enough emphasis given on using reagents that can be derived from lignin itself or controlling the product distribution between aliphatic and phenolic compounds from lignin depolymerization. Hence, there is a need to explore biaryl formation as a pretreatment process and study its effect on the lignin structure that can alter the subsequent depolymerization of product yields.

The present study examined how a pretreatment of lignin with phenol causes modification of lignin, leading to changes in the yields of products such as phenolic monomers, aromatics, aliphatics, and char. This study aims to answer if the pretreatment of lignin results in an increase in the yield of desired products, such as phenolic monomers, during subsequent depolymerization. The results of this study are presented as the yields of various products quantified using GC-MS/FID, and the observations are discussed in the context of their reaction mechanisms.

4.2 Experimental

4.2.1 Materials

Organosolv lignin was extracted from poplar biomass. Poplar wood chips sized between Mesh-12 (1680 μm) and Mesh-30 (595 μm) were used in this study (Forest Concepts LLC, Washington, USA). Phenol (>99.0%), n-hydroxy-5-norbornene-2,3- dicarboximide (NHND), ruthenium on carbon (5 wt.% loading on carbon support matrix), n-decane, chloroform-D, and 2-chloro-4,4,5,5-tetramethyl-1,3,2-dioxaphospholane (TMDP) were purchased from Millipore-Sigma (Burlington, Massachusetts, USA). Sulfuric acid and acetic anhydride were purchased from J.T.Baker Chemicals (Phillipsburg, New Jersey, USA). Pyridine and $Cu(II)Cl_2.2H_2O$ were purchased from Alfa Aesar (Haverhill, Massachusetts, USA). Ethanol (95%), ethyl acetate (99.9%) ethylenediaminetetraacetic acid (EDTA), sodium hydroxide, dimethyl sulfoxide (DMSO)-d6 and 2-propanol were purchased from VWR Chemicals BDH® (Suwanee, Georgia, USA). Ultra-high purity nitrogen (99.999%) and oxygen (99.994%) and ultra-zero grade air (total hydrocarbons < 0.1 ppm) were purchased from Airgas, Inc. (Radnor, Pennsylvania, USA).

4.2.2 Methodology

The overall schematic of the experiments is shown in Figure 4.2. Experiments were directed at extracting lignin from poplar with minimal modifications in its structure and then pretreating it with phenol at mild conditions. Subsequent depolymerization and separation of products were performed for control, treatment, and blank studies. Briefly, a controlled study was used to establish baseline results for lignin depolymerization, which was then compared with the treatment study to contrast with the effect of pretreatment. Product separation and characterization techniques were optimized with preliminary experiments in the laboratory. All of the steps are discussed in Sections 4.2.3, 4.2.4, 4.2.5, and 4.2.6.

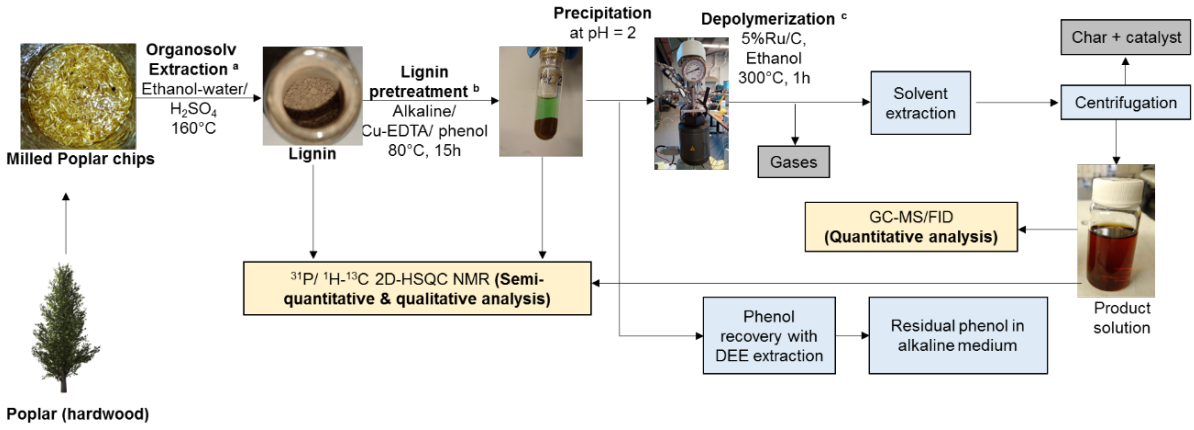

[a] 33.3 g Poplar (Green chips- Hammer Mill, 12 mesh, from Forest Concepts LLC, Auburn, WA), 0.4 g H_2SO_4 (37%), 166.3 g 190 proof ethanol, 72.9 g deionized water
[b] 3 g Organosolv lignin, ~98.5 mL alkaline water (0.5 M NaOH), 7 mol/mol EDTA, 7mol/mol Cu(II)Cl_2, 70 mol/mol phenol (2.3 g, 77 wt% of lignin), 15h at 80°C
[c] *[1g lignin, 40 mL ethanol, 300°C, 1h, 5%Ru/C (15% of feed); 6.9 bar N_2 Quantification using calibration curves and Polyarc® with creosol as the internal standard]*

Figure 4.2 Overall schematic of the experiments

4.2.3 Organosolv lignin extraction

Ethanol organosolv lignin was extracted from poplar wood chips following the general procedure described in the literature (Mahadevan et al., 2016; Meng et al., 2018). Briefly, in a typical batch, about 70 g of poplar wood chips were mixed in 65% ethanol with a 1:7 solid to liquid ratio. To this mixture was added 1% (wt/wt of the poplar) of sulfuric acid. The mixture was soaked overnight and then heated in a 1.8 L Parr® reactor at 170°C for 1 h, stirring at 50 rpm. The reactor was quenched after the reaction by passing chilled water through cooling tubes. The resulting

mixture was filtered under vacuum with Whatman filter paper (#42). A small quantity of ethanol was added to extract more lignin from the residue, and this solution was added to the filtrate. The residue was stored. About a 3-fold volume of deionized water was added to the filtrate to precipitate lignin. Lignin was then washed with water to remove trace water-soluble compounds, and the solids were dried at 50°C for several days.

4.2.4 Lignin pretreatment

Pretreatment of lignin was performed by a method based on the protocols previously described in the literature (Nanayakkara et al., 2014a; Yang et al., 2014). Briefly, 3 g of organosolv lignin extracted from poplar was mixed with 0.5 NaOH (98.5 ml). To this solution, 2.3 g phenol was added. To this mixture, 7 mmol/mmol lignin of $Cu(II)_2Cl_2.2H_2O$ (0.1 g/g lignin) and EDTA (0.2 g/g lignin) were added to create the Cu-EDTA catalytic system. The mixture was stirred at 80°C for 15 h. The resulting solution was brought to a pH of 2 by adding a few drops of 1M HCl to precipitate pretreated lignin. The aqueous phase was separated by centrifugation and stored separately. Phenol was recovered from this phase with liquid-liquid extraction using excess diethyl ether. Filtration was used to separate pretreated lignin. Lignin was then washed with excess deionized water, followed by diethyl ether, and then dried under vacuum at room temperature overnight. Later, it was also found that drying the pretreated lignin at 70°C did not seem to degrade its structure, as it exhibited the desired spectral regions during NMR characterization.

Additionally, the effect of changing the external environment during the pretreatment was examined by performing the pretreatment under inert and oxidative conditions. For this part, instead of using aerobic conditions enabled by pretreatment under air, approximately 1 bar N_2 or O_2 was bubbled in the mixture prepared for pretreatment for 10 minutes. Precipitation, separation, and depolymerization of pretreated lignin were performed in the same way as described before.

4.2.5 Depolymerization of lignin

The depolymerization of pretreated lignin was performed using CTH. A known amount of pretreated lignin (~ 1 g) was mixed with 40 mL ethanol and vortexed for 2 min. To this mixture, 15 wt% (based on the mass of lignin) of catalyst (5wt% Ru/C) was added. The mixture was loaded

in a stainless steel mini-reactor and sealed. Parr® 4567 reactor (450 mL volume) was used to perform a high-pressure liquefaction reaction (Parr Instrument Company, Moline, Illinois, USA). A reaction temperature of 300°C was maintained for 1 h in the reactor. The reactor was initially pressurized with 100 psi $N_{2,}$ whereas it increased to 120-130 psi after cooling the reactor at the end of the reaction. The maximum pressure in the reactor during the reaction was ~1200 psi. After opening the reactor, products were removed by washing the reactor with ~10 mL of dichloromethane. The product mixture was centrifuged to remove catalyst and char. An aliquot (~2 g) was taken out from liquid products for GC-MS/FID. Mass of all of the reagents was noted. The char was dried at 70ºC for 24 hours. The gases produced from the reaction were captured and analyzed with a micro-GC (Agilent Technologies, Santa Clara, California, USA). Control and blank experiments were performed with the same procedure described above. A control experiment is defined as the CTH of untreated organosolv lignin. A blank experiment is defined as the CTH of phenol in the same liquefaction medium used for lignin.

4.2.6 Characterization of reactants and products

4.2.6.1 Proximate and compositional analysis

Proximate analysis of raw materials was performed as per guidelines suggested by NREL (Sluiter et al., 2008a). Briefly, samples were dried for 24 hours at 105ºC to measure moisture content. Dried samples were subjected to 950ºC for 7 min to calculate volatile combustible matter. The resulting solids were subjected to 575ºC for 4 h to calculate ash content. Fixed carbon was estimated as the remaining mass from the sample after subtracting the rest of the portions.

Compositional analysis of raw biomass extracted lignin, and pretreated lignin was performed as per NREL protocol (Sluiter et al., 2008b). Briefly, extractives were removed from samples using ethanol. Thereafter, acid hydrolysis of samples was performed, and lignin was separated from carbohydrates. Acid-soluble lignin was measured with Helios Omega UV-vis spectrophotometer (Thermo Scientific, Waltham, Massachusetts, USA), and acid-soluble lignin was measured by combustion in a muffle furnace. Sugars were analyzed using High-Pressure Liquid Chromatography with Agilent 1260 Infinity HPLC system (Agilent Technologies, Santa Clara, California, USA).

4.2.6.2 ^{1}H-^{13}C 2D-HSQC NMR spectroscopy

Untreated organosolv lignin, pretreated lignin, and depolymerization products were characterized by ^{1}H-^{13}C 2D Heteronuclear Single Quantum Coherence- Nuclear Magnetic Resonance (HSQC-NMR) spectroscopy using a protocol prescribed in the literature (Talebi Amiri et al., 2019). In this technique, one-dimensional ^{1}H and ^{13}C spectra are plotted on X- and Y-axes, respectively, and contours produced from their signals were correlated with lignin's structural features. Briefly, 20-25 mg of lignin or bio-oil was dissolved in about 800 µL of a deuterated solvent, dimethyl sulfoxide (DMSO)-d_6. The solution was vortexed for 2 min and then filtered through a 0.45 µm nylon syringe filter. Filtered solution was added to the NMR tube. ^{1}H and ^{13}C, as well as 2D-HSQC NMR spectra, were recorded on a Bruker Avance 600 MHz spectrometer equipped with a z-gradient triple resonance Cryo-probe (Bruker BioSpin Corporation, Billerica, Massachusetts, USA). Bruker standard pulse sequence 'hsqcetgp' was used for recording spectra. With 16 scans for ^{1}H, 32 scans for ^{13}C, additional 2 scans for HSQC, and 16 dummy scans to ensure a steady-state of the instrument; the acquisition was performed for 10.49 min at 298.1 K. Spectra were analyzed using Bruker Topspin 4.0.6 software.

For both the raw and pretreated organosolv lignin samples, dissolution was poor in deuterated solvents, and hence acetylation was used to increase their solubility (Gan and Pan, 2019). However, it is essential to note that acetylation can help to make only ~90% mass of lignin soluble, and hence the values obtained need to be interpreted with caution (Tolbert et al., 2014). The lignin depolymerization product had monomers and oligomers, and hence it was soluble in the deuterated solvent without acetylation. The regions in the spectra for lignin were assigned based on the reference spectra from literature for similarly derivatized lignin samples (Tarmadi et al., 2018a). Briefly, about 100 mg of lignin was dissolved in a 1:1 v/v mixture of pyridine and acetic anhydride and was vortexed for 2 min. Then, it was kept in the dark at room temperature for 72 h. Later, the mixture was added to 120 mL of ice-cold water containing 1 mL of concentrated hydrochloric acid dropwise. The precipitate was filtered and washed with deionized water. The resulting acetylated lignin was dried under vacuum at room temperature for several days before using it for NMR analysis.

4.2.6.3 ^{31}P NMR spectroscopy

The literature procedure to quantitatively characterize hydroxyl group concentration of lignin and lignin-derived products was used for this analysis (Meng et al., 2019b). Briefly, to make a stock solution, pyridine and deuterated chloroform were mixed in a ratio of 1.6: 1 (v/v). To 10 mL of this mixture, about 40 mg of Cr(III)acetylacetonate was added ad a relaxation agent, and NHND was added as an internal standard. The mixture was vortexed for 2 minutes. About 20-25 mg of the sample was mixed in 800 µL of stock solution and was shaken. Approximately 100 µL of a phosphitylating agent (2-chloro-4,4,5,5-tetramethyl-1,3,2-dioxaphospholane, or TMDP) was added to the sample mixture, and it was vortexed again for 2 min to ensure complete reaction. The solution was filtered with a 0.45 µm nylon syringe filter into an NMR tube to fill it with 5.5 cm height. Mass of all reagents was noted. ^{31}P NMR spectroscopy was performed on Bruker Avance 400 MHz spectrometer with 64 scans, 240 ppm spectral width, and 0.84 s acquisition time (Bruker BioSpin Corporation, Billerica, Massachusetts, USA). Spectra were analyzed using Bruker TopSpin 4.0.6 software.

4.2.6.4 Elemental Analysis

Elemental analysis of lignins was performed using the 'Vario MICRO cube' elemental analyzer (Elemental Americas Inc., New York, USA). About 2 mg of sample was used for analysis. Sulfanilamide, as a standard, was used to calculate daily factor values.

4.2.6.5 FTIR spectroscopy

Fourier Transform Infrared (FTIR) analysis of lignin was performed using Thermo-Nicolet iS10 instruments (Thermo Scientific, Massachusetts, USA). A total of 34 scans were performed on samples with wavenumbers between 400 to 4000 cm^{-1}.

4.2.6.6 Thermogravimetric analysis

Raw and pretreated lignin were subjected to thermal degradation in TGA-50 (Shimadzu Scientific Instruments Inc., Maryland, USA) under an oxidative environment using air (~20 mL $minute^{-1}$). A sample was placed in an alumina crucible and heated from room temperature to 900°C

at a rate of 15°C/minute. A sample was held at the highest temperature for 1 minute before cooling it down to ambient conditions.

4.2.6.7 Gel Permeation Chromatography (GPC) analysis

The weight-average molecular weight (M_w) and number-average molecular weight (M_n) of untreated and pretreated lignin were measured by GPC after acetylation, as previously described (Li et al., 2019). Briefly, lignin derivatization was conducted employing ~3 mg lignin in 1.00 mL of pyridine/acetic anhydride (1:1 *v/v*) in the dark at room temperature for 24 h, 200 RPM. The solvent/reagents were removed by co-evaporation at 45°C with ethanol several times, using a rotatory evaporator until dry. The resultant acetylated lignin was dissolved in tetrahydrofuran (THF), and the solution was filtered through a 0.45 μm membrane filter before GPC analysis. Size-exclusion separation was performed on an Agilent 1200 HPLC system (Agilent Technologies, Inc, Santa Clara, CA, USA) equipped with Waters Styragel columns (HR0.5, HR3, and HR5E; Waters Corporation, Milford, MA, USA). A UV detector (270nm) was used for detection. THF was used as the mobile phase at a flow rate of 0.3 mL/min. Polystyrene narrow standards were used for establishing the calibration curve. Acetylated samples were measured in duplicates, and the average values were reported. The bio-oils from lignin depolymerization are readily dissolved in THF for GPC analysis without acetylation. The sample solution was filtered through a 0.45 μm membrane filter before GPC analysis.

4.2.6.8 GC-MS/FID

An aliquot from liquid product mixture from depolymerization was filtered with a 0.2μm nylon filter and then subjected to analysis with gas chromatography. GC-MS analysis was performed with an Agilent 7890A GC/5975C MS system (Agilent Technologies, Santa Clara, California, USA). The instrument was equipped with a DB-1701 column (30 m; 0.25 mm i.d.; 0.25 mm film thickness). Ultra-high purity (99.999%) helium was used as a carrier gas, supplied by Airgas Inc. (Charlotte, North Carolina, USA). GC system was connected to Polyarc® system (Activated Research Company, Minnesota, USA). Sample vapors were sent through the Polyarc® catalyst before being analyzed with a flame ionization detector (FID). GC column was kept at 50°C for 2

minutes and then ramped up to 280°C at a rate of 4°C/minute and held there for 1 minute. A 5µL injection with split-less mode was used. Compounds were identified by comparing their mass spectra with those for pure compounds from NIST library, retention times, and verifying the formation of similar compounds from the literature. Creosol was consistently seen in the lignin depolymerization product, and hence its FID peak was used as the internal standard. The yield of individual products was calculated as per Equation 4.1 and Equation 4.2 as per Polyarc® guidelines ("Quantification with the Polyarc ®," n.d.).

$$Mass\ yield\ of\ a\ compound\ in\ \ lignin\ depolymerization\ product\ (wt\%\ of\ initial\ dry\ lignin) = \frac{Concentration\ of\ the\ compound\ in\ aliquot\ x\left(\frac{weight\ of\ the\ total\ product\ solution}{100}\right)x100}{weight\ of\ initial\ moisture-free\ lignin} \quad \textit{(Equation 4.1)}$$

$$The\ concentration\ of\ a\ compound\ in\ the\ aliquot\ (\text{wt\%}) = \left(\begin{matrix}\text{Concentration of creosol calculation with a standard}\\ \text{calibration curve}\end{matrix}\right) x \left(\frac{Methanizer - FID\ area\ of\ the\ compound}{Methanizer - FID\ area\ of\ creosol}\right) x \left(\frac{The\ molecular\ weight\ of\ the\ compound}{Molecular\ weight\ of\ creosol}\right) x \left(\frac{Number\ of\ carbon\ atoms\ in\ creosol}{Number\ of\ carbon\ atoms\ in\ the\ compound}\right) \quad \textit{(Equation 4.2)}$$

4.3 Results and discussion

4.3.1 Proximate and ultimate analyses

Proximate analysis of organosolv lignin extracted from poplar (~8 wt% yield based on dry poplar) revealed its fixed carbon content to be 16.2 wt% (based on dry lignin), up from 8.1 wt% in raw biomass (Table 4.1). Fixed carbon content remained almost the same at 16.7 wt% after pretreatment. However, the ash content of pretreated lignin was higher at 2.1 wt%, up from 1.4 wt% of untreated lignin, which likely happened because of a reduction in volatile combustible matter of lignin. The oxygen content of pretreated lignin went up to 29.7 wt% (dry, ash-free basis) from 22.5 wt% (dry, ash-free basis) in untreated organosolv lignin. From the proximate analysis results, it is proposed here that a small fraction of volatile components of lignin was lost during pretreatment. The oxygen content measurements suggested that the process of aerobic oxidation simultaneously occurred during pretreatment. Phenol amount required to modify lignin was previously reported to be optimal at 70 mmol phenol per mmol of lignin (0.8 g phenol/ g lignin)

(Arturi et al., 2017; Nanayakkara et al., 2014b). Since pretreatment was performed under air, alkaline aerobic conditions suitable for lignin oxidation were present (Schutyser et al., 2018). It was also reported that phenol's action under an oxidative environment was helpful in preventing recondensation reactions (Toledano et al., 2014) . The primary mechanism for lignin oxidation could be carbonyl (C=O) group formation on the side chain, which would have blocked the reactive site from undergoing recondensation (Schutyser et al., 2018).

Table 4.1 Proximate and ultimate analysis of raw and pretreated organosolv lignin

Proximate analysis (Wt%)	**Raw biomass (Poplar)**	**Organosolv lignin**	**Pretreated lignin (under air)**
Moisture content, as-received basis	3.9 ± 0.0	1.2 ± 0.0	1.7 ± 0.0
Volatile combustible matter, dry basis	91.2 ± 0.2	82.4 ± 0.1	81.3 ± 1.5
Ash, dry basis	0.7 ± 0.2	1.4 ± 0.7	2.1 ± 0.3
Fixed carbon, dry basis	8.1 ± 0.1	16.2 ± 0.1	16.7 ± 1.3
Elemental composition, dry ash-free basis (Accounted for hydrogen from the moisture)			
C	49.8 ± 0.9	70.2 ± 0.2	63.6 ± 0.0
H	7.5 ± 0.3	7.0 ± 0.1	6.3 ± 1.2
N	1.5 ± 0.0	0.2 ± 0.0	0.1 ± 0.0
S	0.1 ± 0.0	0.2 ± 0.0	0.3 ± 0.2
O (by difference)	41.3 ± 1.2	22.5 ± 0.3	29.7 ± 0.1
H/C (molar)	1.8	1.2	1.2
O/C (molar)	0.6	0.2	0.4

4.3.2 FTIR analysis

FTIR analysis of untreated organosolv and pretreated lignin is shown in Figure 4.3. Peaks indicating OH groups and C-H stretching or vibrations of methyl and methoxyl groups in 3500 – 2300 cm^{-1} region show only a slight increase after pretreatment. This result could indicate hydroxyl groups of lignin at certain positions could have been replaced by hydroxyl group of phenol in equal molar proportions, and no net increase in it is expected. However, unconjugated C=O vibrations at 1708 cm^{-1} decreased after pretreatment. This result is an unwanted side-reaction during pretreatment, which was expected to be small due to the mild temperature of 80ºC used for pretreatment. Analysis of residual filtrate separated after pretreatment shows an accumulation of phenol in it. Aromatic skeletal vibrations in lignin coming from C=C stretching seen at 1592 cm^{-1} and 1511 cm^{-1} decreased after pretreatment. This could be due to the aromatic ring shielding of lignin resulting from phenol attaching to it. Aromatic ring peaks are seen at 1461 cm^{-1}, and 1422 cm^{-1} increased after pretreatment. There was no change in condensed guaiacol structures of lignin which was suggested by the unchanging peak intensity at 1326 cm^{-1}, in C-C and C-O at 1215 cm^{-1}, in C=O stretch of Hibbert ketones resulting from β-O-4 cleavage, in syringyl ring breathing seen at 1115 cm^{-1} or in deformation of aromatic C-H plane at 1028 cm^{-1}. However, guaiacyl ring and C-O stretching in lignin at 1268 cm^{-1} were seen to decrease, which again suggests that demethoxylation might have occurred to a small extent during pretreatment.

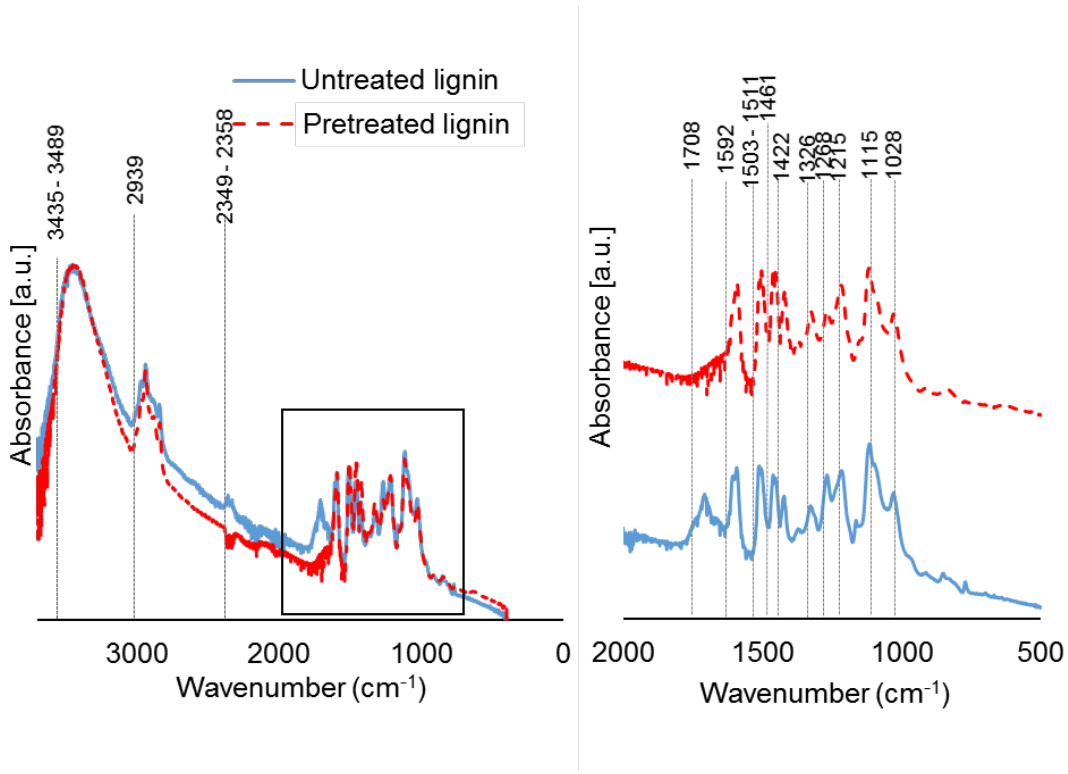

Figure 4.3 FTIR spectra of untreated and pretreated organosolv lignin

4.3.3 Thermogravimetric analysis

TGA and DTG curves obtained for untreated and pretreated organosolv lignin are shown in Figure 4.4. It can be seen from this data that pretreated lignin exhibited a generally lower temperature of thermal degradation than untreated organosolv lignin. This result is evident from the TGA curve, where complete degradation occurred at a higher temperature for untreated organosolv lignin (~650°C) than for pretreated lignin (~600°C). The DTG curve also shows that the temperature for the fastest degradation was higher for untreated organosolv lignin (~600°C) than for pretreated lignin (~550°C). Also, for the untreated organosolv lignin, a peak indicating another higher value for degradation rate was seen at 350°C, which was absent in pretreated lignin, suggesting a more uniform lignin degradation. Previously, lignin degradation has been reported to occur in a wide temperature range, specifically between 100–900°C (Yang et al., 2007; Zhou et al., 2015a). In the present study, solvent liquefaction was used for lignin depolymerization, which enabled the thermal degradation of lignin to be performed at a lower temperature (300°C) than in the TGA analysis. However, the trend seen in the TGA results can also be extended to the range

temperatures (0°C to 300°C) experienced by lignin during the liquefaction process. Overall, the pretreatment resulted in lignin more susceptible to rapid thermal degradation.

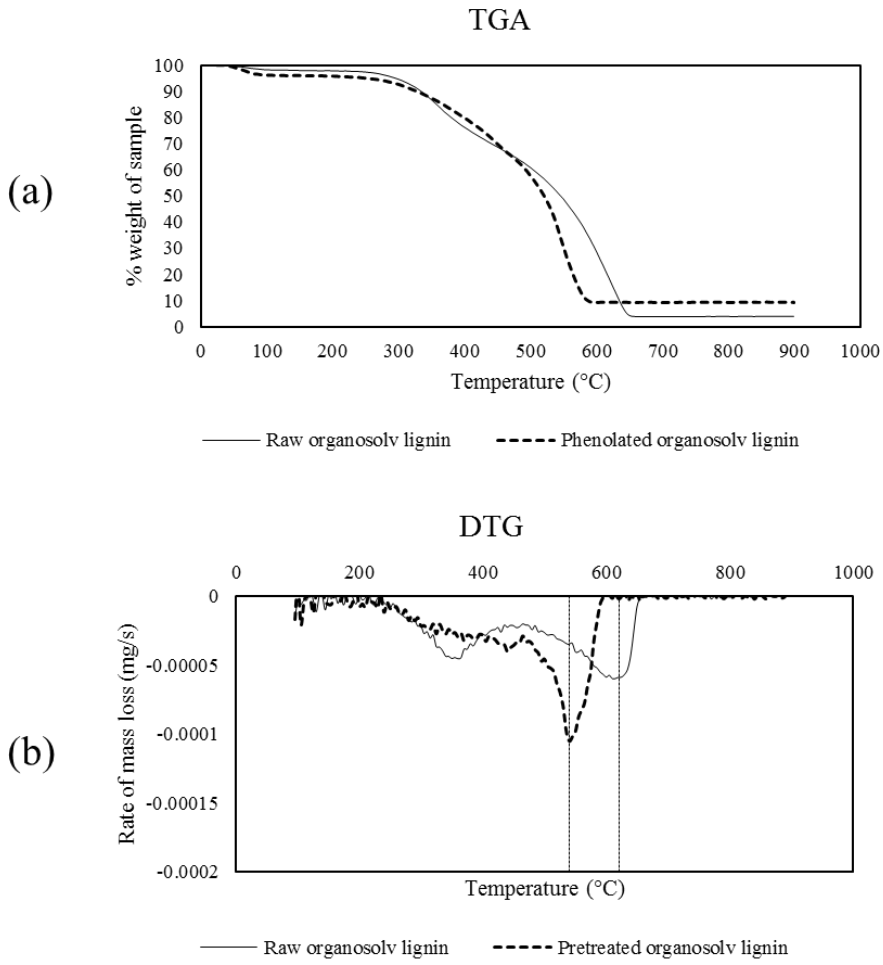

Figure 4.4 (a) Thermogravimetric analysis, TGA and (b) derivative thermogravimetry, DTG analysis of raw and pretreated organosolv lignin

4.3.4 Gel Permeation Chromatography (GPC)

Table 4.2 shows the molecular weights of untreated and pretreated lignin, as well as that of the bio-oil. The molecular weight (Mw) of organosolv lignin increased from 2420 g mol^{-1} to 3581 g mol^{-1}, respectively, after the pretreatment. However, the bio-oil from pretreated lignin had similar molecular weights (1158 and 734 g mol^{-1}, Mw and Mn) compared to the bio-oil from untreated lignin (1174 and 714 g mol^{-1}, Mw and Mn). Similarly, even though the polydispersity index (PDI)

of pretreated lignin was higher (2.6) than that of untreated lignin (2.3), the PDI of resulting bio-oil from both lignins was equal (1.6). The molecular weight (Mw) values for organosolv lignin observed here are lower than those reported for milled wood lignin (~20,000 g mol^{-1}) or Kraft lignin (~3,300-6,500 g mol^{-1}) as expected (Asikkala et al., 2012). Overall, the molecular weight data suggests two main effects. First, the pretreatment with phenol is mild enough to prevent any lignin depolymerization occurring during the pretreatment stage itself. Second, the high M_w and M_n for bio-oils indicate that the depolymerization product consists of long-chain oligomers in addition to phenolic monomers.

Table 4.2 The weight-average (Mw) and number-average (Mn) molecular weights, and polydispersity index (PDI) of lignins and products measured with gel permeation chromatography (GPC)

	Mw (g mol^{-1})	**Mn (g mol^{-1})**	**Polydispersity index (PDI)**
Untreated organosolv lignin	2420.0 ± 8.0	1045.5 ± 1.5	2.3 ± 0.0
Pretreated organosolv lignin	3580.5 ± 92.5	1353 ± 11.0	2.7 ± 0.1
Untreated organosolv lignin bio-oil	1173.5 ± 33.5	714 ± 22.0	1.6 ± 0.0
Pretreated organosolv lignin bio-oil	1157.5 ± 13.5	734 ± 3.0	1.6 ± 0.0

4.3.5 NMR spectroscopy

4.3.5.1 *2D-HSQC NMR*

^{1}H-^{13}C 2D-HSQC NMR spectrum of untreated organosolv lignin is shown in Figure 4.5. The spectrum shows the presence of typical features of lignin reported in the literature (Nishimura et al., 2018; Tarmadi et al., 2018b). These include monolignol units such as syringyl and guaiacyl units, as well as inter-unit linkages such as β-β, β-5, and β-O-4.

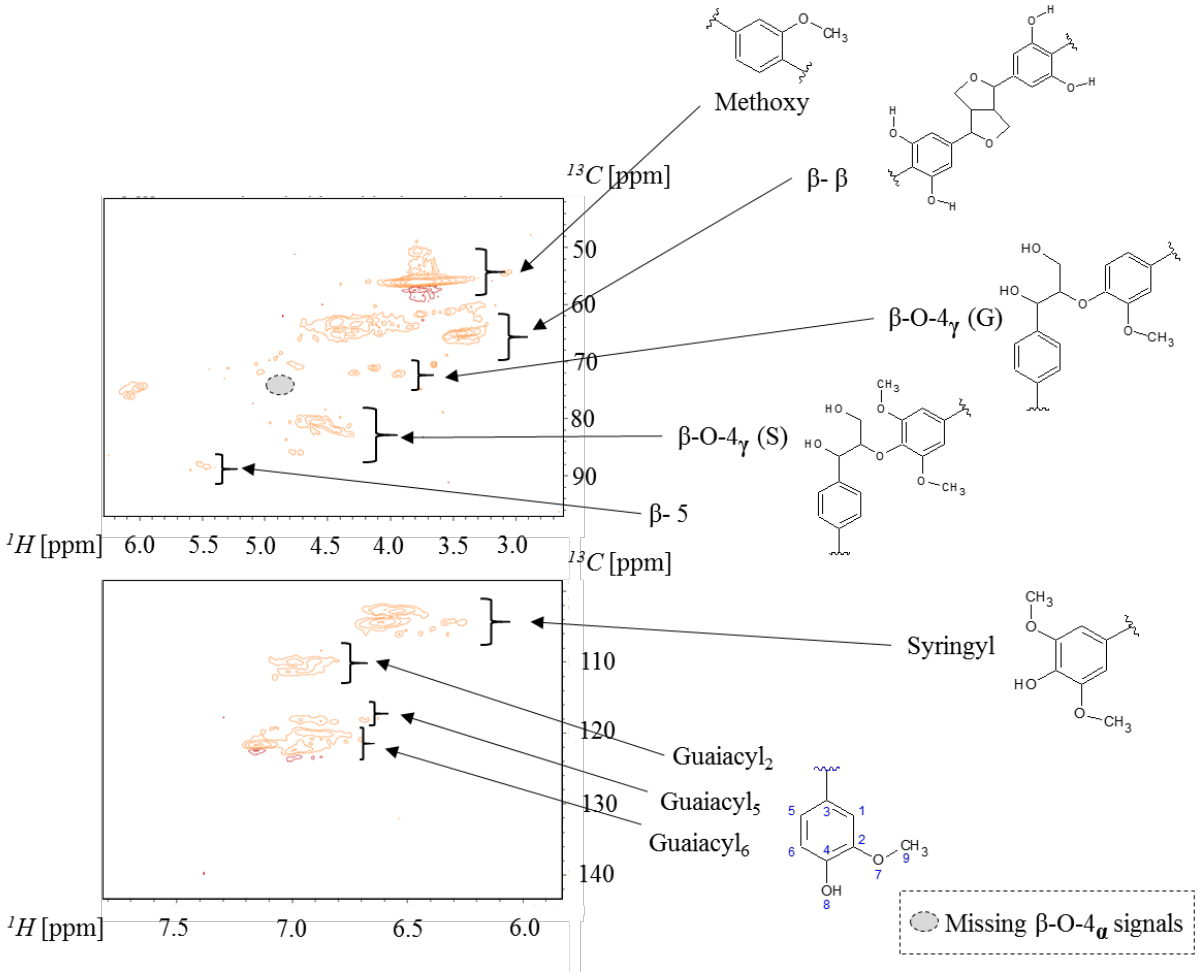

Figure 4.5 Structural features of poplar organosolv lignin detected with ^{1}H-^{13}C 2D-HSQC NMR spectrum

Quantification of various functional groups seen in the lignin structure was compared to literature values and is shown in Table 4.3. Overall, the β-O-4 linkage in lignin was more abundant than other linkages and might be responsible for giving rise to phenolics seen in lignin depolymerization products. S/G ratio calculated for lignin in this study was 1.9, which was slightly higher than that from literature (Cheng et al., 2020). However, this factor did not prevent monomeric product formation, supporting the conclusion of a recent study that contended the correlation of monomer yields with the S/G ratio of poplar lignin in the feed (Anderson et al., 2019).

Table 4.3 Linkage ratio of lignins calculated using 2D HSQC-NMR

Linkage	δH/δC (ppm)		Linkage ratio (%)	
			Poplar lignin (this study)	Poplar lignin (from (Cheng et al., 2020))
β-5	3.0-4.0/ 50.0-55.0		<1	~2
β-O-4	3.1-4.2/ 55.0-65.0		97	82
β-β	3.8-4.6/ 70.0-75.0		2	16
S-type structures	6.2-7.0/ 100.0-110.0		65	62
G-type structures	6.5-7.3/ 110.0-120.0		35	38
S/G ratio			1.8	1.6

2D-HSQC spectra of untreated and pretreated lignin, as well as that of depolymerization product, are compared in Figure 4.6. It can be seen from the spectra that the typical organosolv extraction method itself results in a relatively condensed lignin structure, affecting the availability of cleavable linkages during subsequent depolymerization. This is evident from the absence of α-signals for β-O-4 linkages and the lower intensity of HSQC signals. For a better understanding of lignin β-O-4 linkages, γ signals are also considered in addition to the α-signals. A higher intensity of signals was seen from distinct functional groups (δ_C/δ_H: 90-60/2.5-6.5 ppm) in depolymerization products. This result indicates that pretreated lignin effectively prevented itself from undergoing recondensation. Also, newly introduced phenoxyl groups (δ_C/δ_H: 128-134/7.1-8.0 ppm) were a result of oligomerization of lignin, as hypothesized from proposed reaction chemistry from literature (Gan and Pan, 2019). However, C_4 attack seems to have stopped during the pretreatment step after attaching the phenoxyl group to lignin, rather than proceeding for subsequent bond-cleavage due to the mild conditions. This result was verified by analyzing the filtrate from the pretreatment, which had only residual phenol, rather than any other lignin-derived products. . It can be hypothesized that after the phenolation step, guaiacyl groups in lignin might have been transformed into catechoyl-like structures having two -OH functionalities through a radical decomposition (Schuler et al., 2019). This result can also be attributed to the different functionalities made available in pretreated lignin formed by the redistribution mechanism (Saito et al., 2003). Signals at δ_C/δ_H: 59.9/ 3.22–3.57 ppm indicate Cγ-Hγ_1, Hγ_2 moiety of lignin

(Nishimura et al., 2018). These signals were seen to be reduced in pretreated lignin compared to untreated organosolv lignin, indicating capping of certain sites due to biaryl formation.

The way phenol modifies lignin structure can be understood by focusing on reasons for selecting reagents for this particular pretreatment. Introducing more phenolic structures in lignin can make it more susceptible to thermochemical degradation. This approach was previously seen in the thermal degradation of specific polymers but was not attempted for lignin. The use of 2,6-dimethylphenol (DMP) to depolymerize PPO through a radical-based mechanism was possible with Cu/pyridine catalyst (Saito et al., 2003). However, this process could only give oligomers, and getting monomers was still challenging. Using ethylenediamine-N,N,N′,N′-tetraacetic acid (EDTA) as a catalyst helped apply this strategy for lignin depolymerization (Nanayakkara et al., 2014c). Using 4-tert-butyl-2,6-dimethyl-phenol (TBDMP) instead of phenol was shown to be better for this purpose due to a blocked *para* position (Nanayakkara et al., 2014a). Although molecular weight (M_w) of lignin was observed to decrease with this approach from 8500 g mol^{-1} to 4700 g mol^{-1} by changing the solvent to an ionic liquid, the product was still in an oligomeric form (Nanayakkara et al., 2014c). To enable phenolic monomer formation, the phenol-pretreatment approach with a relatively higher temperature (160°C in place of 80°C) was used (Gan and Pan, 2019; Nanayakkara et al., 2014c). This strategy led to phenolic monomers, but the amount of phenol used was 3-times the weight of lignin (Gan and Pan, 2019). The current study reiterates a lower pretreatment temperature of 80°C that enables grafting of phenoxyl groups at selective sites without breaking lignin inter-unit linkages. Also, phenol recovery with water and diethyl ether washing could enable phenol recycling.

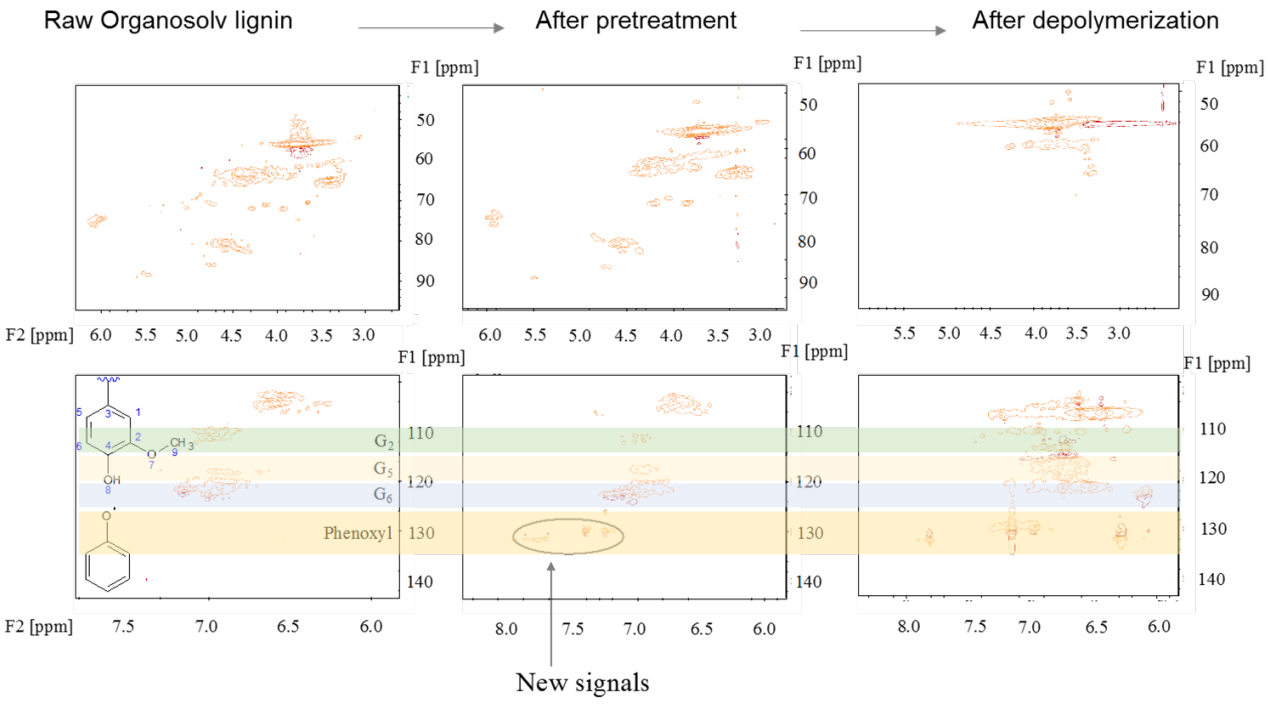

Figure 4.6 Lignin transformation tracked through pretreatment and subsequent depolymerization using ^{1}H-^{13}C 2D-HSQC NMR spectra.

4.3.5.2 ^{31}P NMR

^{31}P-NMR results of untreated organosolv and pretreated organosolv lignin are shown in Table 4.4. After the pretreatment, lignin was first washed only with excess water, and total hydroxyl group concentration increased from 7.6 mmol g^{-1}-lignin to 18.7 mmol g^{-1} lignin. In the final stage, pretreated lignin was washed with excess diethyl ether (DEE) to remove phenol attached with weak forces, reducing the total hydroxyl group content to 10.8 mmol g^{-1} lignin. This value was greater than the total hydroxyl group concentration of the original lignin. Hydroxyl concentration increased in the pretreated lignin, but aliphatic were decreased after the pretreatment, indicating biaryl formation on aliphatic groups. Additionally, after the depolymerization, total hydroxyl group concentration increased to 15.7 mmol g^{-1} bio-oil.

Table 4.4 Changes in hydroxyl group concentration of lignin after the pretreatment and subsequent depolymerization

	Untreated lignin	Pretreated lignin washed only with water	Pretreated lignin washed with water and DEE	Depolymerized lignin
	OH concentration (mmol g^{-1} lignin)			
Aliphatic	4.6	5.2	3.7	6.2
Phenolic	2.9	3.7	3.8	7.1
Carboxylic	0.1	9.9	3.3	2.4
Total	7.6	18.7	10.8	15.7

4.3.6 GC-MS/FID characterization

The GC-MS/FID characterization of the liquid product from lignin depolymerization revealed several monomeric products, including aliphatic and aromatic compounds. The GC-MS spectra obtained from depolymerization of untreated organosolv lignin and pretreated organosolv lignin are shown in Figure 4.7. Only the 20 peaks with the largest peak areas are labeled, whereas more peaks were considered for the analysis. The control experiment is compared with the CTH of pretreated lignin to assess the pretreatment effect. The spectra revealed that the untreated and pretreated organosolv lignin result in a different set of compounds on depolymerization. Pretreated lignin produced a higher number of depolymerization products than untreated organosolv lignin, as seen from the higher number of peaks representing distinct compounds in the spectrum. Also, the formation of an aromatic dimer, also known as biaryl, was possible only from the pretreated lignin. But its peak is not indicated in the spectrum, as it was much smaller compared to the other peaks. Phenolic monomers, one-ring aromatics, and aromatic dimers were the result of lignin ether bond cleavage. Whereas, aliphatic compounds such as esters, linear alkanes, cycloalkanes, and alkenes were also present in the liquid products, which were the residual modified wood extractives. The blank experiment was used to identify the products that might be generated with the degradation of residual phenol or the solvent. From the blank experiment, it was found that phenol (70.6 wt%), benzene, ethoxy- (9.3 wt%), phenol, 2-ethyl- (8.3 wt%), and 4-propyl-1,1'-diphenyl (<0.1 wt%) were the 4 main phenol-derived products. The blank study helped to confirm

that the newly seen products with pretreated lignin were not the results of any residual phenol in the system but were indeed lignin-derived compounds. Also, the gases produced in the reaction mainly consisted of nitrogen (from the initial pressurization of the reactor), ~8 wt% H_2 and a small quantity of n-butane (<3%).

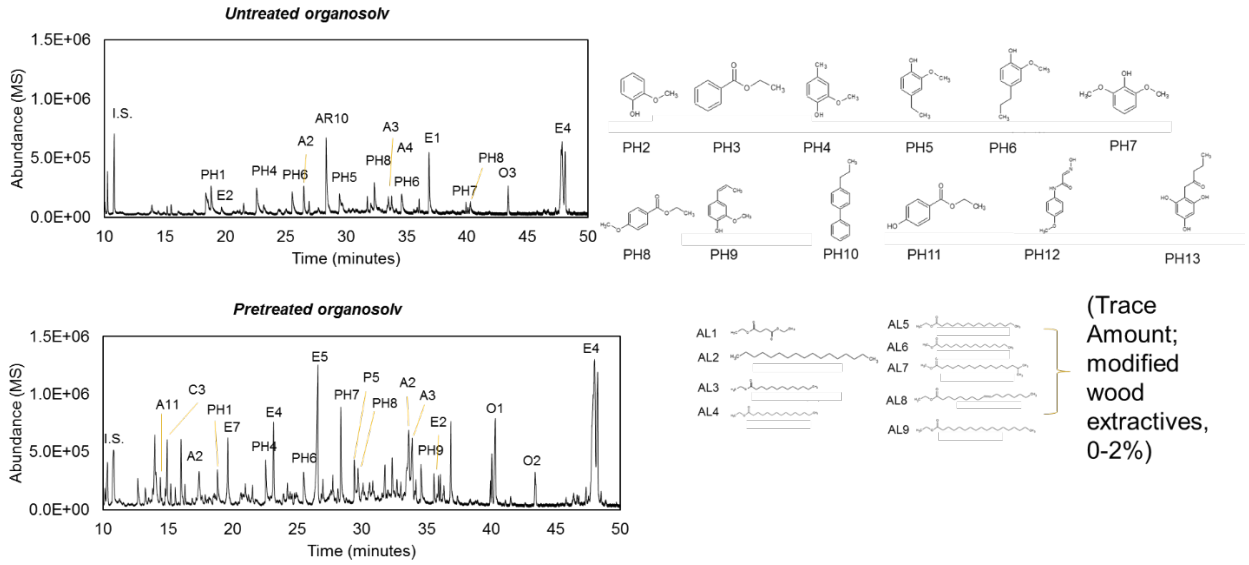

Figure 4.7 GC-MS spectra of depolymerization products from 'untreated organosolv' lignin and 'pretreated organosolv' lignin (depolymerization at 300°C, Ru/C, ethanol)

The pretreatment is responsible for biaryl formation through phenol attachment on lignin through the coupling of phenol with phenolic structure of lignin (Baran and Sargin, 2020; Yang et al., 2014). Later, the some of the attached phenol molecules getting released from lignin could have also attacked the carbon near the C_4 position on the lignin aromatic ring (Saito et al., 2003). This could have cleaved the lignin interunit linkages, resulting in a decreased chain length. Subsequent iterations of this reaction could produce monomer or dimers, but the primary reaction responsible for the depolymerization of lignin in this study was catalytic transfer hydrogenolysis. During this process, the ether linkages in lignin were effectively cleaved to form unstable structures with unsaturated bonds on the lignin side chain, which on rearrangement result in stable monomeric compounds (Roberts et al., 2011).

A comparison of product yields from the depolymerization of untreated organosolv and pretreated organosolv lignin is shown in Figure 4.8. The net result was an increase of ~ 14 % in phenolic monomers (excluding phenol) from pretreated lignin depolymerization compared to the untreated organosolv lignin depolymerization. The pretreatment resulted in ~ 27% lower average amount of char compared to the depolymerization of untreated lignin. It was seen that the bio-oil yield based on dry lignin increased from 26.5 wt% to 50.9 wt% after the pretreatment. However, during the pretreated lignin depolymerization, the oligomeric fraction in bio-oil could have been even higher. The amount of 'residual' phenol (wt% based on initial dry lignin) and the phenol produced from lignin was subtracted from the liquid bio-oil yield.

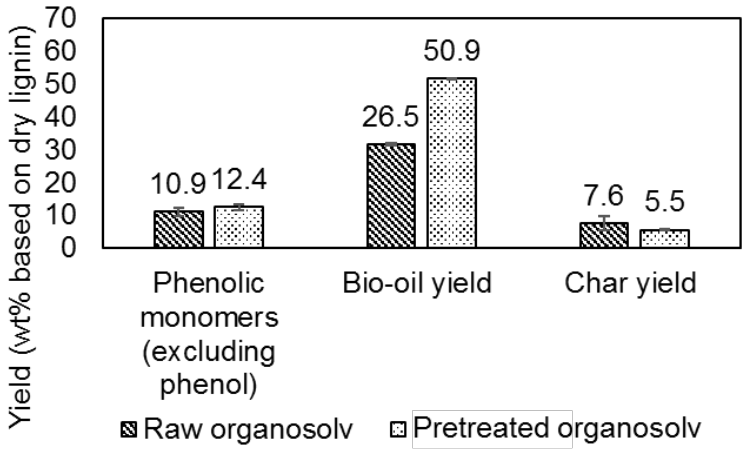

Figure 4.8 Product yields from the depolymerization of untreated and pretreated organosolv lignin

A comparison of individual compound yields common in both the untreated and pretreated lignin depolymerization products is shown in Table 4.5. Some of the product yields were increased, whereas that of others decreased, suggesting altered reaction pathways. Phenol has been known to act as a stabilization agent for the reactive fragments produced from lignin (Toledano et al., 2014). The product yields suggested that the stabilization reaction occurred with a similar effect using pretreated lignin compared with that reported in other strategies (Kim and Kim, 2018; Shuai and Saha, 2017). Pretreated lignin resulted in a different route for the release of phenol moiety, which ended up in phenolic dimers, rather than the single phenol molecule, as evidenced from the first row of Table 4.5. The phenolic monomer yield based on dry lignin excluding phenol was higher

with pretreated lignin (12.4 wt%) than untreated lignin (10.9 wt%). Pretreated lignin curbed the aliphatics formation, shifting the product yields towards phenolics and aromatics. Bio-oil and char yields alone could not explain the entire mass balance, and hence the formation of gases and oligomers needs to be studied more closely. Prior studies suggested that the lignin-derived bio-oil had 50 – 70% oligomers (Anderson et al., 2019).

Table 4.5 Total yields of compounds obtained from the depolymerization of raw and pretreated organosolv lignin

	wt% of lignin				
	Raw organosolv		**Pretreated organosolv (under air)**		
	Avg	**SD**	**Avg**	**SD**	**Increase (%)**
Total monomers	19.2	0.7	13.2	1.2	-
Phenol	4.8	1.9	0.7	0.2	-
Total monomers (excluding phenol)	14.4	2.6	12.5	1.0	-
Phenolic monomers (excluding phenol)	10.9	1.2	12.4	1.0	14
Bio-oil yield	26.4	1.3	50.9	0.2	92
Char yield	7.6	2.2	5.5	0.1	-27

[Yields of individual compounds are given in the supplementary information]

4.3.7 Compositional analysis

Lignin content measurement and compositional analysis of untreated and pretreated organosolv lignins were performed to confirm the role of carbohydrate impurities. Acid-soluble and insoluble lignin contents of untreated organosolv and pretreated organosolv lignin are listed in Table 4.7. It was seen that organosolv lignin samples could contain about 10–12 wt% of

impurities, which are retained even after ethanol washing after the organosolv process, and water/diethyl ether washing after pretreatment.

Table 4.6 Lignin content measurement of samples

Sample	AIL, wt %	UV_{abs}	M.C., wt%	ODW, mg	ASL, wt%	Extractives, wt %	Total lignin, wt.%	Total lignin, wt.% (Average)	Total lignin, wt.% (S.D.)
OL1	91.7	0.4	1.2	296.4	4.1	0.1	95.7	95.1	0.6
OL2	91.2	0.3	1.2	296.4	3.4	0.1	94.5		
POL 1	92.7	0.2	3.0	291.0	2.2	0.1	94.8	95.4	0.6
POL 2	93.5	0.2	3.0	291.0	2.6	0.1	96.0		
P1	22.4	0.7	2.0	293.9	7.7	0.1	30.1	28.7	1.4
P2	22.6	0.4	2.0	293.9	4.8	0.1	27.3		

[OL 1: Organosolv lignin_replica 1; OL 2: organosolv lignin_replica 2; POL 1: pretreated organosolv lignin_replica 1; POL 2: pretreated organosolv lignin_replica 2; P1: raw poplar_replica 1; P2: raw poplar_replica 2; AIL: acid insoluble lignin; M.C.: moisture content, wet basis; ODW: oven dry weight, ASL: acid soluble lignin]

Residual carbohydrates in lignin were quantified as per the NREL method (Sluiter et al., 2008b). The results are shown in Table 4.8. It was found that the untreated organosolv lignin had 2.9 wt% total sugars on a dry basis. Whereas the pretreated organosolv lignin had 7.2 wt% total sugars on a dry basis. The pretreated lignin produced a lower amount of total aliphatics (<0.1 wt%) compared to that from untreated organosolv lignin (0.7 wt%). This is even though the pretreated lignin had a higher amount of sugar impurities. It suggests that pretreatment suppressed the tendency of lignin to produce any additional aliphatic compounds from sugars other than those produced from residual wood extractives.

There was a shift in product selectivity as a result of the pretreatment. Even though some standard deviation was seen in the yields of individual compounds from lignin (as previously seen from Table 4.5), the combined yields of total monomers and phenolic monomers had a low standard deviation. This indicated that pretreatment was altering the depolymerization routes. The products reported here surely include extractives-derived carbohydrate compounds. The organosolv lignin was washed with deionized water to remove the water-soluble impurities. However, some of the impurities remained in lignin, resulting in overall lower yield values of other desired products reported based on the initial lignin amount. Calculating the yields based on Klason lignin content in the future can help overcome the challenges in accurate quantification of monomer yields (Phongpreecha et al., 2017).

Table 4.7 Sugar analysis in raw and pretreated organosolv lignin samples

Sample	**Amount, wt% based on dry weight of lignin**									
	Glucose		**Galactose**		**Arabinose**		**Mannose**		**Total**	
	Avg	S.D.	Avg	S.D.	Avg	S.D.	Avg	S.D.	Avg	S.D.
OL1	0.2	0.2	1.4	0.1	1.2	0.3	0.0	0.0	2.9	0.1
OL2	0.5	<0.1	1.4	<0.1	1.1	0.2	0.0	0.0		
POL 1	0.0	0.0	4.4	0.2	2.9	0.1	0.0	0.0	7.2	0.2
POL 2	0.0	0.0	4.4	<0.1	2.7	0.4	0.0	0.0		

[Avg: average of two measurements; S.D.: standard deviations; OL 1: Organosolv lignin 1; OL 2: Organosolv lignin 2; POL 1: Pretreated Organosolv lignin 1; POL 2: Pretreated Organosolv lignin 2; P1: Raw poplar 1; P2: Raw poplar 2]

4.3.8 Exclusive products from pretreated lignin

There were several compounds produced exclusively with the depolymerization of pretreated lignin, as shown in Figure 4.9. Previously, adding phenol to the lignin liquefaction medium was shown to produce phenolic dimers, anisolic dimers, and two-ring non-condensed aromatic dimers (Arturi et al., 2017). In the present study, two-ring, non-condensed aromatics such as 1-benzyl-4-ethylbenzene were detected from pretreated lignin depolymerization products,

which were the result of biaryl formation. Arturi et al. explained the fate of phenol added to the reaction medium with dimers of anisolic nature, such as 9H-xanthene (Arturi et al., 2017). However, no dimers of anisolic nature were observed in the current study. This could prevent the reaction of free phenol with the lignin depolymerization products that lead to toxic compounds by using phenol in the pretreatment step. Multiple compounds detected with mass spectrometry had sulfur in them, which can be due to the impurities in pretreated lignin. However, the verification of these compounds was not possible due to the unavailability of pure compounds with these pure compounds in the market.

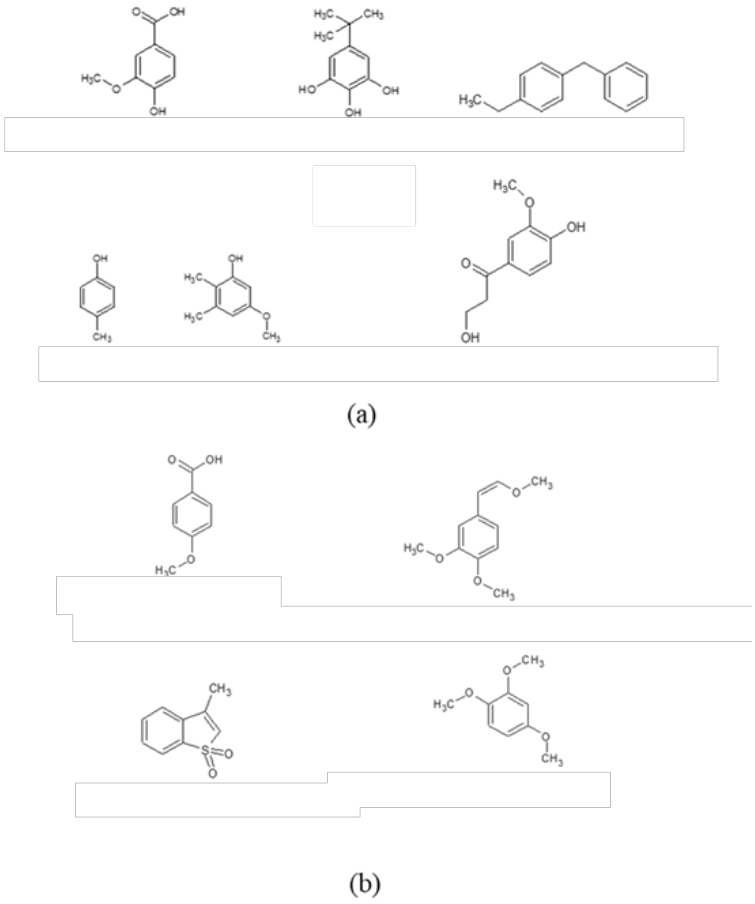

Figure 4.9 Unique products from the depolymerization of pretreated lignin (a) phenolics (b) aromatics

Some of the compounds produced from the depolymerization of pretreated lignin were found to have several applications, which are summarized in Table 4.9. It is yet another feature of

the pretreatment applied for lignin depolymerization that the final products are more likely to be free of toxic contamination of free phenol. In contrast with the scheme where phenol is directly added to the lignin liquefaction medium, the lignin pretreated with phenol can result in uniquely substituted phenolic groups in the lignin moiety, eliminating the chances of residual phenol in the final product.

Table 4.8 Applications of compounds produced from the depolymerization of lignin pretreated with phenol

Compound	Uses	Yield (wt% of dry pretreated lignin)	Reference
Phenolics			
Phenol, 4-methyl-	Flavoring Agent	2.1 ± 0.4	("PubChem Database. P-Cresol, CID=2879," n.d.)
Benzoic acid, 4-hydroxy-3-methoxy-	Flavoring Agent, Astringent, Vanilla, Drug, Human metabolite	2.5 ± 0.0	("PubChem Database. Vanillic acid, CID=8468," n.d.)
Aromatics			
Benzoic acid, 4-methoxy-	Flavoring Agent, Savory, Adjuvant	0.1 ± 0.1	("PubChem Database. 4-Methoxybenzoic acid, CID=7478," n.d.)
1,2,4-trimethoxybenzene	Pesticide (biochemical, biocide)	0.1 ± 0.1	("PubChem Database. 1,2,4-Trimethoxybenzene, CID=67284," n.d.)

Pretreated lignin could have undergone unique reactions due to the selective capping of particular sites on the lignin moiety. Pretreatment with phenol is expected to lead to biaryl formation, consuming phenol, and leading to modified lignin in the process (Baran and Sargin, 2020; Han et al., 2009). Hence, reinventing the stabilization strategy is possible with lignin-derived phenol by using it as a pretreatment reagent. A clever blend of stabilization and alkaline aerobic

oxidation of lignin can be achieved with this pretreatment strategy (Belkheiri et al., 2018; Wouter Schutyser et al., 2018). Keeping the pretreatment and depolymerization steps separate can also enable the optimization of each stage individually and allows studying the effect of each step independent of the other. However, it is also important to note that there can be several positive or negative synergistic effects of combining the pretreatment and depolymerization steps, which could not be explored with the experimental strategy of this study. Additionally, organosolv lignin itself is known to be a condensed form of lignin due to the harsh acidic conditions used for its extraction. Hence, performing the pretreatment during the organosolv process itself can also be tried in the future studies.

4.3.9 Pretreatment with phenol under inert and oxidative conditions

Pretreatment with phenol under air also resulted in increased oxygen content of lignin from 27.5 wt% to 30.9 wt% (dry ash-free basis), as was previously seen from Table 4.1. Moreover, the conditions used for the pretreatment were also conducive to the alkaline aerobic oxidation of lignin, as previously reported in the literature (Schutyser et al., 2018). Hence, to examine the effect of a different atmosphere, the pretreatment was performed in either inert or oxidative conditions. Inert conditions led a further increase in the phenolic monomers to 16.2 wt% (based on dry lignin) from 12.4 wt% (based on dry lignin), as shown from Table 4.10. Under oxidative conditions, the yield was even higher, 27.3 wt% (based on dry lignin). However, the trend for the bio-oil yields was: pretreatment under air (50.9 wt%) > oxidative pretreatment (42.0 wt%) > inert pretreatment (31.6 wt%) > untreated (26.5 wt%), based on dry lignin. Pretreatment under air led to the highest bio-oil quantity among the reaction atmospheres tested, warranting an investigation of its oligomeric content. Whereas, the inert or oxidative conditions led to higher monomeric fractions.

Char formation remained nearly identical between pretreatment under air (5.5 wt% based on dry lignin) or under an inert gas (~5.5 wt%). Whereas, char increased with oxidative pretreatment (~7.4 wt% based on dry lignin), pointing to repolymerization and recondensation. Aliphatic compound yields were higher with oxidative pretreatment, compared to the inert pretreatment. Whereas, pretreatment under air produced modified lignin that suppressed the aliphatics formation. Overall, it can be said that pretreatment under oxygen is potentially more effective than that under inert gas or air. This inference is based on the higher phenolic monomer yields, which came at the

cost of increased char formation. In other words, adding oxygen during pretreatment makes sense only if the focus is on increasing the phenolic monomer yields. Pretreatment under air or inert gas is still able to suppress the char formation. Whereas, during subsequent depolymerization, the oxidative conditions used for pretreatment counteract the preventive effect on char formation.

Table 4.9 Total yields of compounds determined using GC-MS/FID for the depolymerization product of lignin pretreated under inert and oxidative conditions.

	Pretreated under inert wt% of lignin		**Pretreated under oxygen wt% of lignin**	
Compound	**Average[a]**	**S.D. [a]**	**Average[a]**	**S.D. [a]**
Total monomers	21.1	2.3	31.1	3.1
Phenol	0.8	0.1	2.3	1.2
Total GC-eluted monomers (excluding phenol)	20.3	-	28.8	-
Phenolic monomers (excluding phenol)	18.4	-	27.3	-
Bio-oil yield	31.6	1.2	42.0	0.6
Char yield	5.5	-	7.4	-

[[a] Calculated with two GC-MS/FID measurements]

4.4 Conclusion

Depolymerization of pretreated lignin resulted in a 14 % increase in the phenolic monomer yields (excluding phenol) than that from untreated lignin depolymerization. Phenolic monomer yield (excluding phenol) of 12.4 wt% with the pretreatment was comparable to directly adding phenol to the system as previously reported in the literature, which was 1.8–14.7 wt% (Arturi et al., 2017). Pretreatmentof lignin with phenol subsequently enabled effective depolymerization, as demonstrated with the yield values, which could have been a result of biaryl formation. Additionally, undesired lignin oligomerization was suppressed with the pretreatment, as seen from the 27% reduction in char yields. The formation of undesired anisolic dimers was prevented due to the absence of free phenol molecules in the system. In addition to one-ring aromatic compounds,

pretreatment enabled getting several exclusive two-ring aromatic and phenolic compounds. The overall fraction of phenolics was increased, and that of aliphatics was decreased due to the pretreatment. The remaining mass balance from lignin was attributed to gaseous products and handling losses. Biaryl formation through the coupling between phenol and the phenolic structure of lignin can potentially be a useful approach for stabilizing lignin during its depolymerization. Also, an inert or oxidative atmosphere during the pretreatment improved the phenolic monomer yield, which warrants further investigation.

4.5 Acknowledgments

The authors would like to acknowledge the United States Department of Agriculture and the National Institute of Food and Agriculture for funding this research project (Grant # USDA-NIFA-2015-67021-22842).

4.6 References

1. Anderson, E.M., Stone, M.L., Katahira, R., Reed, M., Muchero, W., Ramirez, K.J., Beckham, G.T., Román-Leshkov, Y., 2019. Differences in S/G ratio in natural poplar variants do not predict catalytic depolymerization monomer yields. Nat. Commun. 10, 2033. https://doi.org/10.1038/s41467-019-09986-1
2. Arturi, K.R., Strandgaard, M., Nielsen, R.P., Sogaard, E.G., Maschietti, M., 2017. Hydrothermal liquefaction of lignin in near-critical water in a new batch reactor: Influence of phenol and temperature. J. Supercrit. Fluids 123, 28–39. https://doi.org/10.1016/j.supflu.2016.12.015
3. Asikkala, J., Tamminen, T., Argyropoulos, D.S., 2012. Accurate and reproducible determination of lignin molar mass by acetobromination. J. Agric. Food Chem. 60, 8968–8973. https://doi.org/10.1021/jf303003d
4. Baran, T., Sargin, I., 2020. Green synthesis of a palladium nanocatalyst anchored on magnetic lignin-chitosan beads for synthesis of biaryls and aryl halide cyanation. Int. J. Biol. Macromol. 155, 814–822. https://doi.org/https://doi.org/10.1016/j.ijbiomac.2020.04.003
5. Belkheiri, T., Andersson, S.-I., Mattsson, C., Olausson, L., Theliander, H., Vamling, L., 2018. Hydrothermal Liquefaction of Kraft Lignin in Subcritical Water: Influence of Phenol as Capping Agent. Energy & Fuels 32, 5923–5932. https://doi.org/10.1021/acs.energyfuels.8b00068
6. Cheng, C., Truong, J., Barrett, J.A., Shen, D., Abu-Omar, M.M., Ford, P.C., 2020. Hydrogenolysis of Organosolv Lignin in Ethanol/Isopropanol Media without Added Transition-Metal Catalyst. ACS Sustain. Chem. Eng. 8, 1023–1030. https://doi.org/10.1021/acssuschemeng.9b05820

7. Cotana, F., Cavalaglio, G., Nicolini, A., Gelosia, M., Coccia, V., Petrozzi, A., Brinchi, L., 2014. Lignin as co-product of second generation bioethanol production from ligno-cellulosic biomass. Energy Procedia 45, 52–60. https://doi.org/10.1016/j.egypro.2014.01.007
8. Das, L., Li, M., Stevens, J., Li, W., Pu, Y., Ragauskas, A.J., Shi, J., 2018. Characterization and Catalytic Transfer Hydrogenolysis of Deep Eutectic Solvent Extracted Sorghum Lignin to Phenolic Compounds. ACS Sustain. Chem. Eng. 6, 10408–10420. https://doi.org/10.1021/acssuschemeng.8b01763
9. Gan, L., Pan, X., 2019. Phenol-Enhanced Depolymerization and Activation of Kraft Lignin in Alkaline Medium. Ind. Eng. Chem. Res. 58, 7794–7800. https://doi.org/10.1021/acs.iecr.9b01147
10. Guadix-Montero, S., Sankar, M., 2018. Review on Catalytic Cleavage of C--C Inter-unit Linkages in Lignin Model Compounds: Towards Lignin Depolymerisation. Top. Catal. 61, 183–198. https://doi.org/10.1007/s11244-018-0909-2
11. Güvenatam, B., Heeres, E.H.J., Pidko, E.A., Hensen, E.J.M., 2016. Lewis acid-catalyzed depolymerization of soda lignin in supercritical ethanol/water mixtures. Catal. Today 269, 9–20. https://doi.org/https://doi.org/10.1016/j.cattod.2015.08.039
12. Han, J., Liu, Y., Guo, R., 2009. Facile Synthesis of Highly Stable Gold Nanoparticles and Their Unexpected Excellent Catalytic Activity for Suzuki−Miyaura Cross-Coupling Reaction in Water. J. Am. Chem. Soc. 131, 2060–2061. https://doi.org/10.1021/ja808935n
13. Issa, I., Delbrück, S., Hamm, U., 2019. Bioeconomy from experts' perspectives – Results of a global expert survey. PLoS One 14, e0215917.
14. Jahromi, R., Rezaei, M., Hashem Samadi, S., Jahromi, H., 2020. Biomass gasification in a downdraft fixed-bed gasifier: Optimization of operating conditions. Chem. Eng. Sci. 116249. https://doi.org/https://doi.org/10.1016/j.ces.2020.116249
15. Kim, K.H., Kim, C.S., 2018. Recent Efforts to Prevent Undesirable Reactions From Fractionation to Depolymerization of Lignin : Toward Maximizing the Value From Lignin 6, 1–7. https://doi.org/10.3389/fenrg.2018.00092
16. Li, M., Yoo, C.G., Pu, Y., Biswal, A.K., Tolbert, A.K., Mohnen, D., Ragauskas, A.J., 2019. Downregulation of pectin biosynthesis gene GAUT4 leads to reduced ferulate and lignin-carbohydrate cross-linking in switchgrass. Commun. Biol. 2, 22. https://doi.org/10.1038/s42003-018-0265-6
17. Limarta, S.O., Ha, J.-M., Park, Y.-K., Lee, H., Suh, D.J., Jae, J., 2018. Efficient depolymerization of lignin in supercritical ethanol by a combination of metal and base catalysts. J. Ind. Eng. Chem. 57, 45–54. https://doi.org/https://doi.org/10.1016/j.jiec.2017.08.006
18. Mahadevan, R., Adhikari, S., Shakya, R., Wang, K., Dayton, D.C., Li, M., Pu, Y., Ragauskas, A.J., 2016. Effect of torrefaction temperature on lignin macromolecule and product distribution from HZSM-5 catalytic pyrolysis. J. Anal. Appl. Pyrolysis 122, 95–105. https://doi.org/10.1016/j.jaap.2016.10.011
19. Meng, X., Crestini, C., Ben, H., Hao, N., Pu, Y., Ragauskas, A.J., Argyropoulos, D.S., 2019. Determination of hydroxyl groups in biorefinery resources via quantitative 31P NMR spectroscopy. Nat. Protoc. https://doi.org/10.1038/s41596-019-0191-1
20. Meng, X., Parikh, A., Seemala, B., Kumar, R., Pu, Y., Christopher, P., Wyman, C.E., Cai, C.M., Ragauskas, A.J., 2018. Chemical Transformations of Poplar Lignin during Cosolvent Enhanced Lignocellulosic Fractionation Process. ACS Sustain. Chem. Eng. 6, 8711–8718. https://doi.org/10.1021/acssuschemeng.8b01028

21. Nanayakkara, S., Patti, A.F., Saito, K., 2014a. Chemical depolymerization of lignin involving the redistribution mechanism with phenols and repolymerization of depolymerized products. Green Chem. 16, 1897–1903. https://doi.org/10.1039/C3GC41708E
22. Nanayakkara, S., Patti, A.F., Saito, K., 2014b. Chemical depolymerization of lignin involving the redistribution mechanism with phenols and repolymerization of depolymerized products. Green Chem. 16, 1897–1903. https://doi.org/10.1039/C3GC41708E
23. Nanayakkara, S., Patti, A.F., Saito, K., 2014c. Lignin Depolymerization with Phenol via Redistribution Mechanism in Ionic Liquids. ACS Sustain. Chem. Eng. 2, 2159–2164. https://doi.org/10.1021/sc5003424
24. Nishimura, H., Kamiya, A., Nagata, T., Katahira, M., Watanabe, T., 2018. Direct evidence for α ether linkage between lignin and carbohydrates in wood cell walls. Sci. Rep. 8, 6538. https://doi.org/10.1038/s41598-018-24328-9
25. Patil, V., Adhikari, S., Cross, P., 2018. Co-pyrolysis of lignin and plastics using red clay as catalyst in a micro-pyrolyzer. Bioresour. Technol. 270, 311–319. https://doi.org/10.1016/j.biortech.2018.09.034
26. Patil, V., Adhikari, S., Cross, P., Jahromi, H., 2020. Progress in the solvent depolymerization of lignin. Renew. Sustain. Energy Rev. 133, 110359. https://doi.org/https://doi.org/10.1016/j.rser.2020.110359
27. Phongpreecha, T., Hool, N.C., Stoklosa, R.J., Klett, A.S., Foster, C.E., Bhalla, A., Holmes, D., Thies, M.C., Hodge, D.B., 2017. Predicting lignin depolymerization yields from quantifiable properties using fractionated biorefinery lignins. Green Chem. 19, 5131–5143. https://doi.org/10.1039/c7gc02023f
28. Podschun, J., Saake, B., Lehnen, R., 2015. Reactivity enhancement of organosolv lignin by phenolation for improved bio-based thermosets. Eur. Polym. J. 67, 1–11. https://doi.org/https://doi.org/10.1016/j.eurpolymj.2015.03.029
29. PubChem Database. 1,2,4-Trimethoxybenzene, CID=67284 [WWW Document], n.d. . Natl. Cent. Biotechnol. Information. URL https://pubchem.ncbi.nlm.nih.gov/compound/1_2_4-Trimethoxybenzene (accessed on Mar. 7, 2020)
30. PubChem Database. 4-Methoxybenzoic acid, CID=7478 [WWW Document], n.d. . Natl. Cent. Biotechnol. Information. URL https://pubchem.ncbi.nlm.nih.gov/compound/4-Methoxybenzoic-acid (accessed on Mar. 7, 2020)
31. PubChem Database. P-Cresol, CID=2879 [WWW Document], n.d. . Natl. Cent. Biotechnol. Information.
32. PubChem Database. Vanillic acid, CID=8468 [WWW Document], n.d. . Natl. Cent. Biotechnol. Information. URL https://pubchem.ncbi.nlm.nih.gov/compound/Vanillic-acid (accessed on Mar. 7, 2020)
33. Quantification with the Polyarc ® [WWW Document], n.d. . Http://www.activatedresearch.com/Public_Documents/Quantification%20with%20the%20Polyarc.pdf.
34. Ragauskas, A.J., Williams, C.K., Davison, B.H., Britovsek, G., Cairney, J., Eckert, C.A., Frederick, W.J., Hallett, J.P., Leak, D.J., Liotta, C.L., Mielenz, J.R., Murphy, R., Templer, R., Tschaplinski, T., 2006. The Path Forward for Biofuels and Biomaterials. Science (80-.). 311, 484 LP – 489.
35. Roberts, V.M., Stein, V., Reiner, T., Lemonidou, A., Li, X., Lercher, J.A., 2011. Towards quantitative catalytic lignin depolymerization. Chem. - A Eur. J. 17, 5939–5948. https://doi.org/10.1002/chem.201002438

36. Saisu, M., Sato, T., Watanabe, M., Adschiri, T., 2003. Conversion of Lignin with Supercritical Water - Phenol Mixtures 3124–3130. https://doi.org/10.1021/ef0202844
37. Saito, K., Masuyama, T., Oyaizu, K., Nishide, H., 2003. Depolymerization of Poly(2,6-dimethyl-1,4-phenylene oxide) under Oxidative Conditions. Chem. – A Eur. J. 9, 4240–4246. https://doi.org/10.1002/chem.200204669
38. Schuler, J., Hornung, U., Dahmen, N., Sauer, J., 2019. Lignin from bark as a resource for aromatics production by hydrothermal liquefaction. GCB Bioenergy 11, 218–229. https://doi.org/10.1111/gcbb.12562
39. Schutyser, W., Kruger, J.S., Robinson, A.M., Katahira, R., Brandner, D.G., Cleveland, N.S., Mittal, A., Peterson, D.J., Meilan, R., Román-Leshkov, Y., Beckham, G.T., 2018. Revisiting alkaline aerobic lignin oxidation. Green Chem. 20, 3828–3844. https://doi.org/10.1039/c8gc00502h
40. Shuai, L., Saha, B., 2017. Towards high-yield lignin monomer production 19. https://doi.org/10.1039/c7gc01676j
41. Sluiter, A., Hames, B., Ruiz, R., Scarlata, C., Sluiter, J., Templeton, D., 2008a. Determination of ash in biomass.
42. Sluiter, A., Hames, B., Ruiz, R., Scarlata, C., Sluiter, J., Templeton, D., Crocker, D., 2008b. Determination of structural carbohydrates and lignin in biomass. Lab. Anal. Proced. 1617, 1–16.
43. Talebi Amiri, M., Dick, G.R., Questell-Santiago, Y.M., Luterbacher, J.S., 2019. Fractionation of lignocellulosic biomass to produce uncondensed aldehyde-stabilized lignin. Nat. Protoc. 14, 921–954. https://doi.org/10.1038/s41596-018-0121-7
44. Tarmadi, D., Tobimatsu, Y., Yamamura, M., Miyamoto, T., Miyagawa, Y., Umezawa, T., Yoshimura, T., 2018a. NMR studies on lignocellulose deconstructions in the digestive system of the lower termite Coptotermes formosanus Shiraki. Sci. Rep. 8, 1290. https://doi.org/10.1038/s41598-018-19562-0
45. Tarmadi, D., Tobimatsu, Y., Yamamura, M., Miyamoto, T., Miyagawa, Y., Umezawa, T., Yoshimura, T., 2018b. NMR studies on lignocellulose deconstructions in the digestive system of the lower termite Coptotermes formosanus Shiraki. Sci. Rep. 8, 1290. https://doi.org/10.1038/s41598-018-19562-0
46. Tolbert, A., Akinosho, H., Khunsupat, R., Naskar, A.K., Ragauskas, A.J., 2014. Characterization and analysis of the molecular weight of lignin for biorefining studies. Biofuels, Bioprod. Biorefining 8, 836–856. https://doi.org/10.1002/bbb.1500
47. Toledano, A., Serrano, L., Labidi, J., 2014. Improving base catalyzed lignin depolymerization by avoiding lignin repolymerization. Fuel 116, 617–624. https://doi.org/10.1016/j.fuel.2013.08.071
48. Yang, H., Yan, R., Chen, H., Lee, D.H., Zheng, C., 2007. Characteristics of hemicellulose, cellulose and lignin pyrolysis. Fuel 86, 1781–1788. https://doi.org/https://doi.org/10.1016/j.fuel.2006.12.013
49. Yang, S., Wen, J.-L., Yuan, T.-Q., Sun, R.-C., 2014. Characterization and phenolation of biorefinery technical lignins for lignin–phenol–formaldehyde resin adhesive synthesis. RSC Adv. 4, 57996–58004. https://doi.org/10.1039/C4RA09595B
50. Zhou, H., Long, Y., Meng, A., Chen, S., Li, Q., Zhang, Y., 2015. A novel method for kinetics analysis of pyrolysis of hemicellulose, cellulose, and lignin in TGA and macro-TGA. RSC Adv. 5, 26509–26516. https://doi.org/10.1039/C5RA02715B

5. Effect of Boric Acid Capping During Biomass Fractionation on Subsequent Depolymerization of Lignin

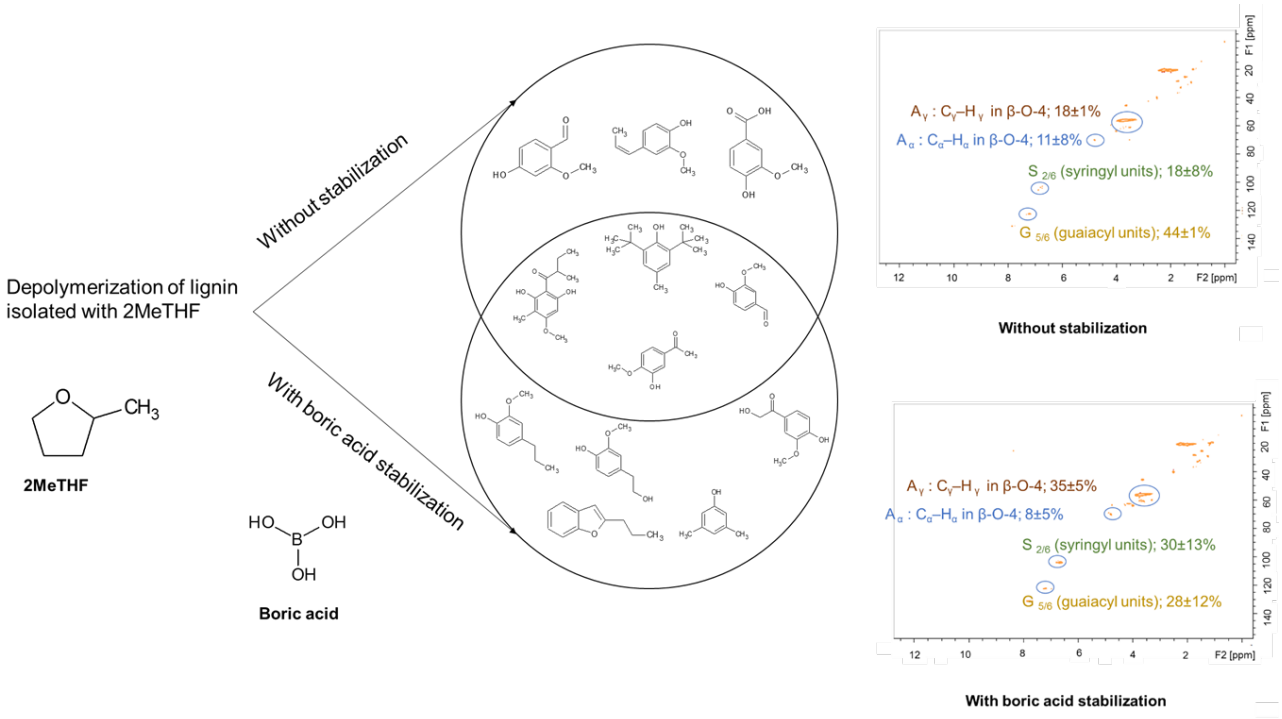

Abstract

Lignin valorization via its depolymerization is challenging due to the many secondary reactions that occur during this process. These secondary reactions can be prevented by selectively capping some of the reactive sites on lignin using certain chemical reagents. Boric acid was explored in this study as one such reagent that can form a protective structure on lignin. Lignin from poplar, a hardwood, was isolated using a mild fractionation involving 2-methyl-tetrahydrofuran as a solvent. The addition of boric acid during lignin isolation led to modification of the lignin structure, which were investigated using ^{1}H-^{13}C 2D HSQC and ^{31}P NMR, and FTIR spectroscopy, as well as elemental analysis. The relative abundance of Cγ-Hγ site in the β-O-4 linkage increased by ~20% while that of Cα-Hα site decreased by 3% after stabilization, suggesting the formation of a new structure. Depolymerization at 300°C with Ru/C as a catalyst in ethanol revealed an increase in mass yields of monomers from 16% to 25% in the modified lignin, as

determined using GC-MS. This study builds on the previous knowledge of lignin stabilization during its isolation by investigating a reagent and a biomass fractionation solvent.

Keywords: *Lignin, Stabilization, Boric Acid, Depolymerization, Phenolic Monomers*

5.1 Introduction

Lignocellulosic biomass can serve the need for producing renewable fuels and chemicals in the coming years, when the supply of fossil-fuels may not be reliable (Adhikari et al., 2020; Jahromi et al., 2020). Additionally, the use of non-food crops for supplying the demand for clean energy can also help mitigate the issues related to climate change and greenhouse gas emissions (Harun et al., 2020; Jahromi et al., 2021). In the United States, the waste lignin from second generation bioethanol industry is expected to reach a volume of about 225 million tons by 2030, whereas that from paper and pulp industry is already about 50 million tons per year (Patil et al., 2020, 2018). The Cα-OH and Cγ-OH groups (Figure 1) in the phenylpropanoid structure of lignin are the reactive sites that often undergo undesired secondary reactions, such as oligomerization and char formation. Preservation of reactive groups of lignin during its isolation from biomass enables optimization of the isolation and depolymerization processes, and at the same time eliminates the need to choose between the yield and quality of isolated lignin (Renders et al., 2017). Temporarily capping these reactive sites can make the lignin structure stable at ambient or relatively mild conditions (Lan et al., 2018).

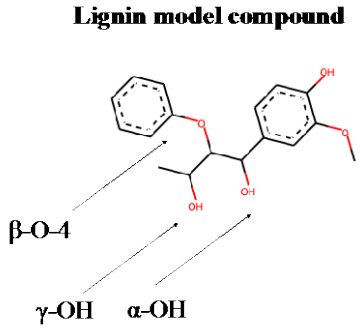

Figure 5.1 A representative structure showing the reactive sites on lignin

Boric acid (H_3BO_3, pKa=9.24) was shown to prevent condensation reactions by forming esters (e.g. $-B(OR)_4$; R being an alkyl group) during depolymerization with the lignin-derived monomers, or capping aromatic OH's in the products (Roberts et al., 2011; Toledano et al., 2014).

Previous studies have shown that the use of boric acid by adding it directly to lignin liquefaction medium along with other reagents, such as NaOH or phenol improves the bio-oil yields up to 52 wt.% based on starting lignin (Rietjens and Steenbergen, 2005; Roberts et al., 2011; Toledano et al., 2014). Boric acid could prevent unwanted product condensation when used in lignin: boric acid mass ratio of 1: 0.75, but also led to an increase in char while giving a smaller amount of residual lignin at the end of depolymerization reaction (Toledano et al., 2014). Boric acid was also used as a homogeneous catalyst to aid the depolymerization of lignin along with another noble-metal catalyst (Luo et al., 2020). Overall, boric acid has been used either as a catalyst or as a capping agent, but under basic conditions (Luo et al., 2020; Roberts et al., 2011). Addition of boric acid to the solvent choline chloride (pH= 4-6) during the extraction of lignin from biomass has also been reported to form esters with lignin hydroxyl groups (Hiltunen et al., 2016). However, the same study did not investigate the subsequent depolymerization of the extracted lignin. Also, it was previously reported that boric acid, when added directly to the lignin liquefaction medium, is needed in about twice the amount of lignin to be effective (Toledano et al., 2014). Hence, the present study aims to examine if a better use of boric acid is for stabilization of lignin structure during its extraction from biomass under acidic conditions. The subsequent depolymerization is hypothesized to have a different product distribution compared to that without the stabilization. The study is aimed at investigating whether this altered pathway leads to higher monomer yield from lignin. A novel biomass-derived solvent, 2-methyl-tetrahydrofuran (2MeTHF), is also investigated for isolation of lignin from biomass. The structure of 2MeTHF and boric acid is shown in Figure 5.2.

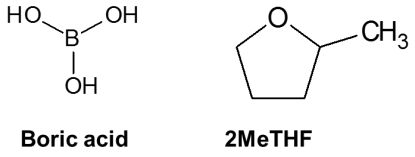

Figure 5.2 Structure of boric acid and 2-methyl tetrahydrofuran (2MeTHF)

5.2 Experimental

5.2.1 Materials

The biomass used for lignin isolation was hammer-milled poplar wood chips with size between mesh 30-60 (Forest Concepts LLC, Washington, USA). Ruthenium on carbon (5 wt.% loading on carbon support matrix), chloroform-D, dimethyl sulfoxide-d_6, 2-chloro-4,4,5,5-tetramethyl-1,3,2-dioxaphospholane (TMDP), and hydrochloric acid (HCl) were purchased from Millipore-Sigma (Burlington, Massachusetts, USA). Boric acid was purchased from Aldon (Avon, New York, USA). Pyridine was purchased from Alfa Aesar (Haverhill, Massachusetts, USA). Ethanol (95%), n-hydroxy-5-norbornene-2,3- dicarboximide (NHND), and dichloromethane (>99.5%) were purchased from VWR Chemicals BDH® (Suwanee, Georgia, USA). Ultra-high purity nitrogen (99.999%), ultra-high purity helium (99.999%) and ultra-zero grade air (total hydrocarbons < 0.1 ppm) were purchased from Airgas, Inc. (Radnor, Pennsylvania, USA).

5.2.2 Lignin isolation and stabilization

The protocol for reactive group-stabilized lignin fractionation was based on that reported in the literature (Talebi Amiri et al., 2019). Briefly, ~4.5 g dry poplar was added to ~25 mL 2-methyltetrahudrofuran (2MeTHF), ~1.7 mL 37% HCl and ~4.1 g boric acid (or ~67 mmol of any other reagent) at 95°C for 3.5 h with stirring. As per the literature protocol for lignin isolation, the quantity of boric acid needed was determined to be ~4.1 g for ~4.5 g of dry biomass (Lan et al., 2018). The solution was neutralized by adding 15.3 g sodium bicarbonate ($NaHCO_3$) and filtered. Filtrate was concentrated with rotary evaporation, dissolved in 10 mL ethyl acetate, and precipitated by adding dropwise to 250 mL hexane. Lignin was washed with deionized water and diethyl ether and dried at 50°C for 48 hours. Stabilization was be performed with duplicates. A control study with duplicates was performed without adding the stabilization agent to the biomass fractionation mixture.

5.2.3 Depolymerization of lignin

The stabilized and extracted lignin samples were depolymerized with a procedure based on that provided in the literature (Ghosh et al., 2016; Kim et al., 2019). Briefly, ~100 mg of dry lignin

and ~15 mg of Ru/C were added to 1.25 mL ethanol in a Swagelok 316SS reactor (total reactor volume of ~2.5 mL). Reactor was sealed tightly and shaken using a vortex mixer for 5 minutes. The reactor was heated in a sand bath ('Techne IFB-51 Industrial Fluidized Sand Bath, 5 L', Cole Parmer, Vernon Hills, Illinois, USA) at 300°C for 60 minutes. The reactor was quenched by placing them in -14°C freezer immediately after the reaction for ~60 minutes and later washed with ~10 mL dichloromethane to recover the products. The biochar was separated with centrifugation at 2400 rpm (g-force of 1095). One depolymerization experiment each performed for two samples each of the lignin isolated with and without stabilization.

5.2.4 Characterization of reactants and products

5.2.4.1 GC-MS

The depolymerization products dissolved in solvent ethanol and dichloromethane were used directly for the GC-MS analysis. An aliquot from this product mixture was filtered through 0.2 µm nylon syringe filter for this purpose. The characterization was performed with Agilent 7890A GC/5975C MS system equipped with DB-1701 column having dimensions of 30 m x 0.25 mm i.d. x 0.25 mm film thickness (Agilent Technologies, Santa Clara, California, USA). The carrier gas used was ultra-high purity (99.999%) helium, supplied by Airgas Inc. (Charlotte, North Carolina, USA). The oven temperature of GC was initially at 50°C for 2 minutes, increased at 4°C minute^{-1} to 280°C, and held at this temperature for 1 minute. Compound identification was performed using their retention times, referring to literature for the formation of similar compounds and comparing their mass spectra with those provided in the NIST library for various compounds. Calibration curves were made for 14 compounds using pure standards. Vanillin, which was already present in the sample, was used as an internal standard to predict the yields of other compounds using 'effective carbon number' method (Kim et al., 2014; Shuai et al., 2016; Szulejko et al., 2013). The equation used for this method is as follows:

$$C_{monomer} = \frac{A_{monomer}}{A_{std}} x \frac{C_{std}}{MW_{std}} x \frac{ECN_{std}}{ECN_{monomer}} x\, MW_{monomer} \quad \textit{(Equation 5.1)}$$

Where,

C $_{monomer}$: Concentration of the monomer wt.%

A $_{monomer}$: The area under a monomer curve in a GC-MS spectrum

A_{std}: The area under a standard compound curve in a GC-MS spectrum

C_{std}: Concentration of the standard, estimated using a calibration curve, wt.%

MW_{std}: Molecular weight of the standard

ECN_{std}: Effective carbon number of the standard

$ECN_{monomer}$: Effective carbon number of a monomer

$MW_{monomer}$: Molecular weight of the monomer

The yield of a compound was calculated in the following way:

$$Y_{monomer} = \frac{C_{monomer} \, x \, W_{product\ mixture}}{W_{lignin}} \quad \textit{(Equation 5.2)}$$

where,

$Y_{monomer}$: Mass yield of a monomer, based on dry lignin

$W_{product\ mixture}$: Mass of product mixture used to get an aliquot (free of char)

W_{lignin}: Initial mass of dry lignin

$$S_{monomer} = \frac{Y_{monomer}}{\Sigma Y_{monomer}} x100 \quad \textit{(Equation 5.3)}$$

Where,

$S_{monomer}$: Selectivity of a monomer

$\Sigma Y_{monomer}$: Sum of mass yields of all monomers, based on dry lignin

5.2.4.2 Ultimate analysis

About 2 mg lignin samples were analyzed using sulfanilamide as a standard in 'Vario MICRO cube' elemental analyzer (Elemental Americas Inc., New York, USA). The values were calculated on moisture and ash-free basis, with hydrogen content of samples accounted for the hydrogen coming from moisture.

5.2.4.3 Thermogravimetric analysis

The moisture and ash contents of lignin samples were measured with thermogravimetric analysis using TGA-50 (Shimadzu Scientific Instruments Inc., Maryland, USA). Briefly, the samples were placed in alumina crucibles and air was supplied to the chamber. The temperature was ramped at 15°C minute^{-1} to 900°C, holding it for 1 minute at this temperature. The weight loss up to 105°C and the weight remaining in the end were taken as approximate values of moisture and ash contents, respectively.

5.2.4.4 FTIR spectroscopy

Lignin samples were characterized with Fourier Transform Infrared (FTIR) using Thermo-Nicolet iS10 instruments (Thermo Scientific, Massachusetts, USA). Total 32 scans were performed on samples between wavenumbers 400 to 4000 cm^{-1}.

5.2.4.5 ^{1}H-^{13}C 2D-HSQC NMR spectroscopy

Lignin isolated from poplar with and without stabilization was characterized with ^{1}H-^{13}C 2D Heteronuclear Single Quantum Coherence- Nuclear Magnetic Resonance (HSQC-NMR) spectroscopy as per the literature protocol (Nishimura et al., 2018; Tarmadi et al., 2018). The dissolution of lignin was improved by using acetylation (Sameni et al., 2017). Briefly, about 100 mg of dry lignin was dissolved in 4 mL of pyridine-acetic anhydride (1:1 v/v) mixture and left to react with agitation for 24 hours. Lignin was precipitated in an HCl solution (pH=1), filtered under vacuum, washed with deionized water, and dried. About 1 mL dimethyl sulfoxide (DMSO-d_6) was used to dissolve ~20-25 mg acetylated lignin. After using 'vortex' to mix the sample for 5 minutes, the solution was filtered through 0.2 µm nylon syringe filter and added to the NMR tube. The spectra were acquired using Bruker Avance 500 MHz spectrometer equipped with a z-gradient triple resonance cryo-probe (Bruker BioSpin Corporation, Billerica, Massachusetts, USA). The Bruker standard pulse sequence 'hsqcetgp' was used for recording the spectra. The acquisition was carried out for 13.57 minutes at 298.1 K with 16 scans for ^{1}H, 32 scans for ^{13}C, additional 2 scans for HSQC, and 16 dummy scans to ensure a steady state of the instrument. Bruker Topspin 4.0.6 software was used to analyze the spectra. It is important to note that even after acetylation, some mass of lignin (~10%) may remain insoluble in the deuterated solvent. This was avoided to as

much extent as possible by making sure that the mixture in deuterated solvent was free of any suspended particles.

5.2.4.6 ^{31}P NMR spectroscopy

The hydroxyl group concentration of lignin was determined by phosphorylating the lignin samples and subsequently using ^{31}P NMR spectroscopy to characterize it. Briefly, a stock solution was made by mixing deuterated chloroform with pyridine in a ratio of 1:1.6 (v/v). About 40 mg of NHND and Cr(III)acetylacetonate each were added as the internal standard and the relaxation agent, respectively. The mixture was vortexed for 2 minutes. About 20-25 mg acetylated lignin was added to ~1 mL stock solution and vortexed for 2 minutes. About 100 µL phosphorylating agent (2-chloro-4,4,5,5-tetramethyl-1,3,2-dioxaphospholane, or TMDP) was added to each sample and vortexed for 2 minutes to make sure that phosphorylation is complete. The mixture was filtered with 0.2 µm nylon syringe filter and transferred to an NMR tube. The spectra were acquired on Bruker Avance 500 MHz spectrometer with 32 scans, 405 ppm spectral width, and 0.4 s acquisition time (Bruker BioSpin Corporation, Billerica, Massachusetts, USA). Bruker Topspin 4.0.6 software was used to process the spectra.

5.3 Results and discussion

5.3.1 GC-MS

The GC-MS characterization of lignin depolymerization product revealed the presence of commonly encountered phenolic and aromatic compounds from this process. The yield and selectivity of lignin-derived compounds are given in Table 5.1. Whereas the abbreviations used for denoting compound names are provided in the supplementary information. Only the guaiacyl-type compounds were detected from the depolymerization of lignin isolated using 2MeTHF. This suggests that partial demethoxylation of some syringyl-type compounds might have occurred during the process. The total yield of lignin-derived monomers increased from 16 wt.% to 25 wt.% (based on dry lignin) as an effect of lignin stabilization with boric acid. Majority of the monomers were phenolics, although the lignin stabilized with boric acid had 2 wt.% of aromatics. Previously, it was reported that in presence of boric acid, lignin produced mainly dimers on its depolymerization (Toledano et al., 2014). However, the results of present study show that using

boric acid during lignin isolation instead of depolymerization can also enable the formation of monomers. Also, it was reported earlier that presence of boric acid in lignin depolymerization medium increased the bio-oil yield from 6 wt% to 15 wt% from lignin (Roberts et al., 2011). The present study resulted in a similar observation, while also exhibiting overall higher yields compared to the previous studies due to the use of a 2MeTHF-based mild fractionation of biomass while isolating lignin.

The selectivity of lignin-derived monomers can be compared with and without boric acid stabilization from Table 5.1. Selectivity may not directly correspond to the mass-yields. However, the changes in selectivity of products can be considered as an indicator to infer how the reaction pathways change as a result of stabilization. Although, the compounds observed from lignin stabilized with boric acid were slightly modified than those from lignin without stabilization, there was little gain in the molecular weight of compounds. This can be approximated as the overall average molecular weight of the monomeric fraction being more or less the same even with boric acid stabilization. This is promising as it shows that any re-polymerization of lignin-derived products is avoided, which was a possible side reaction previously reported from the use of boric acid directly in depolymerization medium (Roberts et al., 2011). The possible reason for the peculiar observation in the present study can be that any residual boric acid-derived group does not act as an acid, but its effect is limited to stabilization of reactive groups. This prevents the additional internal hydrogen bonding that would have been induced in presence of any loose boric acid in the system, which in turn would have led to oligomerization. The biochar yield did not considerably change as a result of boric acid stabilization and was ~25 wt% based on dry lignin.

Table 5.1 Chemical compounds present in lignin depolymerization products, as detected from GC-MS characterization (major compounds)

	Without stabilization Yield, wt% (based on dry lignin)	**Without stabilization Selectivity (wt% of lignin-derived compounds)**	**With stabilization Yield, wt% (based on dry lignin)**	**With stabilization Selectivity (wt% of lignin-derived compounds)**

Compound code	avg	SD		avg	SD	
Phenolics						
PH2	1.1	1.1	6.6	3.4	<0.1	13.4
PH3	0.8	0.8	5.1	<0.1	<0.1	<0.1
PH6	<0.1	<0.1	<0.1	4.4	2.5	17.6
PH7	3.8	0.4	23.6	4.3	1.5	17.3
PH8	0.2	0.2	1.0	<0.1	<0.1	<0.1
PH9	<0.1	<0.1	<0.1	0.5	0.5	2.1
PH15	<0.1	<0.1	<0.1	1.0	1.0	3.8
PH16	1.1	0.3	6.8	0.1	0.1	0.3
PH18	4.6	2.7	28.5	<0.1	<0.1	<0.1
PH19	<0.1	<0.1	<0.1	1.7	1.7	6.7
PH22	<0.1	<0.1	<0.1	4.1	4.1	16.4
PH23	1.9	1.9	11.8	<0.1	<0.1	<0.1
PH24	1.4	1.3	8.9	3.1	0.4	12.2
Other	0.6		3.4	0.3		1.8
Total phenolics	*15.5*		*95.7*	*22.9*		*91.3*
Aromatics						
AR6	0.2	0.2	1.1	<0.1	<0.1	<0.1
AR7	<0.1	<0.1	<0.1	0.5	0.5	1.8
AR9	<0.1	<0.1	<0.1	1.1	1.1	4.3
AR11	<0.1	<0.1	<0.1	0.6	0.6	2.5
Other	0.5		3.2	<0.1		0.1
Total aromatics	*0.7*	*<0.1*	*4.3*	*2.2*	*<0.1*	*8.7*
Total	**16.2**		**100.0**	**25.1**		**100.0**
Biochar	**24.4**	**2.2**		**25.2**	**1.7**	

[*avg: Average; **SD: Standard deviation; compound names provided in supplementary information]

5.3.2 Ultimate analysis

The ultimate analysis of lignin isolated with and without boric acid capping are given in Table 5.2. It was seen that the boric acid stabilization did not have an effect on the elemental composition of isolated lignin. Whereas the small amounts of N and S seen in lignin without stabilization were lowered in the stabilized lignin. The molar ratios of H/C and O/C were equal with and without using boric acid. Hence, it can be said that stabilization did not considerably reduce or oxidize lignin in the process. The lignin produced this was free of ash. The absence of ash can be a result of using HCl as an acid catalyst for biomass fractionation, which has previously been reported to

result in a lignin that had ~99.6% purity (Jääskeläinen et al., 2003). Even with the use of a different solvent for biomass fractionation, such as ethanol or acetone in combination with HCl as a catalyst, negligible ash (~0.1%) was seen in lignin (Bauer et al., 2012). It was previously reported that the 2MeTHF/H_2O-based isolation of lignin does not result in any considerable change in its aromatic structure (Xue et al., 2018). Hence, the effect of boric acid stabilization could not be seen from the ultimate analysis in the present study, as the overall aromatic structure of lignin seems to have remained intact. Additionally, the present study did not use water, but only 2MeTHF as a solvent for lignin isolation. This would be beneficial to the economic feasibility of the overall process as the recovery of water in the end of a typical organosolv process is considerably energy-intensive (Viell et al., 2013). Future studies may be needed to elucidate the reaction mechanism of lignin isolation through 2MeTHF as a solvent to understand this process better. The nitrogen content of lignin isolated using HCl, which comes from the protein residues, was reported to be zero in a previous study (Jääskeläinen et al., 2003). This corroborates with the findings of the present study where negligible nitrogen was seen in lignin.

Table 5.2 Ultimate analysis of lignin isolated with and without boric acid stabilization

Elemental composition, dry ash-free basis	Lignin isolated without stabilization	Lignin isolated with boric acid stabilization
C	63.9 ± 0.4	63.9 ± 1.5
H	5.5 ± 0.2	5.4 ± 0.5
N	0.1 ± 0.0	0.0 ± 0.0
S	0.4 ± 0.1	0.2 ± 0.0
O (by difference)	30.2 ± 0.4	30.4 ± 1.7
H/C (molar)	1.0	1.0
O/C (molar)	0.4	0.4
Moisture content (wt.%, based on wet lignin)	2.1	4.9
Ash content (wt.%, based on dry lignin)	0	0

5.3.3 Thermogravimetric analysis

The thermogravimetric analysis of lignin isolated with and without stabilization is summarized in Figure 5.3. It was seen that the rate of thermal degradation of lignin peaks at a higher temperature (534°C vs 511°C), as a result of stabilization. The other regions of maximum degradation between 150-300°C can also be seen to have shifted towards higher temperatures as a result of stabilization. This observation supports the initial hypothesis that boric acid temporarily stabilizes lignin against unwanted secondary reactions at lower temperatures. This might be an indication that at temperatures below 300°C, lignin is more resistant to thermal degradation as a result of stabilization. Such a shift in property can ensure that secondary reactions of lignin at relatively lower temperatures will occur to a smaller extent. At ~100°C for the stabilized lignin, the degradation of lighter components, such as volatiles, might be getting over and that of heavier components, such as those from fixed-carbon might have started. This transition can be a reason for a possible 'pause' in the degradation and a sudden drop in the thermal degradation rate. The melting point of any residual boric acid is 171°C, but it is expected to turn into a liquid above 200°C, affecting the rate of thermal degradation (Luo et al., 2020). Hence its effect would be seen after ~200°C, as evident from the TGA curve.

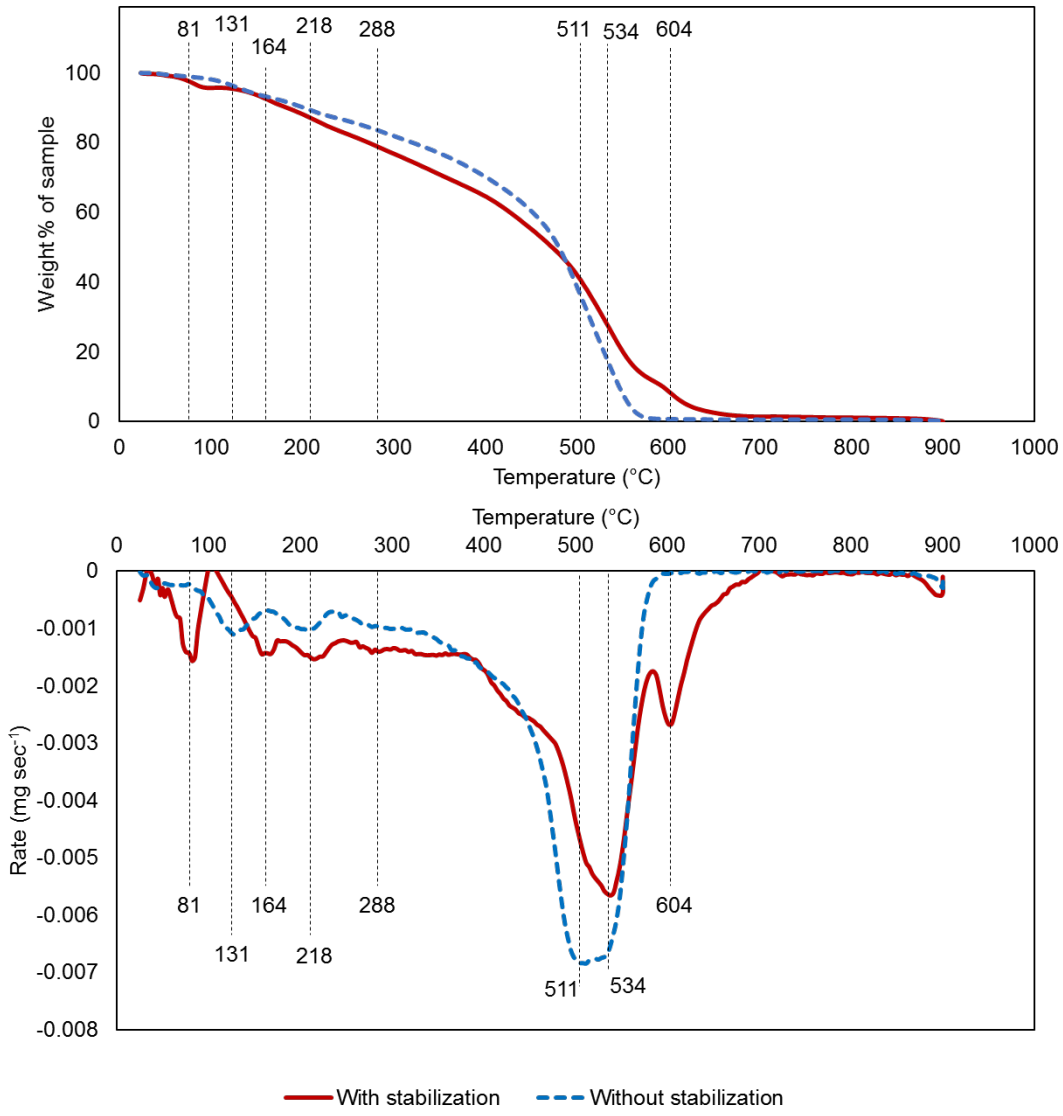

Figure 5.3 Thermogravimetric analysis (TGA) and differential thermogravimetric (DTG) curve of lignin isolated in 2-methyltetrahydrofuran with and without boric acid stabilization

5.3.4 FTIR spectroscopy

The FTIR spectra of lignin isolated in 2MeTHF with and without boric acid stabilization are shown in Figure 5.4. There was a slight increase in the C-H stretching or vibrations of methyl or methoxyl groups at 2934 cm^{-1} in stabilized lignin. This may be an indication that the self-condensation between structural units at methoxy groups might have been prevented to some

extent in this lignin. Signals of aromatic skeletal vibrations from C=C stretching at 1596 $cm^{-1}$and 1512 cm^{-1} decreased in stabilized lignin. This might suggest a slight shielding of aromatic rings in lignin due to a structure formed by boric acid. Whereas there was not much change in the signals at 1463 cm^{-1} and 1419 cm^{-1}, which are also from the aromatic rings. Only the signals from deformation of aromatic rings at 1035 cm^{-1} increased slightly, suggesting that some changes occur there. However, the difference between the spectra of lignin isolated with and without stabilization could not be clearly seen from the FTIR characterization. Hence, other more powerful spectroscopy techniques have been reported in the next sections. Not many residual solvent peaks were seen in the FTIR spectra of these lignins. This affirms the theoretical estimate reported by a previous study that stated that a solvent recovery of about 99.99 wt% is possible when using 2MeTHF for such a process (Viell et al., 2013). A previous study applied additional CO_2 pressure to maintain a liquid phase in the reactor (vom Stein et al., 2011). In the present study, 2MeTHF vapors were condensed back to the biomass fractionation mixture, which served the same purpose. The degradation of solvent 2MeTHF can indeed occur due to the presence of HCl, but the extent of this reaction has been reported to be very low (Aycock, 2007).

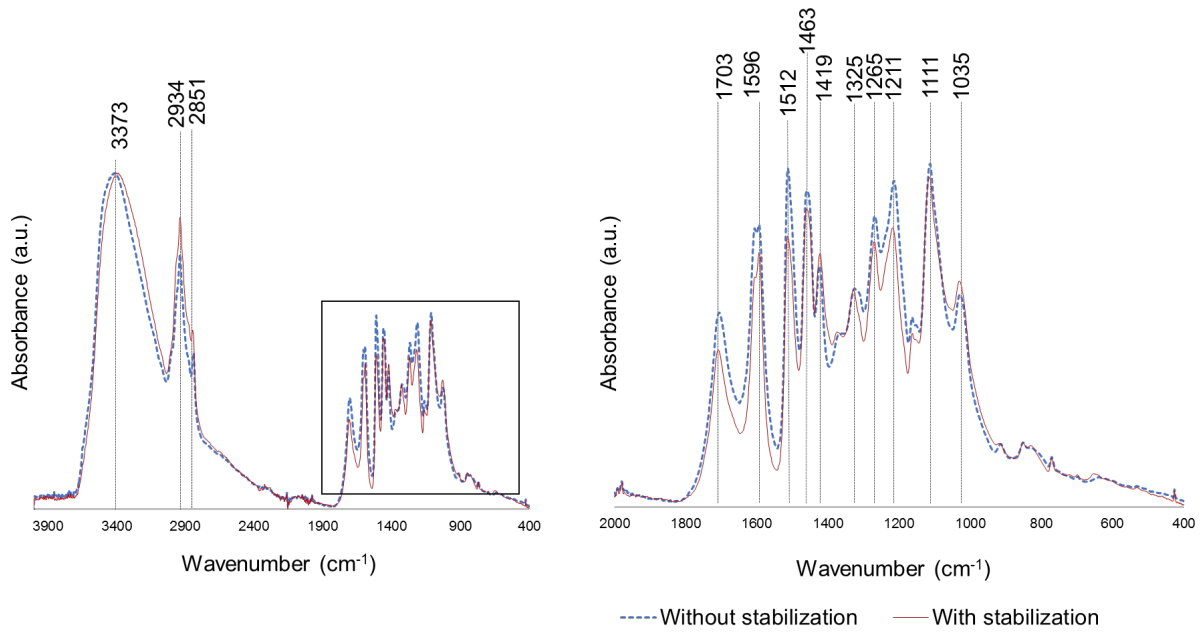

Figure 5.4 Functional groups in lignin isolated from poplar with and without boric acid stabilization as detected from FTIR spectroscopy

5.3.5 2D-HSQC and ^{1}H NMR spectroscopy

The ^{1}H-^{13}C 2D-HSQC NMR spectra of lignin isolated with and without boric acid stabilization is shown in Figure 5.5. The biomass used for isolating lignin in this study was poplar, which was a hardwood. As a result, the lignin had both guaiacyl (G) and syringyl (S) type structures (Hu et al., 2014). The newly formed bonds due to the presence of boric acid that lead to stabilization of lignin can either be covalent or hydrogen bonds (Hiltunen et al., 2016). Hence, the structural changes occurring in lignin can be seen in more than one way, as observed from the changes in relative abundance of multiple structural locations. For example, the relative abundance of Cγ-Hγ site in the β-O-4 linkage of lignin increased from 18% to 35%. This might be an indication that that any interunit linkages that might have been blocking this position in lignin without stabilization were absent when boric acid was added to the biomass fractionation mixture. The relative abundance of Cα-Hα site in the β-O-4 linkage of lignin decreased from 11% to 8%, which might be indicating that boric acid forms a protective structure at this location in lignin, temporarily blocking these groups. Some β-5 (6% relative abundance) and β-β (3% relative abundance) structures were also observed in the lignin isolated without stabilization. However, these groups were capped in lignin isolated with boric acid stabilization and hence did not show signals. Previously, the presence of similar linkages (β-O-4, β-5 and β-β) was reported in the lignin isolated in presence of boric acid (Hiltunen et al., 2016). This might not be an indication of condensation of lignin with this type of stabilization, as such blocking of group is hypothesized to be only temporary in nature (Lan et al., 2018). The extent to which lignin condensation might occur due to the presence of HCl in the biomass fractionation mixture might be higher in the present case compared to a previously reported study where 2MeTHF-H_2O mixture was used (Aycock, 2007). The reason can be that all of the HCl remains dissolved in the same organic phase as that of lignin, instead being taken away by water phase, as was observed in a previous study (Aycock, 2007). This indicates the need to involve yet another strategy to minimize the effect of HCl in isolated lignin after it has already catalyzed the biomass fractionation process.

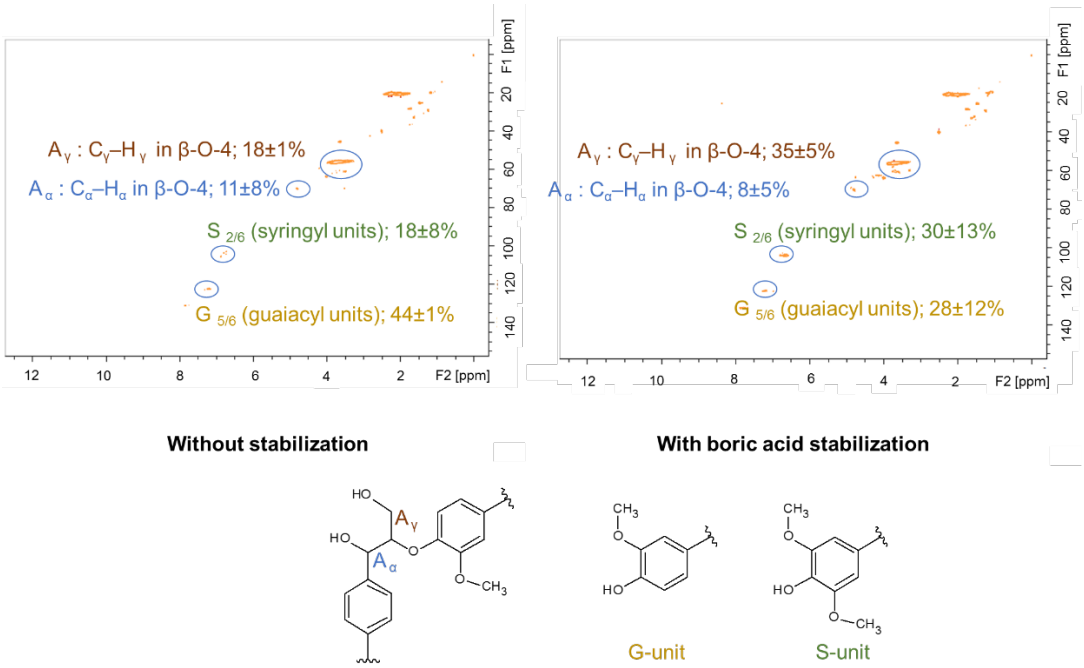

Figure 5.5 Structural features of lignin detected from ^{1}H-^{13}C 2D-HSQC NMR spectra (numbers indicate relative abundance of signals from a particular structure)

Boric acid does not contain carbon atoms and hence it cannot be detected in a 2D-HSQC spectrum. However, with ^{1}H NMR of lignin isolated with boric acid stabilization, a unique peak at 7.35-7.45 ppm was seen, which was also seen from ^{1}H NMR a representative compound, phenylboronic acid (Figure 5.6). This peak, however, was not present in boric acid, and instead, it represents the protons on aromatic rings. It suggests that in the structure formed on lignin, an aromatic ring might be attached to boron instead of a hydroxyl group. Note that the ^{1}H NMR only detects proton, and not boron. It was seen that there were many other ^{1}H peaks indicating a variety of functional groups in lignin isolated with 2MeTHF. This is in agreement with a previous study that reported similar observations by comparing lignin isolated using 2MeTHF/H_2O with that using organosolv process (vom Stein et al., 2011).

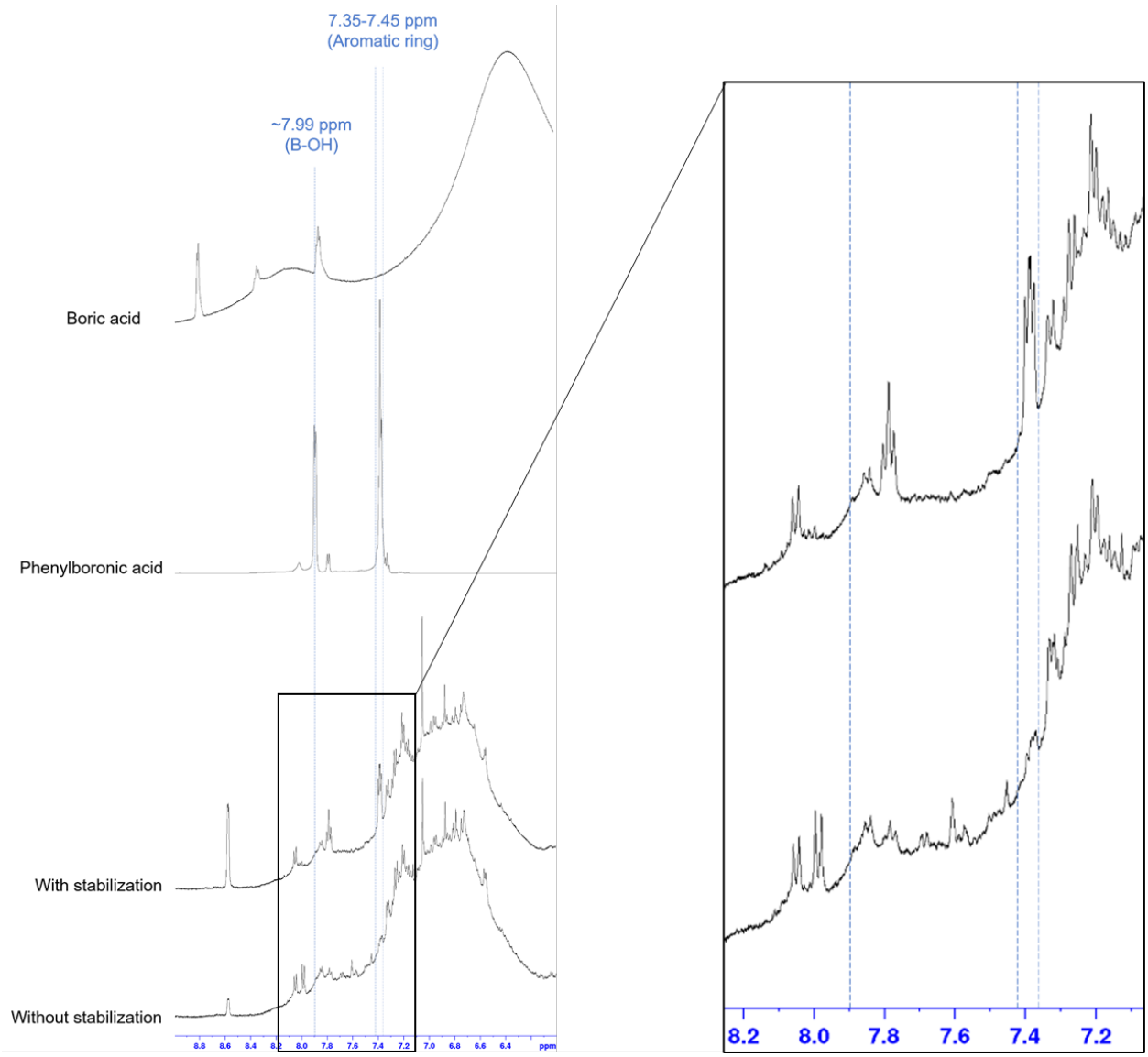

Figure 5.6 Structural changes in lignin isolated with boric acid stabilization observed using ^{1}H NMR spectroscopy

5.3.6 ^{31}P NMR spectroscopy

The hydroxyl group concentration of lignin measured using quantitative ^{31}P NMR spectroscopy is given in Figure 5.7. From the literature, it has been reported that boric acid can form esters with hydroxyl groups of lignin, making them stable in the process (Hiltunen et al., 2016; Roberts et al., 2011). The same phenomena can be predicted to have happened in this case, as the hydroxyl group concentration went down in lignin isolated with boric acid stabilization. For

example, the aliphatic hydroxyl group concentration decreased from 4.8 to 3.5 mmol g^{-1} lignin, whereas that of phenolic hydroxyl groups decreased from 4.1 to 2.9 mmol g^{-1} lignin. These hydroxyl groups correspond to the most reactive sites in lignin, and the changes in their concentration suggests their selective capping. It was previously reported that the presence of a large amount of hydroxyl groups in the solution can hinder the stabilization of lignin that would have occurred via boric acid-induced ester-formation (Roberts et al., 2011). However, the solvent used for lignin isolation in the present case being 2MeTHF, it did not introduce any further hydroxyl groups to the system, preventing any adverse effect such as this. Also, the need to use a higher temperature for phase-separation due to the presence of water was avoided in the present study by using only 2MeTHF for the lignin isolation (Aycock, 2007). This is an advancement that can reinforce the use of 2MeTHF while using boric acid stabilization instead of conventional solvents such as ethanol or water that are typically used for organosolv-type lignin isolation processes (Pan et al., 2006).

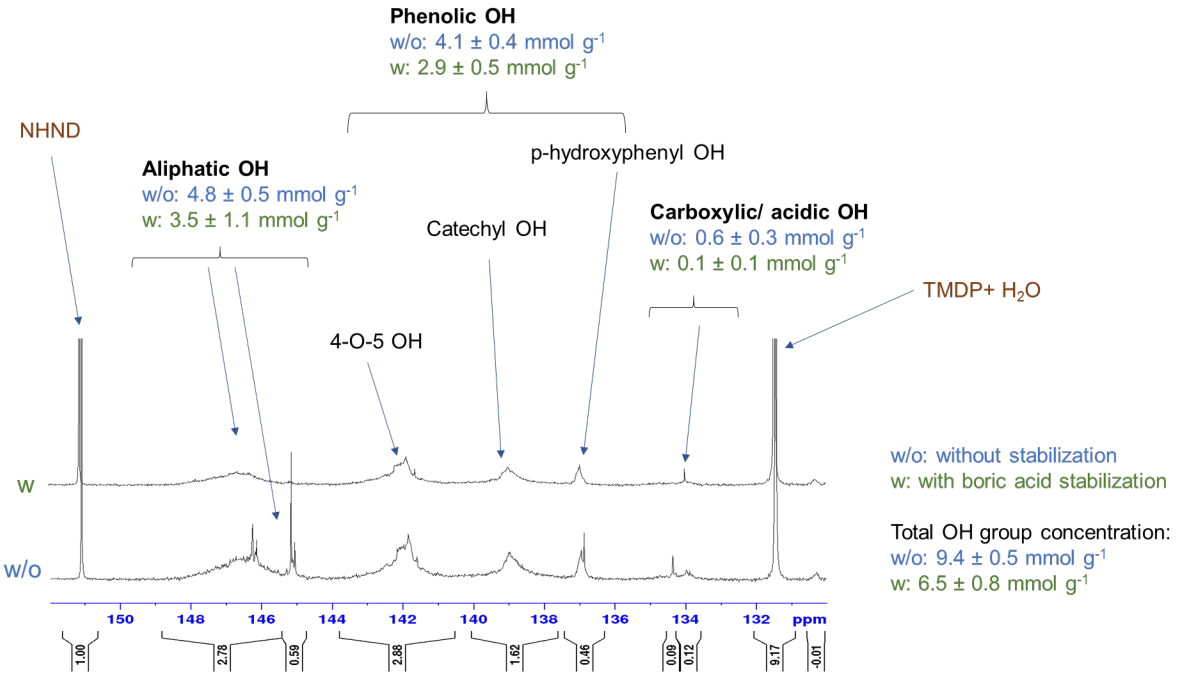

Figure 5.7 ^{31}P NMR spectra and hydroxyl group concentrations of lignin isolated with and without stabilization

5.3.7 Insight in boric acid stabilization

About 70% boric acid was recovered in the holocellulose residue at the end of biomass fractionation process. Boric acid itself is a very weak acid and hence did not change the pH of solution, which was also confirmed during the experiments. However, the addition of boric acid to the biomass fractionation mixture could have created a buffer solution that was resistant to changes in the pH. This is in agreement with the weak acidic nature of boric acid. Hence, the amount of $NaHCO_3$ needed to neutralize the acidic mixture during biomass fractionation in presence of boric acid was double that needed without stabilization (~260 mg mL^{-1} vs ~130 mg mL^{-1}). This is likely due to boric acid being a Lewis acid, and its tendency to accept electron pairs, which might occur during the fractionation (Hiltunen et al., 2016). The difference between major compounds obtained from depolymerization of lignin isolated using 2MeTHF with and without boric acid stabilization can be seen from Figure 5.8. Briefly, with stabilization, products without methoxy groups were slightly less abundant, as seen from the chemical structure of compounds produced. This corresponds to a slight decrease in relative abundance of methoxy groups after boric acid stabilization (from 38% to 37%) that was seen from 2D-HSQC NMR characterization. The reason for such observation can be hypothesized to be the catalytic activity of boric acid and the groups formed from it towards the cleavage of methoxy groups (Luo et al., 2020). Also, as an effect of stabilization, the products were more saturated. For example, phenol, 2-methoxy-4-propyl- (5 wt.%) was seen in lignin-derived monomers after boric acid stabilization, as compared to phenol, 2-methoxy-4-(1-propenyl)- (2 wt.%) seen without stabilization. The sidechains attached to the aromatic ring were longer in depolymerization products from stabilized lignin. For example, 2,4'-Dihydroxy-3'-methoxyacetophenone (4 wt.%) was seen from stabilized lignin instead of vanillic acid (2 wt.%).

Previously, adding boric acid directly to the lignin depolymerization medium was seen to result in an overall increase in the molecular weight of products (Roberts et al., 2011). However, from the present study, such increase in molecular weight was prevented by using boric acid in the lignin isolation step. This can be a beneficial improvement in the strategy of boric acid stabilization, as typical lower-molecular weight monomers are more valuable as commodity-chemicals. It was earlier reported that the effectiveness of boric acid capping on lignin increases by using it in a certain combination with a solvent mixture (Hiltunen et al., 2016). However, the

solvent suggested in that study was an ionic liquid, the high cost of which might be a limitation in its use for large scale conversion of lignin. In the present study, 2MeTHF was used as the solvent, which serves the purpose of enabling effective interaction between boric acid and lignin, as well as provides the benefit of being derivable from biomass (Aycock, 2007). Although the amount of boric acid needed to stabilize lignin was quite high, a previous study came up with a similar conclusion in this regard that almost twice the amount of boric acid is required for capping of a certain amount of lignin (Roberts et al., 2011).

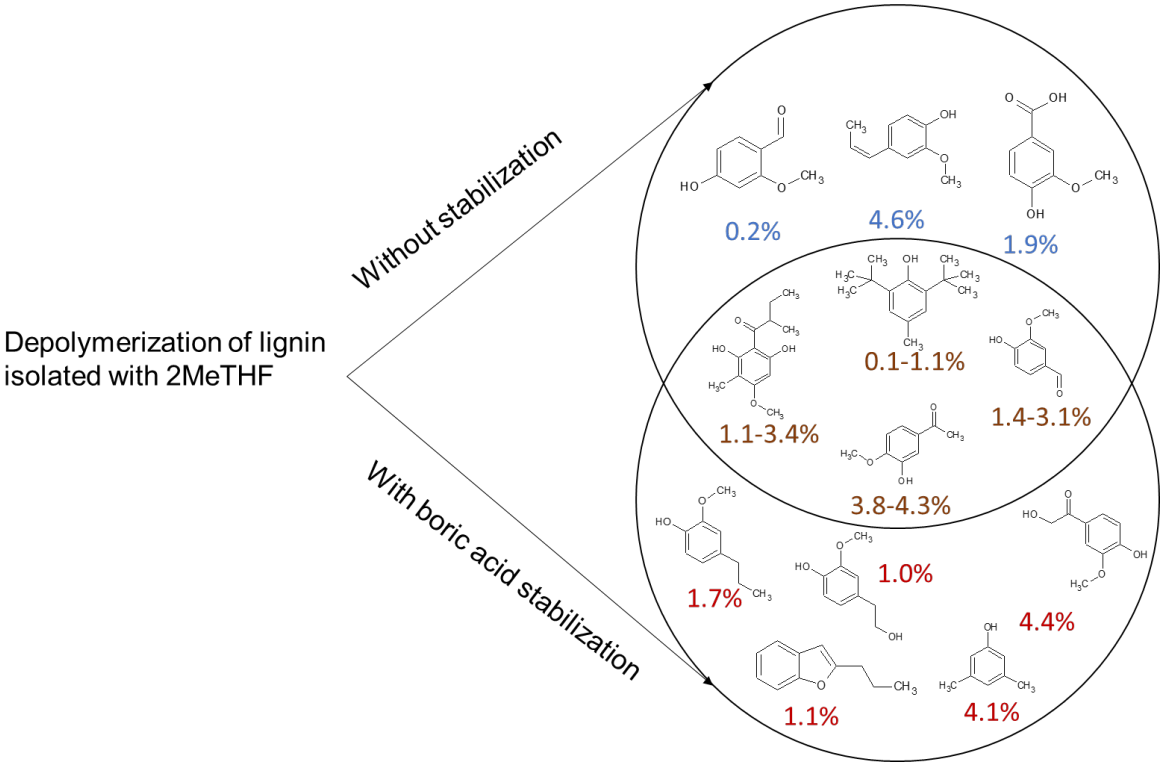

Figure 5.8 Major compounds produced from depolymerization of lignin isolated in 2MeTHF with and without boric acid stabilization

There are also certain side-reactions expected due to the presence of boric acid, such as the formation of dimers, polymeric phenols and coordinated complexes with lignin (Rietjens and Steenbergen, 2005; Toledano et al., 2014). However, these side reactions have been reported to occur when boric acid is present in the reaction medium under harsh conditions (>250°C). The reaction of boric acid has previously been reported to occur with free crosslink sites (OH groups) of a biopolymer (guaran) under basic conditions (Rietjens and Steenbergen, 2005). Such reaction may not be directly applicable to the specific sites found in lignin. The extent of side reactions

might be lower when boric acid is present only during the mild conditions of biomass fractionation (100°C) and the excess boric acid is washed with water before the depolymerization step. Compounds similar to boric acid, such as phenylboronic acid have been shown to achieve capping of lignin during its isolation from biomass (Lan et al., 2019b, 2018). Here, formation of a cyclic boronate had been reported to occur at the Cα-OH and Cγ-OH sites of lignin (Lan et al., 2018). Boric acid can be a cheaper substitute to achieve lignin stabilization instead of phenylboronic acid. Boric acid has also been reported to be useful for capping the Cα-OH and Cγ-OH sites of lignin model compounds, but in presence of an ionic liquid, choline chloride (Hiltunen et al., 2016). However, the high cost of ionic liquids can be a hindrance to scalability of the process. Instead, using a biomass-derived solvent such as 2MeTHF used in the present study can provide a low-cost route to achieve boric-acid assisted stabilization of lignin. The use of 2MeTHF was also helpful in effective recover of lignin at the end of isolation, as this solvent prevents the formation of any rag layers or emulsion (Aycock, 2007). Keeping the initial pH of the biomass fractionation mixture at 1 was found to be useful, because at pH of 4-12, formation of polyboronate could have hindered the desired capping reaction (Toledano et al., 2014). Hence, the more acidic pH of the mixture used for lignin isolation in this study is justified this way for preventing the unwanted reactions of the capping agent.

5.4 Conclusion

The boric acid stabilization of lignin during its isolation from poplar in 2MeTHF could produce compounds that were slightly more saturated, had longer sidechains and had lesser abundance of methoxy groups. Overall, the monomer yield increased from 16 wt.% to 25 wt.% with the stabilization. This strategy to stabilize lignin during its isolation can be helpful in preventing the unwanted secondary reactions such as condensation and oligomerization. The process of boric acid stabilization did not oxidize lignin, but instead led to blocking of certain locations, including the phenylpropanoid chain and the aromatic ring. Using the lignin stabilized with boric acid directly can be a better alternative to adding boric acid during the depolymerization step, since an uncondensed lignin can lead to selective depolymerization, producing a higher yield of monomers. Also, the use of HCl as an acid catalyst for biomass fractionation resulted in lignin that was free of ash and proteins to a great extent. Additionally, the use of solvent 2MeTHF for

lignin isolation was not previously investigated. In the present study, the use of 2MeTHF instead of its combination with water was found to beneficial in terms of solvent recovery but also led to increased degradation due to the presence of HCl. As 2MeTHF can be a byproduct of biorefinery processes, its use in lignin isolation can be a promising area to further investigate in the future. For mild biomass fractionation processes, 2MeTHF can also be a safer substitute for dioxane, which was a toxic solvent previously reported for this type of processes.

5.5 Acknowledgements

The authors would like to acknowledge the United States Department of Agriculture and the National Institute of Food and Agriculture for funding this research project (Grant # USDA-NIFA-2015-67021-22842).

5.6 References

1. Adhikari, S., Auad, M.L., Via, B., Shah, A., Patil, V., 2020. Production of Novolac Resin after Partial Substitution of Phenol from Bio-oil. Trans. ASABE 0. https://doi.org/10.13031/trans.13798
2. Aycock, D.F., 2007. Solvent Applications of 2-Methyltetrahydrofuran in Organometallic and Biphasic Reactions. Org. Process Res. Dev. 11, 156–159. https://doi.org/10.1021/op060155c
3. Bauer, S., Sorek, H., Mitchell, V.D., Ibáñez, A.B., Wemmer, D.E., 2012. Characterization of Miscanthus giganteus Lignin Isolated by Ethanol Organosolv Process under Reflux Condition. J. Agric. Food Chem. 60, 8203–8212. https://doi.org/10.1021/jf302409d
4. Ghosh, A., Brown, R.C., Bai, X., 2016. Production of solubilized carbohydrate from cellulose using non-catalytic, supercritical depolymerization in polar aprotic solvents 1023–1031. https://doi.org/10.1039/c5gc02071a
5. Harun, K., Adhikari, S., Jahromi, H., 2020. Hydrogen production via thermocatalytic decomposition of methane using carbon-based catalysts. RSC Adv. 10, 40882–40893. https://doi.org/10.1039/D0RA07440C
6. Hiltunen, J., Kuutti, L., Rovio, S., Puhakka, E., Virtanen, T., Ohra-Aho, T., Vuoti, S., 2016. Using a low melting solvent mixture to extract value from wood biomass. Sci. Rep. 6, 32420.
7. Hu, J., Shen, D., Wu, S., Zhang, H., Xiao, R., 2014. Composition Analysis of Organosolv Lignin and Its Catalytic Solvolysis in Supercritical Alcohol. Energy & Fuels 28, 4260–4266. https://doi.org/10.1021/ef500068h
8. Jääskeläinen, A.S., Sun, Y., Argyropoulos, D.S., Tamminen, T., Hortling, B., 2003. The effect of isolation method on the chemical structure of residual lignin. Wood Sci. Technol. 37, 91–102. https://doi.org/10.1007/s00226-003-0163-y

9. Jahromi, H., Adhikari, S., Roy, P., Hassani, E., Pope, C., Oh, T.-S., Karki, Y., 2021. Production of green transportation fuels from Brassica carinata oil: A comparative study of noble and transition metal catalysts. Fuel Process. Technol. 215, 106737. https://doi.org/https://doi.org/10.1016/j.fuproc.2021.106737
10. Jahromi, R., Rezaei, M., Hashem Samadi, S., Jahromi, H., 2020. Biomass gasification in a downdraft fixed-bed gasifier: Optimization of operating conditions. Chem. Eng. Sci. 116249. https://doi.org/https://doi.org/10.1016/j.ces.2020.116249
11. Kim, J., Hafezi-sefat, P., Cady, S., Smith, R.G., Brown, R.C., 2019. Premethylation of Lignin Hydroxyl Functionality for Improving Storage Stability of Oil from Solvent Liquefaction. https://doi.org/10.1021/acs.energyfuels.8b03894
12. Kim, Y.-H., Kim, K.-H., Szulejko, J.E., Bae, M.-S., Brown, R.J.C., 2014. Experimental validation of an effective carbon number-based approach for the gas chromatography–mass spectrometry quantification of 'compounds lacking authentic standards or surrogates.' Anal. Chim. Acta 830, 32–41. https://doi.org/https://doi.org/10.1016/j.aca.2014.04.052
13. Lan, W., Amiri, M.T., Hunston, C.M., Luterbacher, J.S., 2018. Protection Group Effects During α,γ-Diol Lignin Stabilization Promote High-Selectivity Monomer Production. Angew. Chemie - Int. Ed. https://doi.org/10.1002/anie.201710838
14. Lan, W., de Bueren, J.B., Luterbacher, J.S., 2019. Highly Selective Oxidation and Depolymerization of α,γ-Diol-Protected Lignin. Angew. Chemie 131, 2675–2680. https://doi.org/10.1002/ange.201811630
15. Luo, B., Li, R., Shu, R., Wang, C., Zhang, J., Chen, Y., 2020. Boric Acid as a Novel Homogeneous Catalyst Coupled with Ru/C for Hydrodeoxygenation of Phenolic Compounds and Raw Lignin Oil. Ind. Eng. Chem. Res. https://doi.org/10.1021/acs.iecr.0c00888
16. Nishimura, H., Kamiya, A., Nagata, T., Katahira, M., Watanabe, T., 2018. Direct evidence for α ether linkage between lignin and carbohydrates in wood cell walls. Sci. Rep. 8, 6538. https://doi.org/10.1038/s41598-018-24328-9
17. Pan, X., Gilkes, N., Kadla, J., Pye, K., Saka, S., Gregg, D., Ehara, K., Xie, D., Lam, D., Saddler, J., 2006. Bioconversion of hybrid poplar to ethanol and co-products using an organosolv fractionation process: optimization of process yields. Biotechnol. Bioeng. 94, 851–861. https://doi.org/10.1002/bit.20905
18. Patil, V., Adhikari, S., Cross, P., 2018. Co-pyrolysis of lignin and plastics using red clay as catalyst in a micro-pyrolyzer. Bioresour. Technol. 270, 311–319. https://doi.org/10.1016/j.biortech.2018.09.034
19. Patil, V., Adhikari, S., Cross, P., Jahromi, H., 2020. Progress in the solvent depolymerization of lignin. Renew. Sustain. Energy Rev. 133, 110359. https://doi.org/https://doi.org/10.1016/j.rser.2020.110359
20. Renders, T., Van Den Bosch, S., Koelewijn, S.F., Schutyser, W., Sels, B.F., 2017. Lignin-first biomass fractionation: The advent of active stabilisation strategies. Energy Environ. Sci. https://doi.org/10.1039/c7ee01298e
21. Rietjens, M., Steenbergen, P.A., 2005. Crosslinking Mechanism of Boric Acid with Diols Revisited. Eur. J. Inorg. Chem. 2005, 1162–1174. https://doi.org/10.1002/ejic.200400674
22. Roberts, V.M., Stein, V., Reiner, T., Lemonidou, A., Li, X., Lercher, J.A., 2011. Towards quantitative catalytic lignin depolymerization. Chem. - A Eur. J. 17, 5939–5948. https://doi.org/10.1002/chem.201002438
23. Sameni, J., Krigstin, S., Sain, M., 2017. Solubility of Lignin and Acetylated Lignin in Organic Solvents. Bioresour. Vol 12, No 1.

24. Shuai, L., Amiri, M.T., Questell-Santiago, Y.M., Héroguel, F., Li, Y., Kim, H., Meilan, R., Chapple, C., Ralph, J., Luterbacher, J.S., 2016. Formaldehyde stabilization facilitates lignin monomer production during biomass depolymerization. Science (80-.). 354, 329–333. https://doi.org/10.1126/science.aaf7810
25. Szulejko, J.E., Kim, Y., Kim, K., 2013. Method to predict gas chromatographic response factors for the trace-level analysis of volatile organic compounds based on the effective carbon number concept. J. Sep. Sci. 36, 3356–3365.
26. Talebi Amiri, M., Dick, G.R., Questell-Santiago, Y.M., Luterbacher, J.S., 2019. Fractionation of lignocellulosic biomass to produce uncondensed aldehyde-stabilized lignin. Nat. Protoc. 14, 921–954. https://doi.org/10.1038/s41596-018-0121-7
27. Tarmadi, D., Tobimatsu, Y., Yamamura, M., Miyamoto, T., Miyagawa, Y., Umezawa, T., Yoshimura, T., 2018. NMR studies on lignocellulose deconstructions in the digestive system of the lower termite Coptotermes formosanus Shiraki. Sci. Rep. 8, 1290. https://doi.org/10.1038/s41598-018-19562-0
28. Toledano, A., Serrano, L., Labidi, J., 2014. Improving base catalyzed lignin depolymerization by avoiding lignin repolymerization. Fuel 116, 617–624. https://doi.org/10.1016/j.fuel.2013.08.071
29. Viell, J., Harwardt, A., Seiler, J., Marquardt, W., 2013. Is biomass fractionation by Organosolv-like processes economically viable? A conceptual design study. Bioresour. Technol. 150, 89–97. https://doi.org/https://doi.org/10.1016/j.biortech.2013.09.078
30. vom Stein, T., Grande, P.M., Kayser, H., Sibilla, F., Leitner, W., Domínguez de María, P., 2011. From biomass to feedstock: one-step fractionation of lignocellulose components by the selective organic acid-catalyzed depolymerization of hemicellulose in a biphasic system. Green Chem. 13, 1772–1777. https://doi.org/10.1039/C1GC00002K
31. Xue, B., Yang, Y., Zhu, M., Sun, Y., Li, X., 2018. Lewis acid-catalyzed biphasic 2-methyltetrahydrofuran/H2O pretreatment of lignocelluloses to enhance cellulose enzymatic hydrolysis and lignin valorization. Bioresour. Technol. 270, 55–61. https://doi.org/https://doi.org/10.1016/j.biortech.2018.09.028

6. Summary and Future Direction

6.1 Summary

This research aimed at finding effective ways for lignin depolymerization and valorization by making use of pyrolysis and solvent liquefaction as thermochemical conversion techniques. The focus of experiments performed was to assess whether various strategies used at different stages of lignin valorization were able to effectively stabilize the structure of lignin and compounds derived from it. Based on quantitative and qualitative analysis of the products derived from lignin depolymerization, it can be concluded that hydrogen from plastics or donor solvents can stabilize the reactive fragments from lignin. Also, pretreatment of lignin with phenol can stabilize its structure, leading to an increased selectivity of phenolics over aliphatics, although consuming phenol in the process. Boric acid stabilization of lignin during its isolation from biomass led to an increase in monomeric yields after its depolymerization. The results indicate that instead of using lignin directly from waste streams of industrial processes, it would be more useful to attempt modifying its structure before depolymerization. Also, the use of chemical reagents for lignin stabilization is possible and can be further optimized to increase the product yields. This approach eliminates the need to reduce the harshness of lignin depolymerization or isolation processes, making sure that the efficiency of the conversion of feedstock is not negatively affected. It is generally known in the research area of lignin valorization that isolation from biomass is the most effective step to introduce stabilization strategies. But this research provided a comprehensive overview for this knowledge by investigating stabilization strategies at various stages of lignin valorization, such as after depolymerization (chapter 2), during depolymerization (chapter 3), during a pretreatment (chapter 4), or during the isolation from biomass (chapter 5). Stabilization during a pretreatment led to a 14% increase in phenolic monomer yields, whereas that during lignin isolation led to a 56% increase in the monomer yield.

By investigating stabilization strategies and making use of biomass-derived solvents for lignin depolymerization, this dissertation has shown how lignin stabilization using protective-groups is still an interesting area of research. Solvents such as 2-methyl tetrahydrofuran and reagents such as phenol and tetralin can be derived from biomass and can be available in a

biorefinery. Their use in lignin valorization can help to bring down the cost of valorization of this novel feedstock and can help biorefineries be independent in terms of their resource use in the future. The identification and quantification of lignin-derived compounds is an important component in the studies on lignin depolymerization. This dissertation made effective use of techniques such as GC-MS/FID equipped with a 'methanizer' to understand how the yields of lignin-derived compounds changed during the various improvements proposed for lignin valorization in different chapters. Additionally, the structure of lignin being one of the most important factors that decide the product yields on its depolymerization, this dissertation used state-of-the-art techniques such as ^{1}H-^{13}C 2D HSQC and ^{31}P NMR to elucidate the structure of lignin and incorporate its importance in the discussion about its reactivity in the depolymerization processes investigated here. The side-reactions leading to products that were not the primary focus of this research, such as aliphatics and di-aromatics were also discussed in this dissertation from place to place wherever they were observed. This ensured the discussion of lignin depolymerization reaction that occurred in the experiments was nuanced and multiple factors affecting the process were taken into consideration.

6.2 Limitations of this dissertation and future direction

This research investigated the effect of various stabilization strategies for aiding lignin depolymerization. The effect of adding chemical stabilization agents before, during, and after lignin depolymerization was revealed. Catalysts ranging from natural red clay to a commercial Ru/C were used for lignin depolymerization. At the same time, chemical stabilization agents such as plastics, tetralin, phenol, and boric acid were investigated with the help of lab-scale experiments. Changes in the structure of lignin were studied with novel NMR techniques and those were correlated with the products of lignin depolymerization. The selectivity of bond cleavage in lignin to form phenolic monomers, as well as the qualitative and quantitative changes in the monomeric products as a result of the stabilization strategies were discussed. However, there were several limitations to this research arising from the types of lignin used, impurities in them, the reactor configurations, and the experimental setup. These limitations can also be looked at as future questions for an investigation that can be explored for the advancement of this research area. These limitations and the future direction of research stemming from them are presented here:

- **Use a single solvent instead of a combination of those**

Even though it is attractive to use a mixture of solvents for the solvent liquefaction process, it may not be the best way to utilize their solvation properties. Different solvents can help aid lignin depolymerization in different ways, such as providing *in situ* hydrogen, dissolving lignin, or stabilizing the fragments derived from. But equally difficult is their separation from the product mixture at the end of the process. Hence, the use of these solvents in pretreatment or during lignin isolation might be preferable, so that unique strategies for their separation from the mixture, such as precipitation, extraction, or phase separation can be used.

- **Explore the reaction mechanism between feedstocks**

For the study with co-pyrolysis of lignin with plastics, although a synergistic effect between the feedstock was observed, the reaction mechanism leading to it remained unknown. However, it might be possible with certain experimental setup and modeling techniques to explore how these two feedstocks or the pyrolysis vapors derived from those react with one another, affecting the formation of depolymerization products.

- **Develop pretreatment strategies accounting for biomass and lignin variability**

The structure of lignin also depends on the biomass from which it is isolated. Hence, any variability in biomass can affect the structure of lignin, and subsequently, its depolymerization. In this dissertation, the lignin type and its properties have been majorly categorized based on the lignin isolation technique. Yet, it would still be valuable to study different types of biomass to isolate lignin with the given methods to investigate how the source affects the structure and properties of lignin. This not only determines the resulting products on depolymerization of lignin but also needs to be considered as an important factor in designing the thermochemical conversion process. Moreover, having a process with easily tunable reaction parameters can be helpful in ensuring that a variable feedstock is effectively handled in a processing facility or an experimental setup.

- **Remove the impurities from technical lignins before depolymerization**

The technical lignin purchased from suppliers (Chapter 2 and Chapter 3) had the presence of many impurities in the form of salts, surfactants, and minerals, as suggested by its solvation in water. These impurities certainly affect lignin depolymerization, most probably leading to an adverse effect on the selectivity of the phenolic monomers getting formed from lignin. However, this research did not take into consideration the effect of these impurities, which is indeed important to have a complete understanding of the process. Hence, future research studies should either try to remove these impurities from lignin before its depolymerization or investigate their effect using techniques such as ICP-MS.

- **Study the solvent liquefaction in a continuous reactor**

The industrial processes for large-scale conversion of biomass or production of commodity chemicals are often operated in a continuous mode. Therefore, the batch-type reactors used in this research may not give an accurate idea for reactivity and conversion of feedstock. Moreover, the bench-scale experiments performed here have limited ability to predict the behavior of lignin in pilot-scale reactors. A continuous reactor-setup can mitigate the limitations stemming from scale of the process to some extent by making available a more useful real-life replica of a pilot-scale conversion unit. Also, continuously feeding the reactor in the form of a slurry is necessary and its feasibility can be examined in a holistic way with the use of a continuous reactor. This type of reactor setup can also pave the way for rapid assessment of different types of feedstocks, catalysts, and solvents used for the solvent liquefaction process.

7. Supplementary Information

7.1 Chapter 2

7.1.1 GC-FID-Polyarc® system calibration

For calibrating the FID system to quantify the GC-detected compounds, five different standards of guaiacol (purchased from Sigma Aldrich) were prepared in dichloromethane as solvent. The GC-MS/FID analysis was carried out with the same GC parameters as that used for the analysis of fast pyrolysis products. The calibration curves are shown in Figure S *7.1*.

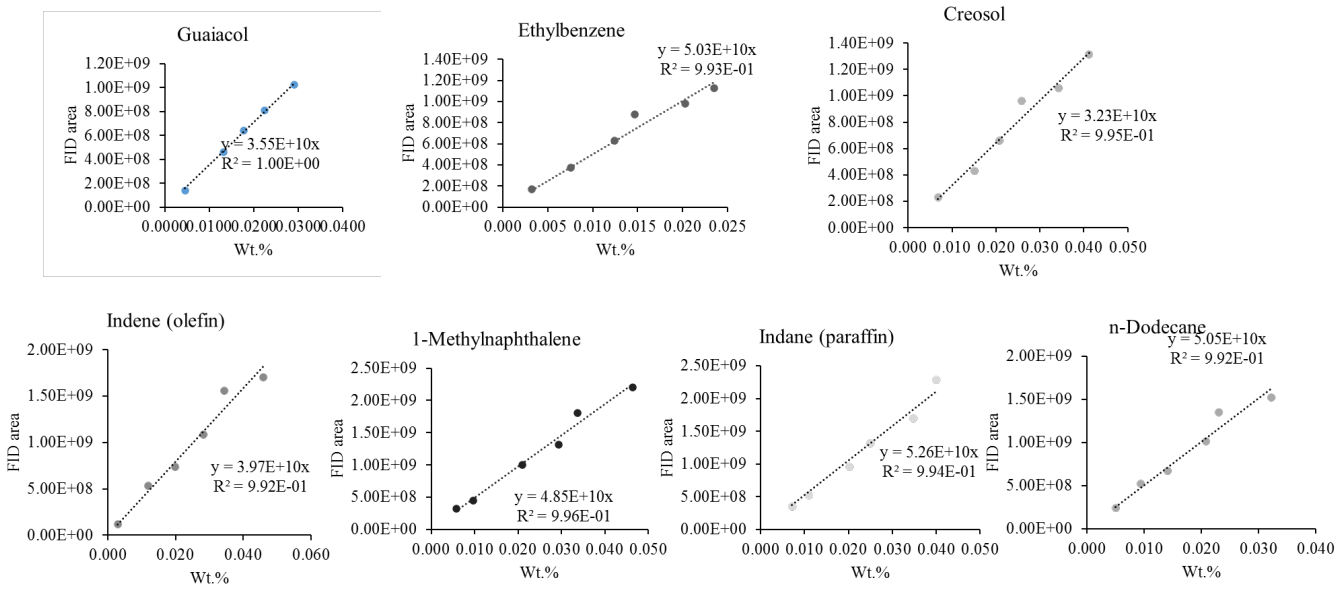

Figure S 7.1 Calibration curves for standard compounds (a) guaiacol (b) ethylbenzene (c) creosol (d) indene (e) 1-methylnaphthalene (f) indane (g) n-dodecane [Density of DCM= 1.330 g/mL; sample injected in GC= 1 µL]

7.1.2 Catalyst characterization

7.1.2.1 XRF analysis

The XRF spectra of red clay catalyst is shown in Figure S 7.2

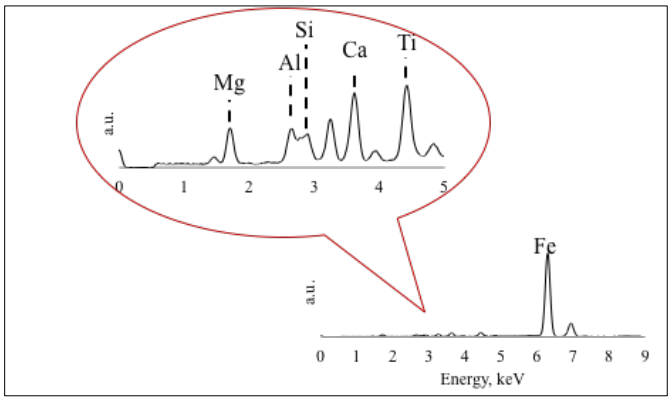

Figure S 7.2 XRF analysis of calcined red clay catalyst

7.1.2.2 XRD analysis

The XRD spectra of red clay catalyst is shown in Figure S 7.3.

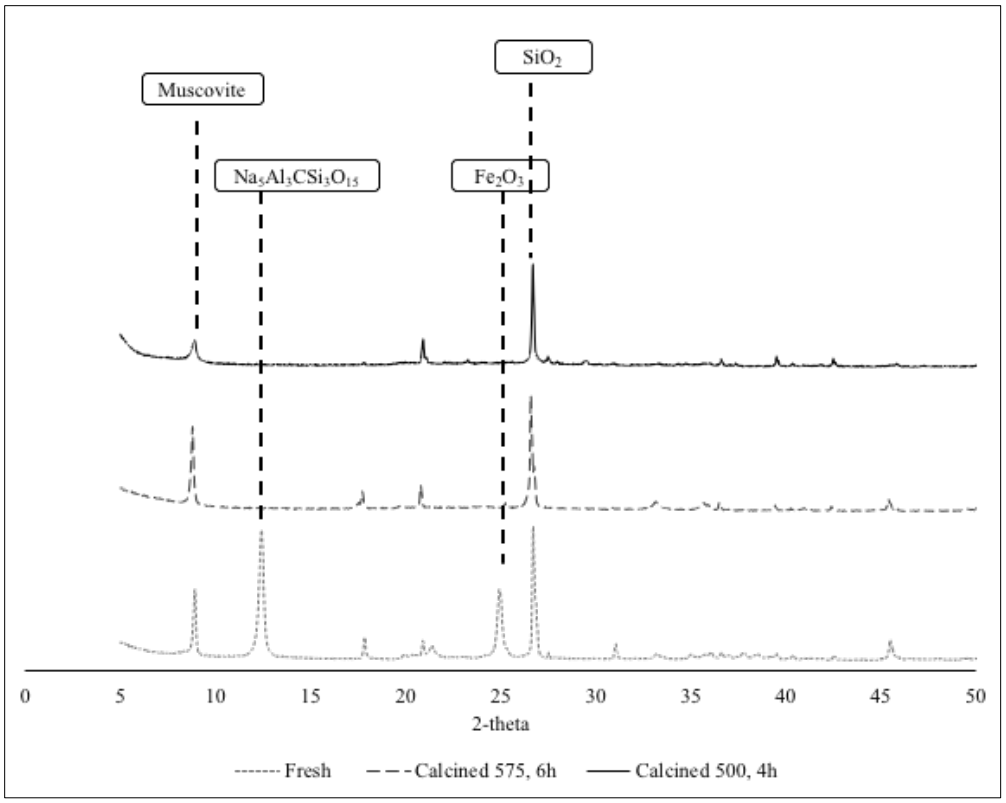

Figure S 7.3 XRD analysis of fresh and calcined red clay catalyst samples

7.2 Chapter 4

Some of the compounds that were exclusively produced from the phenolated lignin were also found to be commercially valuable. The mass spectra of these compounds were used to confirm their identity in addition to the elution time in gas chromatography, and are shown in Figure S 7.4.

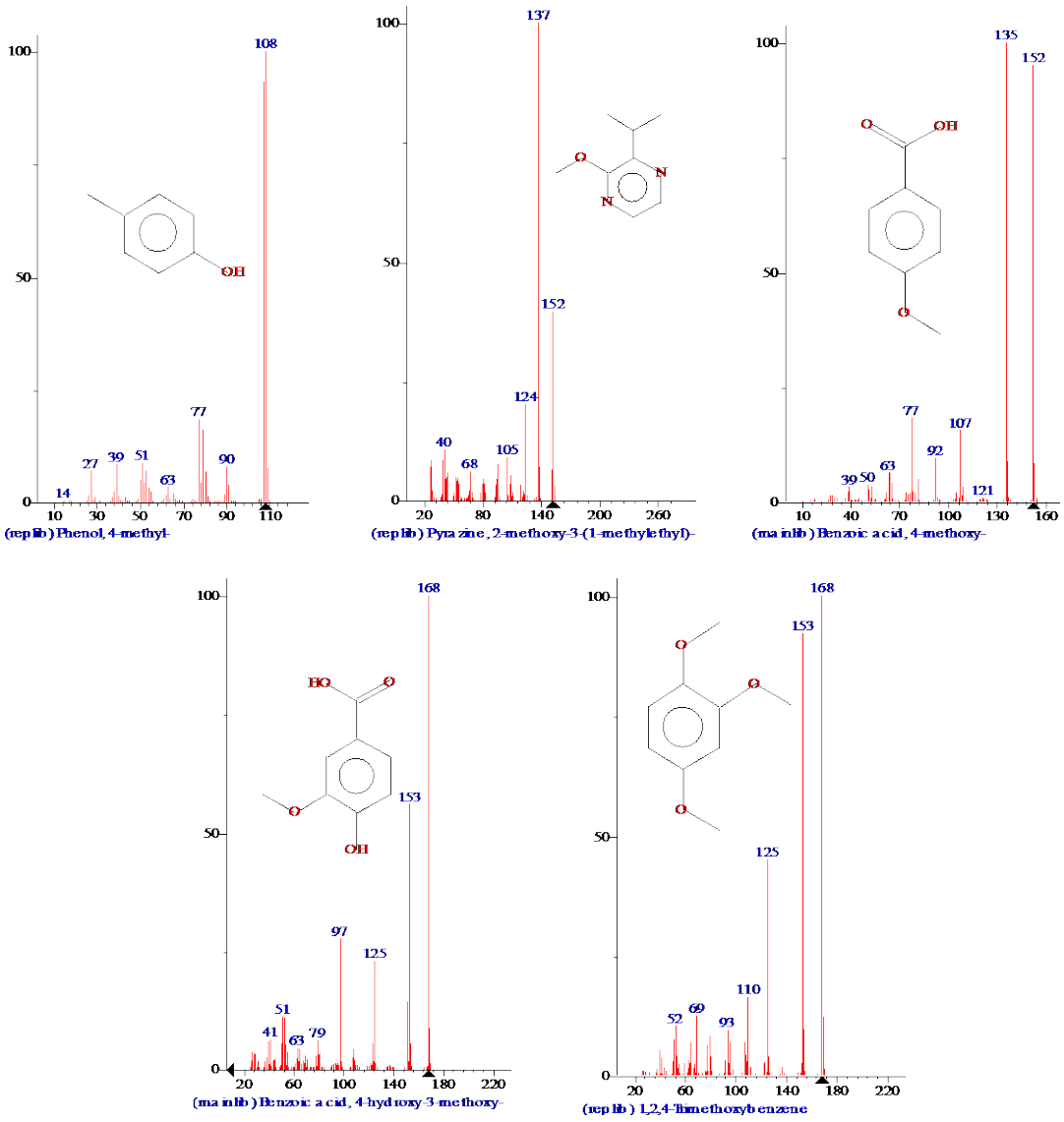

Figure S 7.4 Mass Spectra of commercially useful unique compounds from pretreated lignin as mentioned in the study

The quantification of compounds mentioned in the research article was carried out with Polyarc method ("Quantification with the Polyarc ®," n.d.). The concentration of creosol (Phenol, 2-methoxy-4-methyl-) was used as an 'internal standard concentration' required for the calculations. This was done for the vast majority of compounds for which pure compound standards were not available. The slopes of calibration curves for compounds whose concentrations were calculated using the external calibration are given in Table S *7.1*.

Table S 7.1 Calibration equation parameters used for estimating the compound yields

Compound	m (slope)	R^2 (regression coefficient)
Phenol, 2-methoxy-	5.38E+09	0.841
Benzoic acid, ethyl ester	1.41E+10	0.99
n-Decane	2.84E+10	0.959
n-Pentadecane	1.33E+10	0.985
Phenol, 4-ethyl-2-methoxy-	7.12E+09	0.956
Phenol, 2-methoxy-4-methyl-	5.86E+09	0.998
Vanillin	2.62E+09	0.944
Phenol, 2,6-dimethoxy-	2.84E+09	0.794
Phenol	1.91E+10	0.99
Phenol, 2-methoxy-4-(1-propenyl)-, (E)-	3.81E+10	0.9
Ethylparaben	6.88E+09	0.99
Benzene, methoxy-	2.24E+10	1

y=mx (y: methanizer-FID area, x: concentration, wt%)

Table S 7.2 Yields of individual compounds obtained from the depolymerization of raw and pretreated organosolv lignin

		wt% of lignin				
		Raw organosolv		Pretreated organosolv (under air)		
Compound	Code	Avg	SD	Avg	SD	Increase (%)
Phenolics						
Phenol	PH1	4.8	1.9	0.7	0.2	-85
Phenol, 2-methoxy-	PH2	2.4	0.8	3.0	1.0	22
Benzoic acid, ethyl ester	PH3	0.4	0.1	0.0	0.0	-100
Phenol, 2-methoxy-4-methyl-	PH4	1.2	0.2	1.2	<0.1	-7
Phenol, 4-ethyl-2-methoxy-	PH5	0.8	0.2	0.6	<0.1	-15
Phenol, 2-methoxy-4-propyl-	PH6	1.5	0.2	1.0	0.1	-32
Phenol, 2,6-dimethoxy-	PH7	1.3	0.2	1.5	<0.1	16
Benzoic acid, 4-methoxy-, ethyl ester	PH8	0.3	0.1	0.0	0.0	-100

Phenol, 2-methoxy-4-(1-propenyl)-, (E)-	PH9	0.8	0.6	1.4	0.1	76
4-Propyl-1,1'-diphenyl	PH10	0.0	0.0	0.9	0.1	100
Ethylparaben	PH11	0.3	<0.1	0.1	<0.1	-78
Phenol, 2,6-dimethoxy-4-(2-propenyl)-	PH12	0.3	<0.1	0.1	<0.1	-64
2-Pentanone, 1-(2,4,6-trihydroxyphenyl)	PH13	0.1	<0.1	0.0	0.0	-100
Total		***14.2***		***10.5***		
Phenol, 4-methyl-	PH14	0.0	0.0	0.4	0.2	100
Phenol, 5-methoxy-2,3-dimethyl-	PH15	0.0	0.0	0.2	0.2	100
1-Benzenol,2-methoxy-4-[[[2-(4-hydroxyphenyl)ethyl]amino]methyl]-	PH16	0.0	0.0	0.1	0.1	100
Benzoic acid, 4-hydroxy-3-methoxy-	PH17	0.0	0.0	0.9	<0.1	100
5-tert-Butylpyrogallol	PH18	0.0	0.0	0.5	<0.1	100
p-Ethyldiphenylmethane	PH19	0.0	0.0	<0.1	<0.1	100
1-Propanone, 3-hydroxy-1-(4-hydroxy-3-methoxyphenyl)-	PH20	0.0	0.0	<0.1	<0.1	100
Total		***0.0***		***2.1***		
Aromatics						
Pyrimidine, 4,5,6-tris(dimethylamino)-	ARO1	0.1	0.1	0.0	0.0	-100
3-Methyl-benzo(b)thiophene-1,1-dioxide	ARO2	0.0	0.0	<0.1	<0.1	100
Benzoic acid, 4-methoxy-	ARO3	0.0	0.0	0.1	0.1	100
1,2,4-Trimethoxybenzene	ARO4	0.0	0.0	0.1	0.1	100
Pyrazine, 2-methoxy-3-(1-methylpropyl)-	ARO5	0.0	0.0	<0.1	<0.1	100
1,2-Dimethoxy-4-(2-methoxyethenyl)benzene	ARO6	0.0	0.0	<0.1	<0.1	100
2,3,4-Trimethoxyphenylacetic acid	ARO7	0.0	0.0	<0.1	<0.1	100
Total		***0.1***		***0.3***		
Aliphatics (impurities derived from residual wood extractives)						
Butanedioic acid, diethyl ester	AL1	0.3	0.1	0.0	0.0	-100
Heptadecane	AL2	0.2	<0.1	0.0	0.0	-100
Tetradecanoic acid, ethyl ester	AL3	0.2	0.0	0.0	0.0	-100
Pentadecanoic acid, ethyl ester	AL4	0.1	<0.1	0.0	0.0	-100

Hexadecanoic acid, methyl ester	AL5	0.2	0.0	0.0	0.0	-100
E-11-Hexadecenoic acid, ethyl ester	AL6	0.7	0.1	0.0	0.0	-100
Heptadecanoic acid, ethyl ester	AL7	<0.1	<0.1	0.0	0.0	-100
Ethyl Oleate	AL8	0.1	<0.1	0.0	0.0	-100
Octadecanoic acid, ethyl ester	AL9	0.1	0.0	0.0	0.0	-100
Heptadecanoic acid, 15-methyl-, ethyl ester	AL11	0.0	0.0	<0.1	<0.1	100
Hexadecanoic acid, ethyl ester	AL10	0.0	0.0	<0.1	<0.1	100
Total		1.9		0.0		
TOTAL		**19.2**	**0.7**	**13.2**	**1.2**	
Phenol		**4.8**	**1.9**	**0.7**	**0.2**	
Total monomers (excluding phenol)		**14.4**	**2.6**	**12.5**	**1.0**	
Phenolic monomers (excluding phenol)		**10.9**	**1.2**	**12.4**	**1.0**	**14**
Bio-oil yield		**26.4**	**1.3**	**50.9**	**0.2**	**92**
Char yield		**7.6**	**2.2**	**5.5**	**0.1**	**-27**

Table S 7.3 Individual compound yields determined using GC-MS/FID for the depolymerization product of lignin pretreated under inert and oxidative conditions

		Pretreated under inert wt% of lignin		**Pretreated under oxygen wt% of lignin**	
Compound	**Code**	**Average[a]**	**S.D. [a]**	**Average[a]**	**S.D. [a]**
Phenolics					
Phenol	PH1	0.8	0.1	2.3	1.2
Phenol, 2-methoxy-	PH2	4.3	0.8	8.6	0.0
Phenol, 4-methyl-	PH14	0.6	0.3	1.2	0.0
Phenol, 2-methoxy-4-methyl-	PH4	2.6	0.5	3.0	0.1
Phenol, 4-ethyl-2-methoxy-	PH5	1.4	0.3	2.1	0.0
Phenol, 2-methoxy-4-propyl-	PH6	1.9	0.2	3.1	0.0
Phenol, 2,6-dimethoxy-	PH7	3.8	1.8	3.9	3.3
3-Methyl-benzo(b)thiophene-1,1-dioxide	PH24	0.2	0.2	0.0	0.0
Phenol, 2-methoxy-4-(1-propenyl)-, (E)-	PH9	0.1	0.0	0.1	0.1
Benzoic acid, 4-hydroxy-3-methoxy-	PH18	1.0	1.0	2.5	0.0

4-Propyl-1,1'-diphenyl	PH10	0.6	0.5	0.3	0.3
1-Propanone, 3-hydroxy-1-(4-hydroxy-3-methoxyphenyl)-	PH25	0.2	0.2	0.0	0.0
Phenol, 2,6-dimethoxy-4-(2-propenyl)-	PH12	0.4	0.0	0.5	0.0
1-Benzenol,2-methoxy-4-[[[2-(4-hydroxyphenyl)ethyl]amino]methyl]-	PH16	0.1	0.1	0.6	0.6
5-tert-Butylpyrogallol	PH19	0.3	0.3	1.0	1.0
2-Pentanone, 1-(2,4,6-trihydroxyphenyl)	PH13	0.0	0.0	0.1	0.1
Benzoic acid, 4-methoxy-, ethyl ester	PH8	0.0	0.0	0.3	0.3
Phenol, 2-methyl-	PH22	0.3	0.3	0.0	0.0
2',4'-Dihydroxypropiophenone	PH23	0.3	0.3	0.0	0.0
Benzoic acid, 3-methoxy-, methyl ester	PH26	0.1	0.1	0.0	0.0
p-Ethyldiphenylmethane	PH20	0.1	0.1	0.0	0.0
Phenylacetylformic acid, 4-hydroxy-3-methoxy-	PH27	0.1	0.1	0.0	0.0
Sum (phenolics)		*19.2*		*29.6*	*0.0*
Aliphatics (impurities derived from residual wood extractives)					
Hexadecanoic acid, methyl ester	AL5	0.1	0.0	0.4	0.0
Hexadecanoic acid, ethyl ester	AL10	0.2	0.0	0.5	0.0
Octadecanoic acid, ethyl ester	AL9	0.0	0.0	0.1	0.0
Sum (aliphatics)		*0.3*		*1.0*	
Aromatics					
1,2,4-Trimethoxybenzene	ARO4	0.7	0.7	0.4	0.4
1,4-Benzenediol, 2,3,5-trimethyl-	ARO9	0.1	0.1	0.0	0.0
Durohydroquinone	ARO10	0.2	0.2	0.0	0.0
4-[n-Propylamino]-2,5-dimethoxyaniline	ARO11	0.2	0.2	0.0	0.0
Benzene, 1,2,3-trimethoxy-5-methyl-	ARO12	0.2	0.2	0.0	0.0
Naphthalene, 2,3-dimethoxy-	ARO13	0.0	0.0	0.0	0.0
Sum (aromatics)		*1.5*		*0.4*	

TOTAL	**21.1**	**2.3**	**31.1**	**3.1**
Phenol	**0.8**	**0.1**	**2.3**	**1.2**
Total GC-eluted monomers (excluding phenol)	**20.3**	**-**	**28.8**	**-**
Phenolic monomers (excluding phenol)	**18.4**	**-**	**27.3**	**-**
Bio-oil yield	**31.6**	**1.2**	**42.0**	**0.6**
Char yield	**5.5**	**-**	**7.4**	**-**

7.3 Chapter 5

Table S 7.4 Chemical compounds present in lignin depolymerization products, as detected from GC-MS characterization (all compounds)

	Without stabilization Yield, wt% (based on dry lignin)		**Without stabilization Selectivity (wt% of lignin-derived compounds)**	**With stabilization Yield, wt% (based on dry lignin)**		**With stabilization Selectivity (wt% of lignin-derived compounds)**
Compound code	**avg**	**SD**		**avg**	**SD**	
Phenolics						
PH1	0.1	0.1	0.9	<0.1	<0.1	<0.1
PH2	1.1	1.1	6.6	3.4	<0.1	13.4
PH3	0.8	0.8	5.1	<0.1	<0.1	<0.1
PH4	<0.1	<0.1	0.2	<0.1	<0.1	<0.1
PH5	<0.1	<0.1	0.1	<0.1	<0.1	0.1
PH6	<0.1	<0.1	<0.1	4.4	2.5	17.6
PH7	3.8	0.4	23.6	4.3	1.5	17.3
PH8	0.2	0.2	1.0	<0.1	<0.1	<0.1
PH9	<0.1	<0.1	<0.1	0.5	0.5	2.1
PH10	<0.1	<0.1	0.1	0.1	0.1	0.5
PH11	<0.1	<0.1	<0.1	0.1	0.1	0.3
PH12	<0.1	<0.1	0.3	<0.1	<0.1	<0.1
PH13	<0.1	<0.1	0.3	<0.1	<0.1	<0.1
PH14	0.1	0.1	0.6	<0.1	<0.1	<0.1
PH15	<0.1	<0.1	<0.1	1.0	1.0	3.8
PH16	1.1	0.3	6.8	0.1	0.1	0.3
PH17	0.1	0.1	0.8	<0.1	<0.1	<0.1
PH18	4.6	2.7	28.5	<0.1	<0.1	<0.1

PH19	<0.1	<0.1	<0.1	1.7	1.7	6.7
PH20	<0.1	<0.1	<0.1	0.1	0.1	0.5
PH21	<0.1	<0.1	<0.1	<0.1	<0.1	0.1
PH22	<0.1	<0.1	<0.1	4.1	4.1	16.4
PH23	1.9	1.9	11.8	<0.1	<0.1	<0.1
PH24	1.4	1.3	8.9	3.1	0.4	12.2
Total phenolics	*15.5*		*95.7*	*22.9*		*91.3*
Aromatics						
AR1	0.1	0.1	0.4	<0.1	<0.1	<0.1
AR2	0.1	0.1	0.8	<0.1	<0.1	<0.1
AR3	0.1	0.1	0.4	<0.1	<0.1	<0.1
AR4	<0.1	<0.1	0.2	<0.1	<0.1	<0.1
AR5	<0.1	<0.1	<0.1	<0.1	<0.1	0.1
AR6	0.2	0.2	1.1	<0.1	<0.1	<0.1
AR7	<0.1	<0.1	<0.1	0.5	0.5	1.8
AR8	0.1	0.1	0.8	<0.1	<0.1	<0.1
AR9	<0.1	<0.1	<0.1	1.1	1.1	4.3
AR10	0.1	0.1	0.3	<0.1	<0.1	<0.1
AR11	<0.1	<0.1	<0.1	0.6	0.6	2.5
AR12	0.1	<0.1	0.3	<0.1	<0.1	<0.1
Total aromatics	*0.7*		*4.3*	*2.2*		*8.7*
Total	**16.2**		**100.0**	**25.1**		**100.0**

***avg: Average**

****SD: Standard deviation**

Table S 7.5 Abbreviations used for the names of lignin-derived compounds

Compound	Compound code
Phenolics	
.beta.-(4-Hydroxy-3-methoxyphenyl)propionic acid	PH1
1-(2,6-Dihydroxy-4-methoxy-3-methylphenyl)-1-butanone	PH2
1-Butanone, 1-(2,4,6-trihydroxy-3-methylphenyl)-	PH3
1-Pentanone, 1-(2,4,6-trihydroxy-3-methylphenyl)-	PH4
2-(Acetoxymethyl)-3-(methoxycarbonyl)biphenylene	PH5
2,4'-Dihydroxy-3'-methoxyacetophenone	PH6
3-Hydroxy-4-methoxyacetophenone	PH7
4-Hydroxy-2-methoxybenaldehyde	PH8
4-n-Propylbiphenyl	PH9
Anthracene	PH10

Benzaldehyde, 2-hydroxy-4-methoxy-	PH11
Benzaldehyde, 3-hydroxy-4-methoxy-	PH12
Benzaldehyde, 4-hydroxy-	PH13
Benzeneacetic acid, .alpha.-hydroxy-.alpha.-methyl-, (R)-	PH14
Benzeneethanol, 4-hydroxy-3-methoxy-	PH15
Butylated Hydroxytoluene	PH16
Phenol, 2,6-dimethyl-	PH17
Phenol, 2-methoxy-4-(1-propenyl)-	PH18
Phenol, 2-methoxy-4-propyl-	PH19
Phenol, 4-methoxy-3-(methoxymethyl)-	PH20
Phenol, 5-methyl-2-(1-methylethyl)-	PH21
Phenol, 3,5-dimethyl-	PH22
Vanillic acid	PH23
Vanillin	PH24
Aromatics	
1,2-Dimethoxy-4-(1,2,3-trimethoxypropyl)benzene	AR1
1,4-Benzenedimethanol, .alpha.,.alpha.'-dimethyl-	AR2
3-Ethoxy-4-methoxybenzyl alcohol	AR3
Anthracene, 2-ethyl-	AR4
Benzene	AR5
Benzene, 1,1'-methylenebis-	AR6
Benzenemethanol, 3,4,5-trimethoxy-	AR7
Benzenemethanol, 3,4-dimethoxy-	AR8
Benzofuran, 2-propyl-	AR9
Benzoic acid, methyl ester	AR10
Dibenzofuran, 4-methyl-	AR11
Naphthalene, 1-methyl-	AR12